NAVAL POSTGRADUATE SCHOOL

MONTEREY, CALIFORNIA

THESIS

DETERMINING A COST-EFFECTIVE MIX OF UAV-USV-MANNED PLATFORMS TO ACHIEVE A DESIRED LEVEL OF SURVEILLANCE IN A CONGESTED STRAIT

by

Kim Chuan Chng

December 2007

Thesis Advisor:	Patricia A. Jacobs
Co-Advisor:	Donald P. Gaver
Second Reader:	Wayne P. Hughes Jr.

THIS PAGE INTENTIONALLY LEFT BLANK

REPORT DOCUMENTATION PAGE			Form Approved OMB No. 0704-0188
Public reporting burden for this collection of information is estimated to average 1 hour per response, including the time for reviewing instruction, searching existing data sources, gathering and maintaining the data needed, and completing and reviewing the collection of information. Send comments regarding this burden estimate or any other aspect of this collection of information, including suggestions for reducing this burden, to Washington headquarters Services, Directorate for Information Operations and Reports, 1215 Jefferson Davis Highway, Suite 1204, Arlington, VA 22202-4302, and to the Office of Management and Budget, Paperwork Reduction Project (0704-0188) Washington DC 20503.			
1. AGENCY USE ONLY ***(Leave blank)***	**2. REPORT DATE** December 2007	**3. REPORT TYPE AND DATES COVERED** Master's Thesis	
4. TITLE AND SUBTITLE Determining a Cost-Effective Mix of UAV-USV-Manned Platforms to Achieve a Desired Level of Surveillance in a Congested Strait		**5. FUNDING NUMBERS**	
6. AUTHOR(S) Kim Chuan Chng			
7. PERFORMING ORGANIZATION NAME(S) AND ADDRESS(ES) Naval Postgraduate School Monterey, CA 93943-5000		**8. PERFORMING ORGANIZATION REPORT NUMBER**	
9. SPONSORING /MONITORING AGENCY NAME(S) AND ADDRESS(ES) N/A		**10. SPONSORING/MONITORING AGENCY REPORT NUMBER**	
11. SUPPLEMENTARY NOTES The views expressed in this thesis are those of the author and do not reflect the official policy or position of the Department of Defense or the U.S. Government.			
12a. DISTRIBUTION / AVAILABILITY STATEMENT Approved for public release; distribution is unlimited		**12b. DISTRIBUTION CODE** A	

13. ABSTRACT (maximum 200 words)

This thesis develops concepts of operations (CONOPS) and analytical models to determine the surveillance assets for a congested strait. Two maritime security threats (Reds) are a hijacked large ship carrying dangerous cargo or a SB manned by terrorists attempting to cause damage to other vessels or the port. The Red SB can either conduct a direct attack or a sneak attack by hiding among other neutral SBs. The defense force consists of shore-based sensors, *unmanned aerial vehicles* (UAVs), *unmanned surface vehicles* (USVs), and *patrol craft* (PC). The shore-based radar and the UAVs classify unidentified vessels as suspicious or not suspicious and suspicious SB must be inspected by a USV or PC. Analytical models are introduced to analyze requirements for numbers of surveillance assets and to assess the effectiveness of the CONOPS to achieve a desired probability of detecting and intercepting the threat. They incorporate both differential equations and probabilistic arguments. Results indicate that if the UAVs generate many false positives then the USVs and PCs have a higher workload which decreases the probability of detecting a threat. USVs and PCs should give a high priority to inspecting suspicious SBs rather than identifying unsuspicious SBs to achieve a higher probability of detecting a threat.

14. SUBJECT TERMS Maritime security, Coastal surveillance, Maritime domain protection modeling			**15. NUMBER OF PAGES** 165
			16. PRICE CODE
17. SECURITY CLASSIFICATION OF REPORT Unclassified	**18. SECURITY CLASSIFICATION OF THIS PAGE** Unclassified	**19. SECURITY CLASSIFICATION OF ABSTRACT** Unclassified	**20. LIMITATION OF ABSTRACT** UU

NSN 7540-01-280-5500 Standard Form 298 (Rev. 2-89)
Prescribed by ANSI Std. 239-18

THIS PAGE INTENTIONALLY LEFT BLANK

Approved for public release; distribution is unlimited

DETERMINING A COST-EFFECTIVE MIX OF UAV-USV-MANNED PLATFORMS TO ACHIEVE A DESIRED LEVEL OF SURVEILLANCE IN A CONGESTED STRAIT

Kim Chuan Chng
Major, Republic of Singapore Navy
B.ENG. (Civil, First Class Honours), National University of Singapore, 1999

Submitted in partial fulfillment of the
requirements for the degree of

MASTER OF SCIENCE IN OPERATIONS RESEARCH

from the

NAVAL POSTGRADUATE SCHOOL
December 2007

Author: Kim Chuan Chng

Approved by: Patricia A. Jacobs
Thesis Advisor

Donald P. Gaver
Co-Advisor

Wayne P. Hughes, Jr.
Second Reader

James N. Eagle
Chairman, Department of Operations Research

THIS PAGE INTENTIONALLY LEFT BLANK

ABSTRACT

A congested strait providing entry to a port contains many benign non-hostile vessels. Some of the vessels are large ships (LSs) carrying dangerous cargo. Others are small boats (SBs), undistinguished in type, but not behavior. Two maritime security threats (Reds) are a hijacked LS carrying dangerous cargo, and/or a SB manned by terrorists attempting to cause damage to other vessels or to the port. The Red SB can either conduct a direct attack upon entering the strait, or a sneak attack by hiding among other neutral SBs. The defense force consists of shore-based sensors, *unmanned aerial vehicles* (UAVs), *unmanned surface vehicles* (USVs), and *patrol craft* (PC). The shore-based radar and the UAVs initially classify unidentified vessels as suspicious or not suspicious. Vessels classified as suspicious must be inspected intensively by a USV or PC; PC inspection often requires boarding, a time consuming process that may frequently result in no incriminating findings.

Analytical models are introduced to analyze requirements for numbers and capabilities of surveillance assets and to assess the effectiveness of concepts of operations (CONOPS) for defense forces to achieve a desired probability of detecting and intercepting the threat. The models incorporate both differential equations and probabilistic arguments. The model results indicate that if the UAVs generate many false positives then the USVs and PCs have a high (and often futile) workload, which decreases the probability of detecting a threat. Further, USVs and PCs should give a high priority to inspecting

suspicious SBs rather than identifying unsuspicious SBs in order to achieve a higher probability of detecting a threat.

TABLE OF CONTENTS

THIS PAGE INTENTIONALLY LEFT BLANK

LIST OF FIGURES

THIS PAGE INTENTIONALLY LEFT BLANK

LIST OF TABLES

THIS PAGE INTENTIONALLY LEFT BLANK

ACKNOWLEDGMENTS

I would like to express my sincerest appreciation and gratitude to Professor Patricia A. Jacobs and Distinguished Professor Donald P. Gaver for their valuable advice, guidance, encouragement, and inspiration. Their suggestions are instrumental in shaping this thesis.

I would also like to offer my heartfelt thanks CAPT USN(Ret) Wayne P. Hughes, Jr. for taking on the idea and helping to shape it into this thesis. CAPT Hughes' valuable guidance and feedback have contributed immensely to this thesis.

I would also like to thank my wife, Lynette, for her patience and love throughout this journey in Naval Postgraduate School.

THIS PAGE INTENTIONALLY LEFT BLANK

EXECUTIVE SUMMARY

A littoral state is concerned with the maritime security of the main sea routes in a narrow strait that her ports and economy depend on. Besides high traffic density on the sea routes, the strait is also congested with many small boats (SBs). Potential maritime security threats come from both large ships (LSs) and SBs plying the straits. In order to enforce maritime security in the strait, the littoral state requires additional surveillance assets on top of the existing system of coastal surveillance radars that is used for vessel traffic control. The littoral state would like to know a cost-effective mix of sensor platforms to ensure adequate surveillance coverage of the congested strait. The Order of Battle (ORBAT) mix that will be considered comprises *Unmanned Aerial Vehicles* (UAV), *Unmanned Surface Vehicles* (USV) and manned patrol crafts (PCs).

Two types of maritime terrorism threats are identified, namely LS threats and SB threats. Based on these threats, two concepts of operations (CONOPS) are considered to address each of them separately. The first maritime threat concerns the use of LSs carrying highly dangerous cargo (D-vessels) to inflict extensive damages to port facilities or other ships. The CONOPS against this threat is to use boarding teams from PCs to conduct boarding and inspection of D-vessels in order to detect a LS that has been hijacked by terrorists (Red vessel). The second maritime threat concerns use of SBs to inflict damage on infrastructure or other vessels. The CONOPS

against this second threat (Red boat) uses coastal radars, UAVs, USVs and PCs. The coastal radars detect suspicious activity (unusual course and speed). The UAV is used to rapidly identify unsuspicious SBs, while USVs and PCs are used to inspect suspicious SBs detected by the coastal radar and the UAVs, and desirably to detect the Red boat. Two possible scenarios for the SB threat are considered, one is a direct attack by single Red boat (scenario A) and the other is a sneak attack where the one Red boat attempts to hide among other neutral SBs for some time before attack (scenario B).

Analytic models of the scenarios are presented here incorporate both differential equations and probabilistic components. The differential equations are solved numerically using MATLAB.

In the LS model, the Red vessel is detected when at least one PC is available for inspection and the latter chooses (at random) the Red vessel from all un-inspected D-vessels. Based on an arrival rate of 20 D-vessels per day, it is showed that in order to have a probability of detecting the Red vessel greater than 0.9, an ORBAT of at least six PCs is required to be deployed. An additional PC will be required for every increment of four to five more vessels to arrive per day. Comparison between the deterministic fluid model and a generalized birth-death stochastic model indicates that both provide similar results.

In scenario A for the SB model, a Red boat is detected when at least one USV (or PC) is available when the Red SB starts its attack, and chooses to inspect the suspicious

Red boat from among other suspicious SBs. In scenario B, a Red boat can either be detected while it is hiding among other SBs, or when it commences attack. Once the Red boat commences attack in scenario B, the situation is modeled as scenario A with a shorter reaction time for the USV (or PC). The results are based on an arrival rate of 12 SBs per hour and an average of 48 unidentified SBs in the strait at any time. To achieve a probability of detection of the Red boat of at least 0.9 in good visibility conditions, the recommended ORBAT mix of six USVs and three PCs without any UAV is recommended, at an estimated cost of US$5.7 million per year for a period of 10 years. A mixed USV and PC ORBAT is recommended for a more robust surveillance force in terms of deterrence and exercising ground judgment. USVs are useful in situations when it is not necessary to risk human lives. If a UAV is included, the recommended mix is one UAV, two PCs and six USVs, at an estimated cost of US$6.7 million per year for a period of 10 years. In poor visibility conditions, the probability of detection drops by about 30%.

The analysis of the SB model results also provides insight into the effectiveness of possible *modus operandi* for the surveillance platforms. The UAV contribution is only positive when it highly accurately in classifies neutral (White) SBs. When the UAV mistakenly classifies a non-suspicious SB as suspicious, a USV or PC must do further inspections on the SB. Thus, UAVs can undesirably increase the workload for the USVs and PCs, and result in small improvements in the probability of detection in SB threat scenario A. The UAV ability to quickly identify SBs is more useful in SB threat scenario B as the Red boat is

hiding among other SBs. In this model there is no advantage to having the UAV follow suspicious SBs, especially if the perceived threat is SB threat scenario A. Conversely, the USV should give highest priority to inspecting suspicious SBs rather than identifying unsuspicious SBs in order to achieve the highest probability of detecting the Red SB.

I. INTRODUCTION

A. BACKGROUND

A littoral state (also referred as Blue state) is concerned about the maritime security of the main strait that its ports, and economy, depend on. This strait is also an international strait as it is an essential connection between two major international shipping lanes. Therefore, the shipping traffic in the strait consists of ships that are calling at the littoral state's ports and ships that are transiting through it to get from one major shipping lane to the other. As a high volume of shipping traffic uses the strait daily, the littoral state is concerned that the strait is vulnerable to the threat of maritime terrorism, and aims to enhance maritime security in its strait. As part of the littoral state's strategy to enhance maritime security, it has decided to improve its surveillance coverage. Enhancements in surveillance of the strait are efforts to increase the probability of detection of any potential threats to security, and serve as a deterrent.

The homeland security department (HSD) of the littoral state has decided that it needs a suite of different sensor platforms to supplement its existing system of coastal surveillance radars. The suite of sensor platforms will consist of *manned surface vessels* or *patrol craft* (PC), *unmanned surface vessels* (USV), and *unmanned aerial vehicles* (UAV). The homeland security department wants to

determine a cost-effective mix of platforms to ensure the desired surveillance coverage of the congested strait.

The goal of this thesis is to assist the HSD in their decision making for achieving the best mix of sensor platforms. Specifically, this thesis presents a concept of operations (CONOPS) based on current perceived maritime terrorism threats. Analytical models are then developed and used to determine the best platform mix. It is likely that opponent (Red) reaction will require the platform mix to change, adaptively.

B. THESIS OBJECTIVE

The objective of this thesis is to determine the force structure of an Order of Battle (ORBAT[1]) consisting of PCs, USVs, and UAVs, in order to achieve given levels of surveillance coverage of a congested strait for the purpose of enforcing maritime security. This will be achieved using a set of analytical models that are robust, low-resolution tools for force-structuring surveillance in the context of a congested strait.

[1] According to JP 1-02 (2007) Department of Defense Dictionary of Military Terms, an order of battle (ORBAT) is defined as the identification, strength, command structure, and disposition of the personnel, units, and equipment of any military force.

C. RESEARCH QUESTIONS

1. Characteristics of Operational Environment

An abstract geographical area is the setting for this analysis. The strait is bounded on two sides by landmasses belonging to the littoral states. The main sea routes in the strait are defined by a traffic separation scheme (TSS), which is a two-lane traffic way running east-west. The main points of entry and exit are at the terminals of the TSS and along the strait leading to the ports of the littoral state. Cross-strait traffic exists along several locations along the strait.

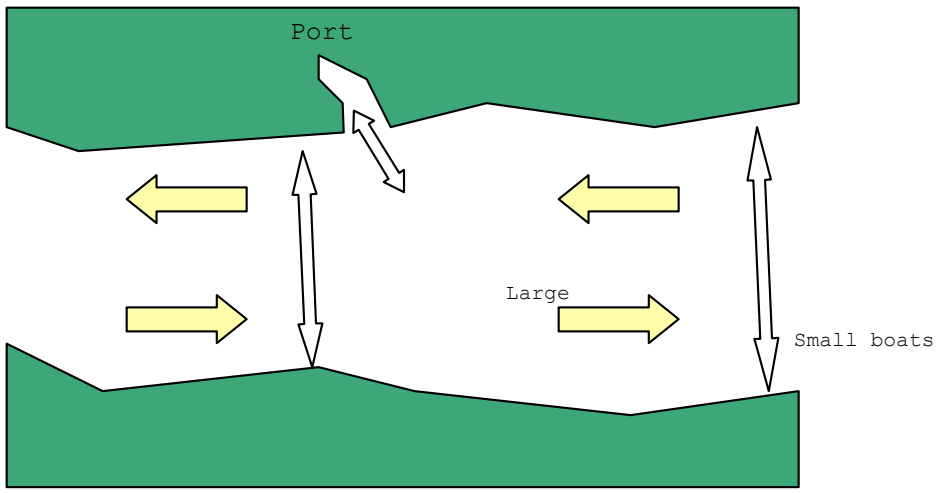

Figure 1. Pictorial representation of the abstract strait of the littoral state.

The notional strait has a set of key characteristics that pose challenges to surveillance.

Geographical Challenges:

- There are many small islands scattered along the coast, which may cause blind spots and clutter to radar and visual surveillance.
- There are multiple crossing points throughout the length of the strait that are used mainly by local traffic, such as pleasure and fishing crafts and ferries. These also add clutter and distraction to radar and visual surveillance.

Environmental Challenges:

- The high traffic density in the strait poses a high demand on the resources required for surveillance. The typical traffic density for a major international shipping strait is about 500 ships transiting per day for vessels above 75 gross ton.
- The presence of numerous small vessels and boats present possible concealment for illicit activities. The density can be about 100 small vessels in the strait continuously.
- There are many unaccounted vessels in the strait. These are the vessels that are not equipped with automatic identification systems (AIS) and are not required to report their movements. Most of these vessels are SBs involved in private leisure

activities or fishing. However, some can be involved in illicit activities that Blue (B) wishes to prevent.

2. Threats of Maritime Terrorism

After the 9/11 terrorist attacks in the U.S., there has been, and continues to be, a heightened international awareness of the threat of terrorism in transportation, including that in the maritime domain. Maritime terrorism threats generally fall into two categories: those carried out by small boats (SBs) and those carried out with larger ships. The use of SBs in guerilla-style attacks and suicide attacks targeted at vessels in transit, at pier-side or anchorage, belongs to the first category. Examples of such attacks in recent years are the attacks on the USS *Cole* in Aden (2000) and on the French tanker MV *Limburg* off the coast of Yemen (2004). In these attacks the terrorists used SBs laden with explosives as their mode of delivery.

The second category concerns the use of LSs, particularly those carrying highly dangerous cargoes, to inflict extensive damage. Terrorists can hijack a ship carrying dangerous cargoes such as liquefied natural gas (LNG) and/or hazardous chemicals and use it as a floating bomb to blow up in the port. The hijacked ship can also be used to import weapons of mass destruction (WMD). Although there is a low probability of such a scenario, the possible fallout and other consequences from even one such occurrence is enough reason for states with high dependency on maritime trades to act in a precautionary manner.

The littoral (Blue) state is concerned with these two categories of threats. They will be modeled and analyze in this study.

3. Surveillance Capabilities

The underlying problem faced by the littoral state in the surveillance of its operational environment is that each of the approximately 500 to 600 vessels plying the strait everyday could potentially be a threat. Hence, a comprehensive surveillance system is necessary to provide the required level of situational awareness to pick out the threat amongst the legitimate traffic.

The littoral state has an existing system of coastal surveillance radars (CSRs) and electro-optic/infrared (EO/IR) systems positioned along the coastline. These systems, together with Vessel Traffic Management Information System (VTMIS) and the Automatic Identification System (AIS)[2], enables the littoral state's maritime authority to know the location and identification[3] of most of the vessels in the strait. The effectiveness of the current suite of radars and modes of detection are limited in the strait's highly cluttered and congested environment.

---

[2] International Maritime Organization (IMO) (2007) regulations require ships of certain tonnage and class to be fitted with the AIS. The AIS is capable of providing information about the ship to other ships and to coastal authorities automatically. It provides information - including the ship's identity, type, position, course, speed, navigational status, destination and other safety-related information.

[3] Name, registration, country of origin, owners, general physical description, etc.

First, the CSRs are generally used for long-range, wide-area detection and tracking of large vessels. In the highly cluttered environment of a congested strait, the CSRs can be overloaded and sometimes give false echoes. The radar clutter and shadows can mask legitimate targets. Second, the CSRs' detection range of small vessels, such as a speedboat, is typically very short. Moreover, the CSRs are positioned on only one side of the strait, so that the detection of small vessels at the far side of the strait is degraded, a situation that may be known and exploited by opponents. The land-based EO/IR systems also have a shallow angle of view when looking at vessels far away, which means that these systems cannot see behind large objects such as LSs and islands.

In addition to the surveillance sensors, the maritime authority also uses the AIS to automatically detect vessels fitted with the AIS. The AIS automatically identifies and provides authorities with information on the positions of the vessels in the strait. This allows the maritime authority to have an improved situational picture of the strait. Also, by cross-referencing the vessels' identities against its database, the Blue's maritime authority can get more information, such as whether the vessel is scheduled to call in to its port. However, there are still many vessels that do not have AIS, such as non-compliant vessels and smaller vessels that do not come under IMO regulations due to their small gross tonnage. It is possible for the local maritime authority to enforce AIS for smaller vessels (not required under IMO regulations), but such a measure is limited to vessels registered in that state. Furthermore, even if a vessel's identification is known, it is possible

that Blue cannot positively ascertain that the vessel poses no harm. For such situations, it may be necessary to further investigate those vessels through individual inspections. These inspections can include a detailed close-up look by a standoff platform like a UAV or USV. The inspections can also be physical inspections conducted by boarding parties.

In order to close the surveillance gaps that are not covered by the AIS and the current land-based systems of CSRs and EO/IR sensors, the littoral state has not, but one day might decide to acquire, new surveillance assets. The ideal surveillance system for this congested strait should not only be multi-spectral, which includes radar, optical and infrared sensing, but should also consist of mobile sensor platforms to overcome the short detection ranges for small vessels and blind zones.

In this analysis, the three types of surveillance platforms that are considered by the littoral state to enhance its land surveillance capabilities are UAVs, USVs and/or PCs. The unmanned platforms are controlled from a command and control (C2) center situated on the mainland. Line-of-sight communications between the C2 center and the unmanned platforms are maintained throughout the strait via a network of transmitters and relay stations located along the coast. The C2 center will coordinate all surveillance efforts by the manned and unmanned platforms in order to achieve the most effective coverage. All three types of surveillance platforms will be equipped with short-range surface radar and EO/IR systems. The radars complement the CSRs in providing coverage in blind zones or in a high-

clutter environment where short-range radar generally has better resolution. Through the use of high-resolution EO/IR systems on the surveillance platforms, the C2 center can conduct detailed and close-up visual inspections on vessels. Under reduced visibility conditions, the mobile sensors can move closer to the targets, something land-based systems cannot do. Finally, in order to generate a coherent situational picture, fusion of all information collected by both land-based and mobile sensors will be necessary. Data fusion of a surveillance system with multiple sensors is complex and is subjected to error and delay, but there are also proposed solutions to address them (Efe, Yilmaz, & Dura Donmez, 2005).

In terms of speed and maneuverability, the UAV is typically three to four times faster than the USV or PC (about 100-120kts compared with 30-40kts). Having greater speed, the UAV will spend less time transiting from one target to another. As an airborne platform, it can quickly conduct an all-around inspection of its target and allow the C2 center to see behind large obstacles that may conceal SB threats. Downward-looking air-borne sensors also have fewer blind zones. As a result, the UAV can expeditiously survey a large area and reduce the risk of overlooking small targets. The EO/IR sensors on the UAV give a plain view of the exposed decks of a vessel that may not be possible for upward- or level-looking sensors on a surface platform. This non-invasive inspection capability, to some extent, allows authorities to ascertain normality of the onboard activities of the vessel. This type of information is useful in assessing the classification of targets. VTOL UAVs, such as the Northrop-Grumman's

Firescout (RQ-8B) [see Figure 2(a)] and DARPA's A160 HummingBird, have the added advantage of having the capability to hover. A hovering VTOL UAV will require less airspace, both horizontally and vertically, when it has to focus continuously on a target.

(a)

(b)

Figure 2. Examples of unmanned platforms. (a) The Firescout UAV with EO/IR camera. (Picture taken from Northrop Grumman website.) (b) The Protector USV with radar, EO/IR camera, and small caliber weapon. (Picture taken from Rafael website).

The USV will be a small and remotely controlled surface vessel, like the Rafael Protector [see Figure 2(b)]. Although the radar on the USV has a short detection range, it can still be used to cover CSRs' radar blind spots or shadow zones, especially for the detection of small vessels. Besides a sensor payload of radars and EO/IR cameras, the USV can also be equipped with searchlights and public address systems, and it can be armed with small caliber weapons. One key advantage that the USV has over the manned platform is that crew safety is guaranteed when operating unmanned surveillance assets. The USV may not be as fast or maneuverable as the UAV, but it can go up close to a SB to observe the activities onboard, and if necessary, the C2 center can give instructions through its public address system. The public address system can be used to interrogate suspicious small vessels and instruct them to carry out specific actions, such as proceeding out of the strait. By doing so, it may coax them to reveal their true intentions.

The manned platform is in the form of a small PC and it has an organic boarding team. It has similar surveillance capabilities as the USV, except that its boarding team can carry out physical inspections onboard a vessel. In certain circumstances, boarding and inspecting a vessel is necessary to ascertain the legitimacy of the crew, such as detecting a hijacked vessel.

D. SCOPE OF THE THESIS

The following is the scope of this thesis:

First, the two key types of maritime terrorism threats, LSs and SBs, will be examined individually. For each of them, a CONOPS will be developed with the purpose of detecting the threat among the other neutral shipping in the environment of a congested strait. The CONOPS will specifically involve using a mix of UAV, USV, and PC.

Second, analytical mathematical models are developed to model the CONOPS and used to estimate the required platform mix to achieve a probability at least 0.9 for the detection of a threat. The models will be solved[4] numerically using MATLAB.

Third, the computed results from the models will be analyzed to develop insights that aid decision-making on the force structuring of a cost-effective ORBAT mix of sensor platforms.

E. THESIS FLOW

Chapter II presents the CONOPS for the surveillance of the strait against the two specific threats considered in this thesis. Based on the CONOPS, analytical models will be developed and presented.

Chapter III covers model exploration and sensitivity analysis discussion of the models.

[4] The codes for solving the models are written by the author.

Chapter IV presents the results from the quantitative evaluation of the mathematical models.

Chapter V consists of a summary of the work done as well as the conclusions developed from this thesis and recommendations for further work.

THIS PAGE INTENTIONALLY LEFT BLANK

II. DESCRIPTION OF MODELS

A simple CONOPS for two types of maritime terrorism (Red) threats will be addressed and developed in this chapter. The threats can be classified as large-sized shipping threats, and small boat (SB) threats; of course not all large or small vessels are threats, but many searches by Blues (Bs) are distracted by benign traffic. Speedy and accurate identification by B is a valuable asset. For the purpose of this thesis, a large ship (LS) is defined as a vessel above 300 gross tons (GT) that carries the IMO-mandated AIS. A SB is defined as a vessel that is below 300 GT and hence does not come under IMO regulations to carry AIS.

The concern in large-sized shipping threats is that a LS that carries hazardous cargo could be hijacked by, or fall under the control of terrorists and used as a floating bomb. Dangerous cargo refers to inflammable and explosive cargo that could be used as fuel for a bomb. The objective of the LS threat would be to ignite the explosive cargo in port or at the dangerous cargo terminals (Bateman 2006). The concern in the SBs threat is the use of SBs in guerilla-style or suicide attacks. These SBs could attempt to disguise themselves to blend into the local small vessel traffic, for example pretending to be local fishing boats. The objective of the SB threat is to deliver and detonate an explosive payload to a high-value target berthed in the harbor or transiting the strait.

Generally there are fundamental differences in the behaviors of LSs and SBs in the strait. Large merchant

ships are required to transit in designated shipping lanes according to the local maritime rules for navigation safety. They typically want to get to their destinations expeditiously to meet commercial deadlines. They are also required to transmit signal via IMO-mandated AIS to identify themselves. Hence, LSs typically enter the strait and proceed in the most direct and allowable route to their destinations (either the port or to the exit of the strait at the other end) in a predictable manner. LSs can be easily tracked by their AIS reports. Therefore, if a LS were to behave suspiciously by not conforming to the traffic rules, it would be easily picked out from the other shipping. If a LS threat were to conform to the behavior of the general shipping patterns, the only way that its possible ill intent can be discovered is by boarding for inspection.

The SBs do not have such predictable behaviors. Their movements in the strait are not as well regulated and they do not typically follow well-defined shipping lanes. Some of them, such as fishing boats, loiter in an area within the strait for a certain period of time when engaging in their activities. Though the SBs are not required under IMO regulations to be equipped with AIS, the local maritime authority could mandate that those registered in their state carry similar identification systems. SBs registered in other states using this international strait may ignore this requirement.

As a result of the differences between the LS and SB threats, they will be considered separately and different CONOPS will be developed for each of these threats.

A. CONOPS FOR LS THREATS

1. Strait Traffic Management

For navigational safety, all LSs entering the strait conform to a standard reporting procedure. They report to the littoral state Vessel Traffic Service (VTS) authorities when entering and leaving the straits.

When a vessel reports in, the Vessel Traffic Information System (VTIS) starts tracking the vessel, and its passage will be monitored continuously until it leaves the strait. An advantage of reporting in is that the vessels will be provided with traffic and navigational information to assist them in navigating safely through the strait.

The VTIS gets information on the traffic condition from the coastal radars, the AIS reports and the vessels' reports. The system of coastal radars provides complete radar coverage of the entire strait, including information on a vessel's location, course and speed, but it does not provide information on a vessel's identity. The AIS complements the coastal radars by automatically providing a vessel's identity and position. The AIS transmits the vessel's position, heading and speed at 10-second intervals. The information on vessel identity is transmitted every six minutes, according to U.S. Coast Guard Navigation Center (2007).

2. Threat Scenario

The threat scenario that is examined in this thesis is common amongst many coastal states especially after the 9/11 terrorist attacks in the U.S. The main concern is that terrorists will attempt to use vessels carrying dangerous cargoes as weapons to cause harm to the vulnerable human population or to valuable properties. In this scenario, terrorists hijack a vessel carrying dangerous cargoes and attempt to blow it up in the harbor or to ram it into a berthed or anchored vessel, such as a cruise liner or navy warship.

The types of vessels that are likely to cause damage akin to the devastation of 9/11 in such a scenario are those that carry dangerous cargoes such as liquefied natural gas (LNG) and chemicals. Henceforth, vessels carrying dangerous cargoes will be known as D-vessels. However, not all will be boarded by Reds.

It is assumed that, if successfully boarded, a D-vessel is covertly hijacked outside the strait. It is further assumed that only the crew of the D-vessel knows that the vessel has been hijacked. The hijacked D-vessel attempts to continue its passage into the strait and ultimately into the port. The hijackers will attempt to avoid detection by complying with all required VTS protocols until they reach a suitable position to execute their plan of attack.

3. CONOPS for Detection of Hijacked D-Vessels

It is extremely difficult to detect a hijacked D-vessel (called Red vessel henceforth) with merely standoff surveillance by UAV and radar, transiting under the false pretence of being a legitimate merchant. The UAV, radars, and AIS can provide information on identity and position, but would never be able to reveal the true intent of the hijackers. As a result, the detection of such vessels requires verification of the intent of D-vessels, which is only possible with onboard inspection of *all* D-vessels and their crews. Hence in this scenario, the boarding parties on the PCs are the primary assets for the detection of Red vessels. The UAVs and USVs are secondary assets because they are unable to conduct onboard inspections but they can be used for first level visual surveillance to complement the AIS. In the case where the VTIS is not receiving any information from the AIS of a particular vessel, the UAVs or USVs can be used to seek out its identity.

All D-vessels transiting through the strait, including those that are not calling at the (B) port, can be potential targets of the hijackers. However, there are a large number of them and boarding to inspect all of them would be impractical and cause delays to the traffic flow in the strait. The littoral state (B) decides that only D-vessels that are scheduled to call at the port will be considered for boarding and inspection. The risk of terrorists using one of the other D-vessels, which are transiting the strait but not calling at the port, will have to be mitigated by other measures and will not be considered in this thesis. One such measure could be

deterrence through the random escorting of the pass-through D-vessels.

A D-vessel calling at the port will enter the strait from either the east or west end of the strait. As long as a PC is available, a D-vessel can be boarded at any point from the entrance of the strait to the entrance of the port. A boarded D-vessel continues to proceed toward the entrance of the port but is only allowed to pass through the entrance of the port when the inspection is completed and the D-vessel has been certified "safe". A "safe" D-vessel is one that has not been hijacked. Upon completion of an inspection, the boarding party will go back to the PC, and the PC will proceed to the next available D-vessel that has not been inspected. If the inspection is not been completed by the time the D-vessel reaches the entrance of the port, the D-vessel will be held in a holding area (near the entrance of the port) until the inspection is completed by other personnel.

B. LS MODEL DETECTION OF HIJACKED D-VESSELS BY PCs

In the formulation of the analytical model, several assumptions about the D-vessels are made. All D-vessels that call at the port are assumed to be the hijackers' potential target will have to be boarded and inspected. Any D-vessel that is identified as the Red vessel is assumed to be apprehended by a response force, and the terrorist act thereby averted. Due to the time taken for post-detection response actions, such as sending special forces to storm the hijacked ship, the hijacked D-vessel must be detected

at the time when it first enters the strait. Post-detection response actions will not be modeled in this study.

1. Formulation

The model will be formulated in two parts. In the first part, the movements of D-vessels in the strait and the process of PCs conducting boarding and inspection on the D-vessels are modeled as a deterministic "fluid" model. A representation of the sequence of events in the CONOPS against LS threat is displayed in Figure 3. The objective of this deterministic fluid model is to reveal the long run mean number of D-vessels that are not inspected by PCs and the long run mean number of PCs that are engaged in the boarding and inspection process. These measures will be the inputs to the second part of the model that will determine the probability of detection of a single Red vessel.

The portion of the strait from one end of the strait to the entrance of the port, called domain S, will be divided along the direction of transit into equally sized sub-regions, $S_i, i \in \{1, 2, ..., n\}$. A D-vessel enters the strait by entering into the sub-region, S_1, and moves towards the port by moving from S_1 to S_2 until S_n. From S_n, the D-vessel will proceed into port (see Figure 4). The mean time D-vessels spend in each sub-region is assumed to be the same for all sub-regions.

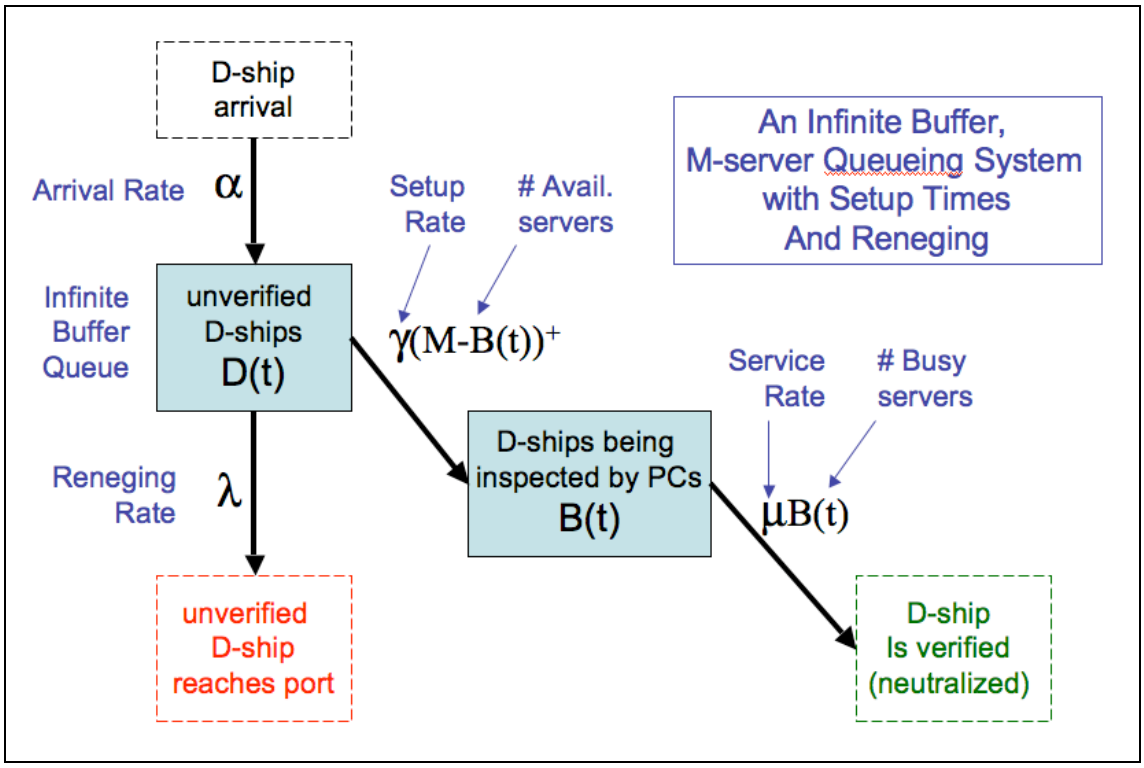

Figure 3. A schematic flow diagram of the sequence of events for a LS model (From Gaver, Jacobs, Chng and Alderson 2007)

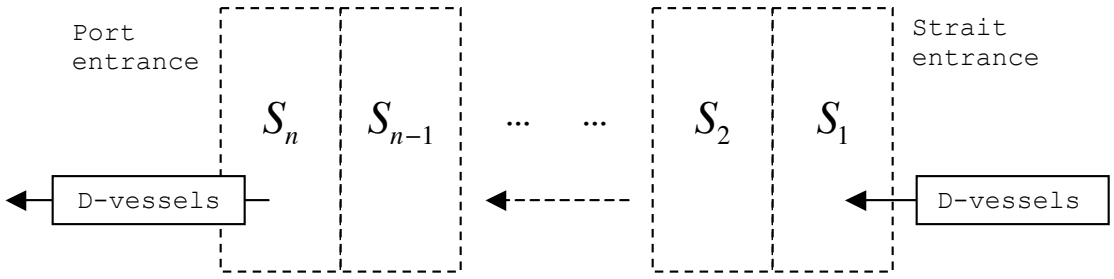

Figure 4. Schematic diagram of the domain S and the movement of the D-vessels through the sub-regions.

The boarding and inspection process by the PCs will be divided into a series of m service time periods. Each service time period is assumed to have the same length. Upon completion of an inspection, the PC will choose the

next D-vessel to be inspected at random. Each un-inspected D-vessel is equally likely to be chosen for inspection.

2. State Variables

Let

$D_i(t)$ = Number of D-vessels in sub-region i that have not been inspected at time t, where $i = 1, \ldots, n$;

$B_j(t)$ = Number of PCs that are busy with j periods of service time remaining at time t, where $j = 1, \ldots, m$.

3. Parameters

Let

M = Number of PCs active in the region (strait);

n = Number of sub-regions in the strait;

m = Number of service time periods in a boarding and inspection process; the first service period for a PC is labeled the m^{th}; the final service period for a PC is labeled 1.

$\frac{1}{\lambda}$ = Mean time a D-vessel spends in each sub-region and is available for inspection (before it reaches the adjacent sub-region);

$\frac{1}{\mu}$ = Mean time in each service time period during which boarding teams from a PC board and inspect a D-vessel;

$\frac{1}{\gamma}$ = Mean time for one idle[5] PC to travel to a D-vessel; and

α = Arrival rate of D-vessels to the region.

4. Equations for Part I Time-Dependent "Fluid" Formulation

For each sub-region, a differential equation is used to represent the rate of change of the mean number of un-inspected D-vessels.

$$\frac{dD_1(t)}{dt} = \alpha - \underbrace{\lambda D_1(t)}_{\substack{\text{Mean number of D-vessels to leave sub-region 1 uninspected}}} - \underbrace{\gamma \underbrace{\left[M - \sum_{j=1}^{m} B_j(t) \right]^{+}}_{\text{Number of idle PCs}} \underbrace{D_1(t)}_{\substack{\text{Mean number of uninspected D-vessels in sub-region 1}}}}_{\text{Mean number of inspected D-vessels in region 1 during } (dt)} \qquad (2.1)$$

[5] An idle PC is one that is currently not engaged in the process of boarding and inspection.

$$\frac{dD_i(t)}{dt} = \underbrace{\lambda D_{i-1}(t)}_{\substack{\text{Mean number of D-vessels entering sub-region } i \text{ uninspected}}} - \underbrace{\lambda D_i(t)}_{\substack{\text{Mean number of D-vessels leaving sub-region } i \text{ uninspected}}} - \gamma \underbrace{\left[M - \sum_{j=1}^{m} B_j(t) \right]^+}_{\text{Mean number of idle PCs}} \underbrace{D_i(t)}_{\substack{\text{Mean number of D-vessels in sub-region } i}} \qquad \forall\, i = 2, \ldots, n$$

(2.2)

where $x^+ = x$ if $x \geq 0$ and $x^+ = 0$ if $x<0$.

For each PC service time period, a differential equation is used to represent the rate of change in the mean number of busy PCs.

$$\frac{dB_m(t)}{dt} = \underbrace{-\mu B_m(t)}_{\substack{\text{Mean number of PCs completing service period } m}} + \underbrace{\gamma \left[M - \sum_{j=1}^{m} B_j(t) \right]^+ \sum_{i=1}^{n} D_i(t)}_{\substack{\text{Mean number of free PCs approaching an uninspected D-vessel}}} \qquad (2.3)$$

$$\frac{dB_j(t)}{dt} = \underbrace{-\mu B_j(t)}_{\substack{\text{Mean number of PCs completing service period } j}} + \underbrace{\mu B_{j+1}(t)}_{\substack{\text{Mean number of PCs completing service period } j+1}} \qquad \forall\, j = 1, \ldots, m-1 \qquad (2.4)$$

where $x^+ = x$ if $x>0$ and $x^+ = 0$ if $x<0$.

Equations (2.1) to (2.4) are subject to boundary conditions so that the following conditions are true:

$$0 \leq \sum_{j=1}^{m} B_j(t) \leq M \quad \text{and} \quad D_i(t) \geq 0, \quad \forall\, i = 1, \ldots, n.$$

Equations (2.1) to (2.4) are solved numerically using implementation of the Euler method in MATLAB to determine the limits of $D_i(t)$ and $B_j(t)$ when $t \to \infty$. These limits are the long run expected number of un-inspected D-vessels in i^{th} sub-region and the long run expected number of PCs that are engaged in the j^{th} service period, respectively. They are then used in the equations in Part II for the computation of the probability of detection.

5. Equations for Part II Probability of Detection When Inspection Process is in Steady State

This part of the model determines the probability that a single Red vessel (***R***), is boarded and inspected by a PC before the ***R*** enters the port.

D-vessels scheduled to call in at the port arrive at the strait at anytime throughout the day and there is no "time-of-day" effect. When ***R*** enters the strait, the number of un-inspected D-vessels in the strait, ***D***, is assumed to have a Poisson distribution with a mean of $\bar{D} = \lim_{t\to\infty} \sum_{i=1}^{n} D_i(t)$.

The number of PCs that are busy boarding and inspecting a D-vessel when ***R*** arrives is assumed to have a Binomial distribution with the number of trials equal to the number of PCs, M, and the mean $\bar{B} = \lim_{t\to\infty} \sum_{j=1}^{m} B_j(t)$; an estimate of the probability a PC is idle is $p = \frac{M - \bar{B}}{M}$. An idle PC chooses the next ship to be inspected from among

the ***D*** un-inspected ships or the ***R*** at random; each ship is equally likely to be chosen. Let K be the event in which ***R*** is inspected. It is assumed that ***R*** will only be inspected if at least one PC is idle at ***R***'s arrival time and one of the idle PCs chooses to inspect ***R***. If the number of idle PCs exceeds ***D*** when ***R*** arrives, then ***R*** will be inspected. The probability of the event, K, is

$$P(K) = \sum_{r=1}^{M} \underbrace{\binom{M}{r} p^r \left[1-p\right]^{M-r}}_{\text{Probability at least one PC is idle}} \left[\underbrace{\sum_{k=0}^{r-1} e^{-\bar{D}} \frac{\bar{D}^k}{k!}}_{\substack{\text{Probability there are fewer} \\ \text{than } r \text{ D-vessels} \\ \text{uninspected}}} + \sum_{k=r}^{\infty} e^{-\bar{D}} \frac{\bar{D}^k}{k!} \underbrace{\left[1-\left(\frac{k-(r-1)}{k+1}\right)\right]}_{\substack{\text{Probability R is} \\ \text{chosen for inspection} \\ \text{(sampling without} \\ \text{replacement)}}} \right]$$

$$= 1-\left[1-p\right]^M - \sum_{r=1}^{M} \binom{M}{r} p^r \left[1-p\right]^{M-r} \left[\sum_{k=r}^{\infty} e^{-\bar{D}} \frac{\bar{D}^k}{k!} \left(1-\frac{r}{k+1}\right) \right]$$

$$= 1-\left[1-p\right]^M$$

$$-\sum_{r=1}^{M} \binom{M}{r} p^r \left[1-p\right]^{M-r} \left[1-\sum_{k=0}^{r-1} e^{-\bar{D}} \frac{\bar{D}^k}{k!} \right]$$

$$+\sum_{r=1}^{M} \binom{M}{r} p^r \left[1-p\right]^{M-r} r \frac{1}{\bar{D}} \left[1-\sum_{k=0}^{r} e^{-\bar{D}} \frac{\bar{D}^k}{k!} \right]$$

(2.5).

6. Measure of Effectiveness (MOE)

The MOE for the LS model is the probability of detecting just one Red vessel given there are a certain number of PCs in the strait.

C. CONOPS FOR SBs THREATS

1. SB Traffic Management in the Strait

The littoral state utilizes a series of CSRs and mobile radars on its UAVs, USVs, and PCs to provide radar coverage for the entire strait. It can detect most SBs in the strait, but the present radar system is unable to provide identification of them.

To circumvent this problem, the littoral state has mandated that all SBs registered in the state be equipped with automatic identification devices similar in function to the IMO mandated AIS. However, other SBs in the strait that are not registered in the littoral state are not required to carry such a device.

When a SB in the strait is detected and identified, it is tagged in the VTIS. Once a SB is tagged, the VTIS has information of its location and identification. It remains tagged as long as one of the sensors (coastal radar, PC, USV, or UAV) continues to track it; otherwise it is considered "lost." When a SB that is "lost" is re-detected by a sensor, it is treated as a new detection. A tagged SB is not known to be armed/hostile/Red without further investigation.

2. Threat Scenarios

The hostile SB's (called Red boat) aim and goal is to get within range of a High Value Target (HVT) which is either berthed in the littoral state's (called Blue) harbor or transiting Blue's strait. Once within range of the HVT,

the Red boat will detonate explosives. Two possible SB threat scenarios will be addressed in this thesis.

In the first scenario, the Red boat waits outside the strait at an ambush location for an opportunity to attack the HVT in the strait or harbor. The Red boat is not subjected to Blue's surveillance when it is outside of Blue's strait. At the time of attack, the Red boat will breach Blue's waters in an attempt to reach or intercept the HVT within the shortest time by proceeding at high speed.

In the second scenario, the Red boat conceals its intention to attack an HVT until the very last minute. Red boat could disguise itself to blend in with legitimate SB traffic in the strait. Red boat could also wait outside the strait at an ambush location for the opportunity to attack the HVT in the strait or harbor. While proceeding toward the HVT for the attack, the Red boat will attempt to keep a low signature by proceeding at an inconspicuous speed, usually quite slowly. In both situations, Red boat's intention is to remain innocuous until the time of attack.

3. A CONOPS for Detection of SB Threat

The CSRs and land-based EO/IR systems, complemented by the mobile sensors, are the primary means for the detection of SBs in the strait. In addition, the PCs, USVs, and UAVs are used to conduct preliminary investigations and provide identification of the SBs. This level of inspection (Type I) classifies the SBs as either friendly, neutral, or suspicious. When Type I inspection determines that a SB is

suspicious, only a PC or a USV is able to determine if it is a threat through a Type II inspection. Type II inspections require the personnel on the PC to conduct boarding operations. A Type II inspection for a USV has personnel situated at the C2 center ashore to communicate with personnel on the SB using a public address system on the USV. If the suspicious SB is detected by the UAV, the next available PC or USV will be tasked to investigate it. In such situations, the UAV will continue to monitor the SB until the arrival of the PC or USV. PCs and USVs engaged in Type I inspections can be reassigned to conduct Type II inspections on another suspicious SBs. PCs that are used in the inspection of SBs differ from those used in the inspection of large dangerous vessels. Once a SB is determined to be a threat, resources for subsequent response actions are readily available.

When the VTIS loses track of a previously tagged SB, all information on the vessel is considered lost. Track loss occurs when none of the radars is able to continue tracking a SB; this can happen in two ways. First, track loss can occur when the SB exits the CSR coverage, which in our model means leaving the strait. Second, track loss of SBs that are within the CSR surveillance can result from other factors, such as the environmental clutter of rain and land. If the same SB is subsequently re-detected, it is treated as a new target, and is subjected to the same inspection process again.

In the first SB threat scenario, once the Red boat is in the strait it will be considered suspicious because of its high speed. Any available Blue USVs or PCs immediately

subjects the Red boat to inspection. The time available for Blue to start investigating the Red boat is short. The Red boat will be considered detected if it is subjected to inspection by a USV or PC before it reaches its target.

In the second SB threat scenario the Red boat can be detected in two ways. First, it must be subjected to Type I inspection, classified as suspicious, and then subjected to a Type II inspection before it commences attack. Second, if it is not inspected before it commences attack, then the situation essentially becomes the first threat scenario with a shorter reaction time for Blue.

D. SB MODEL DETECTION OF SB THREAT BY PCs, USVs, AND UAVs

It is assumed that the SBs are dispersed uniformly throughout the strait. Because of airspace restriction in the strait, a maximum of two UAVs can operate simultaneously there. Since the PCs and USVs essentially perform the same function, for the purpose of this model they are treated as the same entity and collectively referred to as USVs henceforth in this formulation.

1. Formulation

The model will be formulated in two parts. In the first part, the states of SBs in the strait (also referred to as region) and the processes of Type I and II inspections of the SBs are modeled as a deterministic fluid model. A schematic representation of the sequence of events for the CONOPS against the SB threat is displayed in Figure

5. The objective of this is to study the long-run mean number of un-identified SBs and the long-run mean number of USVs and UAVs that are engaged in the inspection processes. These measures are the inputs to the second part of the model that determine the probability of detection of a single Red boat.

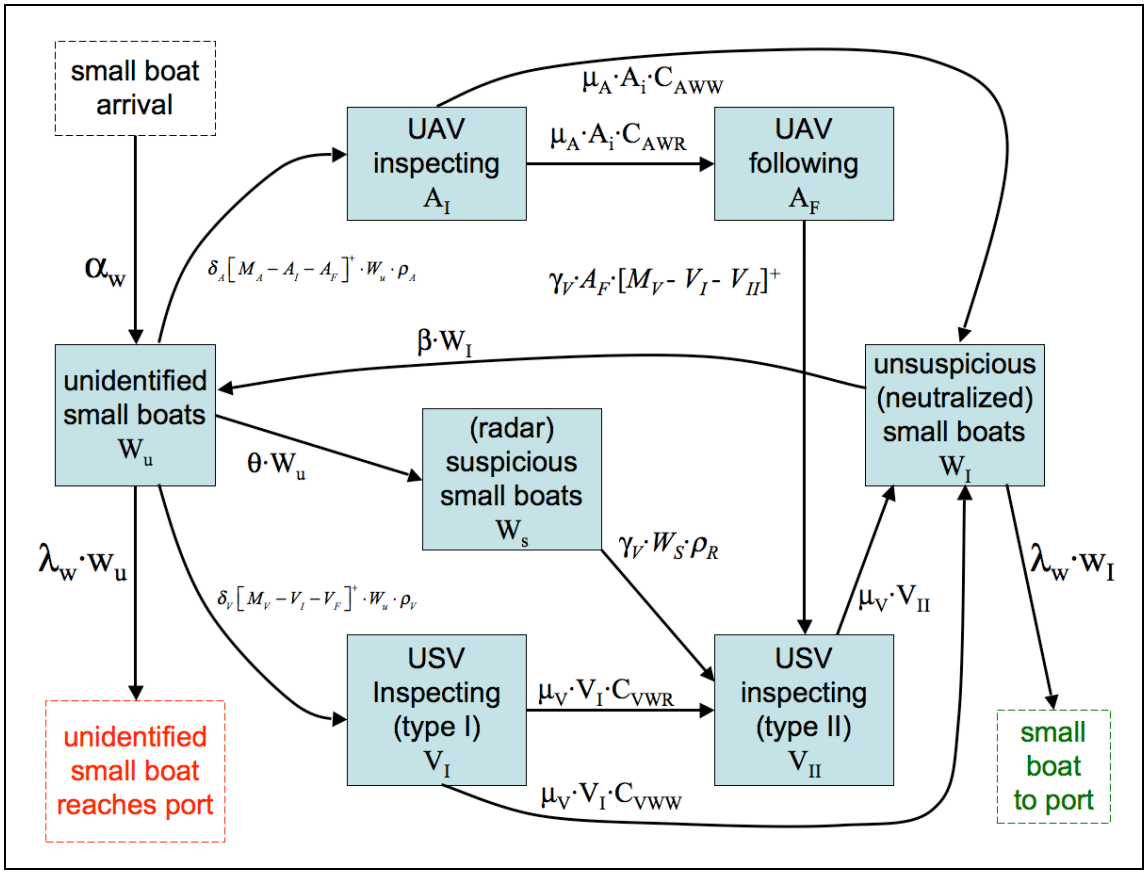

Figure 5. A schematic flow diagram of the sequence of events for a SB model[6] (From Gaver, Jacobs, Chng and Alderson 2007).

[6] ρ_A and ρ_V are factors concerning priority in inspection which are functions of κ_A and κ_V as presented in Section 3 on model parameters.

2. State Variables

Let

$W_U(t)$ = Mean number of unidentified SBs that are not suspicious at time t;

$W_S(t)$ = Mean number of unidentified suspicious SBs at time t;

$W_I(t)$ = Mean number of identified SBs at time t;

$A_I(t), (\text{respectively}, V_I(t))$ = Mean number of platforms engaged in identifying SB (one on one) at time t (Type I inspection) for UAV or respectively USV;

$V_{II}(t)$ = Mean number of USVs engaged in investigating a suspicious SB at time t (Type II inspection); and

$A_F(t)$ = Mean number of UAVs shadowing suspicious SBs (one on one) at time t (which is equal to the number of suspicious SBs being followed by a UAV).

3. Parameters

α_W = Arrival rate of SBs into the region/strait;

$\frac{1}{\lambda_W}$ = Mean time a SB remains in the region/strait;

p_{SS} = Probability that a SB will act suspiciously before it leaves the region. Assume that the time a SB remains in the region and the time an unidentified SB

remains unsuspicious before becoming suspicious are independent and exponentially distributed with means of $\frac{1}{\lambda_W}$ and $\frac{1}{\theta}$, respectively; then $p_{SS} = \frac{\theta}{\theta + \lambda_W}$. The value of θ is chosen so that the equation is satisfied for given values of λ_W and p_{SS}. A SB may become suspicious after leaving the region, but it is outside the B's surveillance area, and is ignored.

$\frac{1}{\beta}$ = Mean time identified SBs remain tracked by the surveillance system (CSRs, UAVs, and USVs);

$\frac{1}{\mu_A}, \left(\text{respectively}, \frac{1}{\mu_{V,I}} \right)$ = Mean time taken to classify a SB as harmless or suspicious (Type I inspection) by UAV or respectively, USV;

$\frac{1}{\mu_{V,II}}$ = Mean time taken by a USV to classify if a suspicious SB is a threat (Type II inspection);

$\frac{1}{\delta_A}, \left(\text{respectively}, \frac{1}{\delta_V} \right)$ = Mean time taken to proceed to an unidentified SB by an idle UAV or respectively, USV. See Appendix A for estimation method;

$\frac{1}{\gamma_V}$ = Mean time taken to proceed to a suspicious SB by an idle USV (if followed by UAV or identified by shore assets). See Appendix A for estimation method;

$M_A, (\text{respectively}, M_V)$ = Number of UAV (respectively USV) platforms active in the region;

$c_{Aww}, (\text{respectively}, c_{Vww})$ = Probability that, during a Type I inspection, a White SB is classified as harmless by a UAV or respectively, USV;

c_{Awr} = Probability that a White SB is misclassified as suspicious by a UAV during a Type I inspection and must be followed until a USV arrives to complete a Type II inspection;

c_{Vwr} = Probability that, during a Type I inspection, a White SB is classified as suspicious by a USV, and must undergo a Type II inspection.

$c_{Arr,} (\text{respectively}, c_{Vrr})$ = Probability that the Red boat is classified correctly by a UAV or respectively, USV;

$\kappa_A, (\text{respectively}, \kappa_V)$ = A decision parameter the larger κ_A or κ_V, the more likely an idle UAV or respectively, USV, will investigate an unidentified suspicious SB rather than an unsuspicious SB;

κ_{VS} = A decision parameter the smaller κ_{VS}, the more likely a USV engaged in a Type I investigation will be reassigned to an unidentified suspicious SB; and

$\tau_A, (\text{respectively } \tau_V \text{ and } \tau_{VS})$ = A model tuning factor applied with the decision parameter κ_A (respectively κ_V and κ_{VS}). The larger $\tau_A, (\text{respectively } \tau_V \text{ and } \tau_{VS})$, the more quickly will Blue concentrate on suspicious SBs.

4. Equations for Part I Dynamic Evaluation of States

The following system of differential equations represents the change dynamics of the mean number of SBs in their respective states over time. Note that many/all "parameters" may be time-dependent, allowing the modeling of arrival surges.

$$\frac{dW_U(t)}{dt} = \underbrace{\alpha_W}_{\substack{\text{Arrival}\\ \text{of}\\ \text{SBs}}} + \underbrace{\beta W_I(t)}_{\substack{\text{Mean}\\ \text{number}\\ \text{of}\\ \text{ID'd}\\ \text{SBs}\\ \text{lost}\\ \text{from track}}} - \underbrace{\lambda_w W_U(t)}_{\substack{\text{Mean}\\ \text{number of}\\ \text{unID'd}\\ \text{SBs}\\ \text{that}\\ \text{leave}\\ \text{region}}} - \underbrace{\theta W_U(t)}_{\substack{\text{Mean number}\\ \text{of}\\ \text{unID'd}\\ \text{SBs}\\ \text{that}\\ \text{act}\\ \text{suspicious}}}$$

$$\underbrace{-\left\{\delta_A\left[M_A - A_I(t) - A_F(t)\right]^+\right\}\left[e^{-\kappa_A\left(\frac{W_S(t)}{W_U(t)}\right)^{\tau_A}}\right]W_U(t)}_{\text{Mean number of idle UAVs that approach unID'd SBs}}$$

$$\underbrace{-\left\{\delta_V\left[M_V - V_I(t) - V_{II}(t)\right]^+\right\}\left[e^{-\kappa_V\left(\frac{W_S(t)}{W_U(t)}\right)^{\tau_V}}\right]W_U(t)}_{\text{Mean number of idle USVs that approach unID'ed SBs}} \qquad (2.6)$$

$$\underbrace{+\left\{\gamma_V V_I(t)\right\}\left[e^{-\kappa_{VS}\left(\frac{\left[M_V - V_I(t) - V_{II}(t)\right]^+}{V_I(t)}\right)^{\tau_{VS}}}\right]\left[W_S(t) + A_F(t)\right]}_{\substack{\text{Mean number of USVs engaged in Type I inspection that are reassigned}\\ \text{to unID'd suspicious SBs and suspicious}\\ \text{SBs being followed by UAV}}}$$

where $x^+ = x$ if $x \geq 0$ and $x^+ = 0$ if $x<0$.

$$\frac{dW_S(t)}{dt} = \underbrace{\theta W_U(t)}_{\substack{\text{Mean number of unID'd SBs that are detected by shore-based radar as acting suspicious}}} - \underbrace{\lambda_w W_S(t)}_{\substack{\text{Mean number of suspicious unID'd SBs that leave the region}}}$$

$$-\underbrace{\left\{\delta_A\left[M_A - A_I(t) - A_F(t)\right]^+\right\}\left[1 - e^{-\kappa_A\left(\frac{W_S(t)}{W_U(t)}\right)^{\tau_A}}\right]W_S(t)}_{\text{Mean number of idle UAV that approach unID'd suspicious SBs}} \qquad (2.7)$$

$$-\underbrace{\left\{\gamma_V\left[M_V - V_I(t) - V_{II}(t)\right]^+\right\}\left[1 - e^{-\kappa_V\left(\frac{W_S(t)}{W_U(t)}\right)^{\tau_V}}\right]W_S(t)}_{\text{Mean number of idle USVs that approach unID'd suspicious SBs}}$$

$$-\underbrace{\left\{\gamma_V V_I(t)\right\}\left[e^{-\kappa_{VS}\left(\frac{\left[M_V - V_I(t) - V_{II}(t)\right]^+}{V_I(t)}\right)^{\tau_{VS}}}\right]W_S(t)}_{\substack{\text{Mean number of USVs engaged in Type I inspection}\\ \text{that are reassigned to unID'd suspicious SBs}}}$$

$$\frac{dW_I(t)}{dt} = \underbrace{-\beta W_I(t)}_{\substack{\text{Mean number of ID'd SBs lost from track}}} - \underbrace{\lambda_w W_I(t)}_{\substack{\text{Mean number of ID'd SBs that leave region}}}$$
$$+ \underbrace{\mu_A A_I(t) c_{Aww}}_{\substack{\text{Mean number unsuspicious SBs ID'd by UAV}}} + \underbrace{\mu_{VI} V_I(t) c_{Vww}}_{\substack{\text{Mean number unsuspicious SBs ID'd by USV}}} + \underbrace{\mu_{VII} V_{II}(t)}_{\substack{\text{Mean number suspicious SBs ID'd by USV}}} \quad (2.8)$$

The following set of differential equations represents the change dynamics of the mean number of UAVs in their respective states over time.

$$\frac{dA_I(t)}{dt} = \underbrace{\left\{\delta_A\left[M_A - A_I(t) - A_F(t)\right]^+\right\}\left[e^{-\kappa_A\left(\frac{W_S(t)}{W_U(t)}\right)^{\tau_A}}\right] W_U(t)}_{\text{Mean number of UAVs that approach unknown SBs for ID}}$$
$$- \underbrace{\mu_A A_I(t)}_{\substack{\text{Mean number of UAVs that complete Type I inspection}}} - \underbrace{\lambda_W A_I(t)}_{\substack{\text{Mean number of unsuspicious SBs that leave region}}} \quad (2.9)$$

$$\frac{dA_F(t)}{dt} = \underbrace{\mu_A A_I(t) c_{Awr}}_{\substack{\text{Mean number of UAVs following SBs that UAVs classified as suspicious and require Type II inspection}}}$$

$$+\underbrace{\left\{\delta_A\left[M_A - A_I(t) - A_F(t)\right]^+\right\}\left[1 - e^{-\kappa_A\left(\frac{W_S(t)}{W_U(t)}\right)^{\tau_A}}\right]W_S(t)}_{\text{Mean number of UAVs that follow suspicious SBs until USVs arrive}}$$

$$-\underbrace{\left\{\gamma_V\left[M_V - V_I(t) - V_{II}(t)\right]^+\right\}\left[1 - e^{-\kappa_V\left(\frac{W_S(t)}{W_U(t)}\right)^{\tau_V}}\right]A_F(t)}_{\text{Mean number of idle USVs that arrive at suspicious SBs being followed by UAVs}} \qquad (2.10)$$

$$-\underbrace{\left\{\gamma_V V_I(t)\right\}\left[e^{-\kappa_{VS}\left(\frac{\left[M_V - V_I(t) - V_{II}(t)\right]^+}{V_I(t)}\right)^{\tau_{VS}}}\right]A_F(t)}_{\text{Mean number of USVs engaged in Type I inspection reassigned to suspicious SBs being followed by UAVs}} - \underbrace{\lambda_W A_F(t)}_{\substack{\text{Mean number of suspicious SBs being followed by UAVs that leave region}}}$$

The following set of differential equations represents the change dynamics of the mean number of USVs in their respective states over time.

$$\frac{dV_I(t)}{dt} = \underbrace{\left\{\delta_V\left[M_V - V_I(t) - V_{II}(t)\right]^+\right\}\left[e^{-\kappa_V\left(\frac{W_S(t)}{W_U(t)}\right)^{\tau_V}}\right]W_U(t)}_{\text{Mean number of idle USVs that approach unknown SBs for ID (Type I inspection)}}$$

$$\underbrace{-\left\{\gamma_V V_I(t)\right\}\left[e^{-\kappa_{VS}\left(\frac{\left[M_V - V_I(t) - V_{II}(t)\right]^+}{V_I(t)}\right)^{\tau_{VS}}}\right]\left[W_S(t) + A_F(t)\right]}_{\text{Mean number of USVs engaged in Type I inspections that are reassigned to unID'd suspicious boat and suspicious SBs being followed by UAVs}} \qquad (2.11)$$

$$-\underbrace{\mu_{VI}V_I(t)}_{\substack{\text{Mean number of USVs that complete Type I inspection}}} - \underbrace{\lambda_W V_I(t)}_{\substack{\text{Mean number of suspicious SBs that leave region}}}$$

$$\frac{dV_{II}(t)}{dt} = \underbrace{\mu_{VI} V_I(t) c_{Vwr}}_{\substack{\text{Mean number of USVs that are inspecting (Type II) SBs ID'd as suspicious by USVs}}}$$

$$+\underbrace{\left\{\gamma_V\left[M_V - V_I(t) - V_{II}(t)\right]^+\right\}\left[1 - e^{-\kappa_V\left(\frac{W_S(t)}{W_U(t)}\right)^{\tau_V}}\right] W_S(t)}_{\text{Mean number of idle USVs that approach unID'd suspicious SBs for Type II inspection}}$$

$$+\underbrace{\left\{\gamma_V\left[M_V - V_I(t) - V_{II}(t)\right]^+\right\}\left[1 - e^{-\kappa_V\left(\frac{W_S(t)}{W_U(t)}\right)^{\tau_V}}\right] A_F(t)}_{\text{Mean number of USVs that arrive at suspicious SBs being followed by UAVs}} \qquad (2.12)$$

$$+\underbrace{\left\{\gamma_V V_I(t)\right\}\left[e^{-\kappa_{VS}\left(\frac{\left[M_V - V_I(t) - V_{II}(t)\right]^+}{V_I(t)}\right)^{\tau_{VS}}}\right]\left[W_S(t) + A_F(t)\right]}_{\text{Mean number of USVs engaged in Type I inspection that are reassigned to unID'd suspicious boat and suspicious SBs being followed by UAVs}}$$

$$-\underbrace{\lambda_W V_{II}(t)}_{\substack{\text{Mean number of suspicious SBs that leave region}}} - \underbrace{\mu_{VII} V_{II}(t)}_{\substack{\text{Mean number of USVs that complete Type II inspection}}}$$

Equations (2.6) to (2.12) are subject to the following set of boundary conditions:

$$\begin{cases} W_U(t),\ W_S(t),\ W_I(t) \geq 0 \\ 0 \leq A_I(t) + A_F(t) \leq M_A \\ 0 \leq V_I(t) + V_{II}(t) \leq M_V \end{cases} \qquad (2.13)$$

Equations (2.6) to (2.12) are solved numerically using implementation of the Euler method in MATLAB to determine the limits of the state variables.

5. Equations for Part II-A Probability of Detection for SB Threat Scenario A

In SB threat scenario A, a Red boat (***R***) waits outside the strait at an ambush location for the opportunity to attack the HVT in the strait or harbor. Once ***R*** is in the strait its actions would be similar to those of a suspicious SB and it can be subjected to inspections. A suspicious SB can either be inspected by an idle USV that is not engaged in any type of inspection, or a USV that is reassigned from a Type I to a Type II inspection. It is assumed that ***R*** will only be inspected if at least one USV is available at ***R'***s arrival time and it chooses to inspect ***R***.

Assume the number of unidentified SBs, W_U, and unidentified suspicious SBs, W_S, in the region when ***R*** enters the straits both have Poisson distributions with means that are the steady state means $\bar{W}_U = \lim_{t\to\infty} W_U(t)$ and $\bar{W}_S = \lim_{t\to\infty} W_S(t)$, respectively. An idle USV chooses the next SB to be inspected from among $\bar{W}_S + 1$ suspicious SBs (including ***R***), with probability $p_S = \left\{1 - \exp\left\{-\kappa_V \left(\frac{\left[\bar{W}_S + 1\right]}{\bar{W}_U}\right)^{\tau_V}\right\}\right\}$. Assume the number of USVs (A_V) that are idle and not engaged in any

inspection when ***R*** arrives has a Binomial distribution with number of trials the number of USVs, M_V, and mean $M_V - B_V$, where $B_V = \bar{V}_I + \bar{V}_{II}$ and the steady state values $\bar{V}_I = \lim_{t\to\infty} V_I(t)$ and $\bar{V}_{II} = \lim_{t\to\infty} V_{II}(t)$; the estimate of the probability a USV is idle and available to intercept ***R*** is $p_{AV} = \frac{M_V - B_V}{M_V}$. Assume the number of busy USVs that are engaged in Type I inspections and are reassigned to inspect a suspicious SB when ***R*** arrives $(\boldsymbol{B}_R)$ has an independent Binomial distribution with number of trials the number of busy USVs; the estimate of the probability that a USV is engaged in a Type I inspection and is subsequently reassigned to Type II inspection is $p_{BR} = \frac{\bar{V}_I}{\bar{V}_I + \bar{V}_{II}} p_{VI,R}$; USVs engaged in Type I inspection are reassigned with probability

$$p_{VI,R} = \exp\left\{-\kappa_{VS}\left(\frac{\left[M_V - \bar{V}_I - \bar{V}_{II}\right]^+}{\bar{V}_I}\right)^{\tau_{VS}}\right\}.$$

The joint probability of the number of USV available to inspect suspicious SBs is (assuming independence)

$$P\left(A_V = a, B_R = b\right)$$
$$= \binom{M_V}{a}\left(p_S p_{AV}\right)^a \left(1 - p_S p_{AV}\right)^{M_V - a} \binom{M_V - a}{b}\left(p_{BR}\right)^b \left(1 - p_{BR}\right)^{M_V - a - b} \quad (2.14)$$

for a and b nonnegative integers satisfying $0 \le a + b \le M_V$.

Among the $\bar{W}_S$ suspicious SBs and the ***R***, the next suspicious SB to be investigated is chosen at random; each

unidentified suspicious SB is equally likely to be chosen. Let K be the event in which the ***R*** is inspected. An expression for $P(K)$ appears in (2.15).

$$
\begin{aligned}
&P(K) \\
&= \sum_{a=0}^{M_V} \sum_{b=0}^{M_V - a} \underbrace{P\left(A_V = a, B_R = b\right)}_{\substack{\text{Probability that } a+b \\ \text{USVs are available to} \\ \text{inspect suspicious} \\ \text{small boat}}} \left[\underbrace{\sum_{j=0}^{a+b-1} e^{-\bar{W}_S} \frac{\bar{W}_S{}^j}{j!}}_{\substack{\text{Probability there are} \\ \text{fewer than } a+b \\ \text{suspicious SBs} \\ \text{(including the R)}}} + \sum_{j=a+b}^{\infty} e^{-\bar{W}_S} \frac{\bar{W}_S{}^j}{j!} \underbrace{\left[1 - \left[\frac{j - (a+b) + 1}{j+1} \right] \right]}_{\substack{\text{Probability the R is chosen} \\ \text{for inspection (sampling} \\ \text{without replacement)}}} \right] \\
&= \sum_{a=0}^{M_V} \sum_{b=0}^{M_V - a} P\left(A_V = a, B_R = b\right) \left[1 - \sum_{j=a+b}^{\infty} e^{-\bar{W}_S} \frac{\bar{W}_S{}^j}{j!} \left[1 - \frac{(a+b)}{j+1} \right] \right] \\
&= \sum_{a=0}^{M_V} \sum_{b=0}^{M_V - a} P\left(A_V = a, B_R = b\right) \left[\sum_{j=0}^{a+b-1} e^{-W_S(\infty)} \frac{\bar{W}_S{}^j}{j!} + \frac{a+b}{\bar{W}_S} \left[1 - \sum_{j=0}^{a+b} e^{-W_S(\infty)} \frac{\bar{W}_S{}^j}{j!} \right] \right]
\end{aligned}
\tag{2.15}
$$

Assume that the time ***R*** takes to travel across the region to the target is a random variable, $\boldsymbol{T}_{R,A}$. Given a USVs are idle and b USVs engaged in Type I inspections are reassigned, assume that the USVs that will inspect a suspicious SB each cover a segment of the coast of length $\frac{M_y}{a+b}$, where M_y is the length of the region. The mean time for a USV to approach a suspicious SB is given by

$$
\frac{1}{\gamma_{V,R}(a,b)} = \left(\frac{M_y}{(a+b)2} \right) \left(\frac{1}{v_V} \right) \tag{2.16}
$$

where v_V is the speed of the USV and the USV is assumed to be stationed in the middle its segment of the coast, hence the distance to a suspicious SB is half its segment length.

The conditional probability that a USV reaches ***R*** before ***R*** gets across the region, given $a+b$ USVs are assigned to suspicious vessels is approximated by $E\left[1-\exp\left\{-\gamma_{V,R}(a,b)\boldsymbol{T}_{R,A}\right\}\right]$.

Let K_A be the event in which ***R*** is chosen to be inspected and an idle USV reaches ***R*** before ***R*** gets across the region. An approximation to $P(K_A)$ appears in equation (2.17).

$$P(K_A)$$

$$= \sum_{a=0}^{M_V}\sum_{b=0}^{M_V-a} \underbrace{P(A_V=a,B_R=b)}_{\substack{\text{Probability that } a+b \\ \text{USVs are available to} \\ \text{inspect suspicious SB}}} \left[\sum_{j=0}^{a+b-1} e^{-\bar{W}_S}\frac{\bar{W}_S{}^j}{j!}\underbrace{E[1-\exp\left\{-\gamma_V(a,b)\boldsymbol{T}_R\right\}]}_{\substack{\text{Probability that USVs reach} \\ \text{R before R gets to target} \\ \text{given } a+b \text{ USVs are available}}}\right]$$

$$+\sum_{a=0}^{M_V}\sum_{b=0}^{M_V-a} \underbrace{P(A_V=a,B_R=b)}_{\substack{\text{Probability that } a+b \\ \text{USVs are available to} \\ \text{inspect suspicious SB}}} \left[\frac{a+b}{W_S(\infty)}\left[1-\sum_{j=0}^{a+b} e^{-\bar{W}_S}\frac{\bar{W}_S{}^j}{j!}\right]\underbrace{E[1-\exp\left\{-\gamma_V(a,b)\boldsymbol{T}_R\right\}]}_{\substack{\text{Probability that USVs reach} \\ \text{R before R gets to target} \\ \text{given } a+b \text{ USVs are available}}}\right]$$

(2.17)

6. Equations for Part II-B Probability of Detection for SB Threat Scenario B

In the SB threat scenario B, ***R*** will enter the region and attempt to blend in with or hide among the other unsuspicious SBs for some time T_R. ***R*** then comes out of hiding and is suspicious for a short time until it reaches its target. The Blue forces can detect ***R*** while it is hiding in two ways. If a USV detects and correctly classifies it, ***R*** is neutralized. If a UAV detects it and classifies it as suspicious, ***R*** is neutralized if a USV is available to inspect it. When ***R*** becomes suspicious, ***R*** may be neutralized if at least one USV is not busy with an inspection or is reassigned from a Type I inspection.

Another set of differential equations is used to model the state of ***R*** during the period of time when it attempts to stay hidden.

7. Additional State Variables

Let

$R(t)$ = Mean number of ***R*** that is not inspected at time t, $0 \le R(t) \le 1$. (The probability ***R*** is subjected to Type I inspection at time t is $\left[1 - R(t)\right]$);

$A_{I,R}(t)$ = Mean number of UAVs engaged in attempting to identify ***R*** at time t (Type I inspection);

$A_{F,R}(t)$ = Mean number of UAVs shadowing ***R*** at time t while waiting for available USVs to conduct Type II inspection;

$V_{I,R}(t)$ = Mean number of USVs in process of identifying ***R*** at time t (Type I inspection); and

$V_{II,R}(t)$ = Mean number of USVs engaged in Type II inspection on ***R*** at time$t$.

Let the mean number of busy UAVs at time t be $B_A = A_I(t) + A_F(t) + A_{I,R}(t) + A_{F,R}(t)$.

Let the mean number of busy USVs at time t be $B_V = V_I(t) + V_{II}(t) + V_{I,R}(t) + V_{II,R}(t)$.

8. Differential Equations for Probability of Detection in Scenario B

The following set of equations represents the dynamical development of the SBs in their various states over time.

$$\frac{dW_U(t)}{dt} = \underbrace{\alpha_W}_{\substack{\text{Arrival}\\ \text{of}\\ \text{SBs}}} + \underbrace{\beta W_I(t)}_{\substack{\text{Mean}\\ \text{number}\\ \text{of ID'd}\\ \text{SBs}\\ \text{lost}\\ \text{from track}}} - \underbrace{\lambda_w W_U(t)}_{\substack{\text{Mean}\\ \text{number}\\ \text{of unID'd}\\ \text{SBs that}\\ \text{leave}\\ \text{region}}} - \underbrace{\theta W_U(t)}_{\substack{\text{Mean number}\\ \text{of unID'd}\\ \text{SBs}\\ \text{that act}\\ \text{suspicious}}}$$

$$\underbrace{-\left\{\delta_A\left[M_A - A_I(t) - A_F(t)\right]^+\right\}\left[e^{-\kappa_A\left(\frac{W_S(t)}{W_U(t)+R(t)}\right)^{\tau_A}}\right]\left[\frac{W_U(t)}{W_U(t)+R(t)}\right]W_U(t)}_{\text{Mean number of idle UAVs that approach unID'd SBs, excluding Red}}$$

$$\underbrace{-\left\{\delta_V\left[M_V - B_V(t)\right]^+\right\}\left[e^{-\kappa_V\left(\frac{W_S(t)}{W_U(t)+R(t)}\right)^{\tau_V}}\right]\left[\frac{W_U(t)}{W_U(t)+R(t)}\right]W_U(t)}_{\text{Mean number of idle USVs that approach unID'd SBs, excluding Red}} \qquad (2.18)$$

$$\underbrace{+\left\{\gamma_V\left[V_I(t)+V_{I,R}(t)\right]\right\}\left[e^{-\kappa_{VS}\left(\frac{\left[M_V - B_V(t)\right]^+}{V_I(t)+V_{I,R}(t)}\right)^{\tau_{VS}}}\right]\left[W_S(t)+A_F(t)\right]}_{\substack{\text{Mean number of USVs engaged in Type I inspection that are reassigned}\\ \text{to unID'd suspicious SBs and suspicious}\\ \text{SBs being followed by UAVs}}}$$

where $x^+ = x$ if $x \geq 0$ and $x^+ = 0$ if $x<0$.

$$\frac{dW_S(t)}{dt} = \underbrace{\theta W_U(t)}_{\substack{\text{Mean number of unID'd SBs that are detected by shore-based radar as acting suspicious}}} - \underbrace{\lambda_w W_S(t)}_{\substack{\text{Mean number of suspicious unID'd SBs that leave the region}}}$$

$$\underbrace{-\left\{\delta_A\left[M_A - B_A(t)\right]^+\right\}\left[1 - e^{-\kappa_A\left(\frac{W_S(t)}{W_U(t)+R(t)}\right)^{\tau_A}}\right]W_S(t)}_{\text{Mean number of idle UAVs that approach unID'd suspicious SBs}}$$

$$\underbrace{-\left\{\gamma_V\left[M_V - B_V(t)\right]^+\right\}\left[1 - e^{-\kappa_V\left(\frac{W_S(t)}{W_U(t)+R(t)}\right)^{\tau_V}}\right]W_S(t)}_{\text{Mean number of idle USVs that approach unID'd suspicious SBs}}$$

$$\underbrace{-\left\{\gamma_V\left[V_I(t) + V_{I,R}(t)\right]\right\}\left[e^{-\kappa_{VS}\left(\frac{\left[M_V - B_V(t)\right]^+}{V_I(t)+V_{I,R}(t)}\right)^{\tau_{VS}}}\right]W_S(t)}_{\text{Mean number of USVs engaged in Type I inspection that are reassigned to unID'd suspicious SBs}} \qquad (2.19)$$

$$\frac{dW_I(t)}{dt} = \underbrace{-\beta W_I(t)}_{\substack{\text{Mean number of ID'd SBs lost from track}}} - \underbrace{\lambda_w W_I(t)}_{\substack{\text{Mean number of ID'd SBs that leave region}}} + \underbrace{\mu_A A_I(t) c_{Aww}}_{\substack{\text{Mean number of unsuspicious SBs ID'd by UAV}}} + \underbrace{\mu_{VI} V_I(t) c_{Vww}}_{\substack{\text{Mean number of unsuspicious SBs ID'd by USV}}} + \underbrace{\mu_{VII} V_{II}(t)}_{\substack{\text{Mean number of suspicious SBs ID'd by USV}}} \tag{2.20}$$

The following set of differential equations represents the change dynamics of the mean number of UAVs in their respective states over time.

$$\frac{dA_I(t)}{dt} = \underbrace{\left\{\delta_A\left[M_A - B_A(t)\right]^+\right\}\left[e^{-\kappa_A\left(\frac{W_S(t)}{W_U(t)+R(t)}\right)^{\tau_A}}\right]\left[\frac{W_U(t)}{W_U(t)+R(t)}\right]W_U(t)}_{\substack{\text{Mean number of UAVs that approach an unknown SBs, excluding Red, for ID}}} - \underbrace{\mu_A A_I(t)}_{\substack{\text{Mean number of UAVs that complete Type I inspection}}} - \underbrace{\lambda_W A_I(t)}_{\substack{\text{Mean number of unsuspicious SBs that leave region}}} \tag{2.21}$$

$$\frac{dA_{I,R}(t)}{dt} = \underbrace{\left\{\delta_A\left[M_A - B_A(t)\right]^+\right\}\left[e^{-\kappa_A\left(\frac{W_S(t)}{W_U(t)+R(t)}\right)^{\tau_A}}\right]\left[\frac{R(t)}{W_U(t)+R(t)}\right]R(t)}_{\text{Mean number of UAVs that approach hidden Red for ID}} - \underbrace{\mu_A A_{I,R}(t)}_{\substack{\text{Mean number}\\ \text{of UAVs}\\ \text{that complete}\\ \text{ID of}\\ \text{hidden Red}}} \tag{2.22}$$

$$\frac{dA_F(t)}{dt} = \underbrace{\mu_A A_I(t) c_{Awr}}_{\substack{\text{Mean number of UAVs following SBs that UAVs classified as suspicious and require Type II inspection}}}$$

$$+\underbrace{\left\{\delta_A\left[M_A - B_A(t)\right]^+\right\}\left[1 - e^{-\kappa_A\left(\frac{W_S(t)}{W_U(t)+R(t)}\right)^{\tau_A}}\right]W_S(t)}_{\substack{\text{Mean number of UAVs that follow suspicious SBs, excluding Red, until USVs arrive}}}$$

$$-\underbrace{\left\{\gamma_V\left[M_V - B_V(t)\right]^+\right\}\left[1 - e^{-\kappa_V\left(\frac{W_S(t)}{W_U(t)+R(t)}\right)^{\tau_V}}\right]\left[\frac{A_F(t)}{A_F(t)+A_{F,R}(t)}\right]A_F(t)}_{\substack{\text{Mean number of idle USVs that arrive at suspicious SBs, excluding Red, being followed by UAVs}}} \quad (2.23)$$

$$-\underbrace{\left\{\gamma_V\left[V_I(t)+V_{I,R}(t)\right]\right\}\left[e^{-\kappa_{VS}\left(\frac{\left[M_V - B_V(t)\right]^+}{V_I(t)+V_{I,R}(t)}\right)^{\tau_{VS}}}\right]A_F(t)}_{\substack{\text{Mean number of USVs engaged in Type I inspection reassigned to suspicious SBs, excluding Red, being followed by UAVs}}} - \underbrace{\lambda_W A_F(t)}_{\substack{\text{Mean number of suspicious SBs being followed by UAV that leave region}}}$$

$$\frac{dA_{F,R}(t)}{dt} = \underbrace{\mu_A A_{I,R}(t) c_{Arr}}_{\substack{\text{Mean number of UAVs following hidden Red that UAVs classified as suspicious and require Type II inspection}}}$$

$$\underbrace{-\left\{\gamma_V \left[M_V - B_V(t)\right]^+\right\}\left[1 - e^{-\kappa_V\left(\frac{W_S(t)}{W_U(t)+R(t)}\right)^{\tau_V}}\right]\left[\frac{A_{F,R}(t)}{A_F(t)+A_{F,R}(t)}\right]A_{F,R}(t)}_{\text{Mean number of idle USVs that arrive at hidden Red being followed by UAVs}} \quad (2.24)$$

$$\underbrace{-\left\{\gamma_V \left[V_I(t)+V_{I,R}(t)\right]\right\}\left[e^{-\kappa_{VS}\left(\frac{\left[M_V - B_V(t)\right]^+}{V_I(t)+V_{I,R}(t)}\right)^{\tau_{VS}}}\right]A_{F,R}(t)}_{\substack{\text{Mean number of USVs engaged in Type I inspection reassigned to Red being followed by UAVs}}}$$

The following set of differential equations represents the change dynamics of the mean number of USVs in their respective state over time.

$$\frac{dV_I(t)}{dt}$$

$$= \underbrace{\left\{\delta_V\left[M_V - B_V(t)\right]^+\right\}\left[e^{-\kappa_V\left(\frac{W_S(t)}{W_U(t)+R(t)}\right)^{\tau_V}}\right]\left[\frac{W_U(t)}{W_U(t)+R(t)}\right]W_U(t)}_{\text{Mean number of idle USVs that approach unknown SBs, excluding Red, for ID (Type I inspection)}}$$

$$\underbrace{-\left\{\gamma_V V_I(t)\right\}\left[e^{-\kappa_{VS}\left(\frac{\left[M_V - B_V(t)\right]^+}{V_I(t)+V_{I,R}(t)}\right)^{\tau_{VS}}}\right]\left[W_S(t)+A_F(t)+A_{F,R}(t)\right]}_{\text{Mean number of USVs engaged in Type I inspection that are reassigned to unID'd suspicious SBs, suspicious SBs and hidden Red being followed by UAVs}} \qquad (2.25)$$

$$\underbrace{-\ \mu_{VI}V_I(t)}_{\text{Mean number of USVs that complete Type I inspection}} \ \underbrace{-\ \lambda_W V_I(t)}_{\text{Mean number of SBs that leave region}}$$

$$\frac{dV_{I,R}(t)}{dt}$$

$$= \underbrace{\left\{\delta_V\left[M_V - B_V(t)\right]^+\right\}\left[e^{-\kappa_V\left(\frac{W_S(t)}{W_U(t)+R(t)}\right)^{\tau_V}}\right]\left[\frac{R(t)}{W_U(t)+R(t)}\right]R(t)}_{\text{Mean number of idle USVs that approach hidden Red for ID (Type I inspection)}}$$

$$-\underbrace{\left\{\gamma_V V_{I,R}(t)\right\}\left[e^{-\kappa_{VS}\left(\frac{\left[M_V - B_V(t)\right]^+}{V_I(t)+V_{I,R}(t)}\right)^{\tau_{VS}}}\right]\left[W_S(t)+A_F(t)+A_{F,R}(t)\right]}_{\begin{array}{l}\text{Mean of number of USVs engaged in Type I inspection of hidden Red}\\ \text{that are reassigned to unID'd suspicious SBs, suspicious SBs}\\ \text{and hidden Red being followed by UAVs}\end{array}} \qquad (2.26)$$

$$-\underbrace{\mu_{VI}V_{I,R}(t)}_{\begin{array}{l}\text{Mean number}\\ \text{of USVs}\\ \text{that complete}\\ \text{Type I}\\ \text{inspection}\\ \text{of hidden}\\ \text{Red}\end{array}}$$

$$\frac{dV_{II}(t)}{dt} = \underbrace{\mu_{VI} V_I(t) c_{Vwr}}_{\substack{\text{Mean number of USVs that are inspecting (Type II) SBs ID'd as suspicious by USV}}}$$

$$+ \underbrace{\left\{\gamma_V \left[M_V - B_V(t)\right]^+\right\}\left[1 - e^{-\kappa_V\left(\frac{W_S(t)}{W_U(t)+R(t)}\right)^{\tau_V}}\right] W_S(t)}_{\substack{\text{Mean number of idle USVs that approach unID'd suspicious SBs}}}$$

$$+ \underbrace{\left\{\gamma_V \left[M_V - B_V(t)\right]^+\right\}\left[1 - e^{-\kappa_V\left(\frac{W_S(t)}{W_U(t)+R(t)}\right)^{\tau_V}}\right]\left[\frac{A_F(t)}{A_F(t)+A_{F,R}(t)}\right] A_F(t)}_{\substack{\text{Mean number of USVs that arrive at suspicious SBs being followed by UAVs}}} \quad (2.27)$$

$$+ \underbrace{\left\{\gamma_V \left[V_I(t) + V_{I,R}(t)\right]\right\}\left[e^{-\kappa_{VS}\left(\frac{\left[M_V - B_V(t)\right]^+}{V_I(t)+V_{I,R}(t)}\right)^{\tau_{VS}}}\right]\left[W_S(t) + A_F(t)\right]}_{\substack{\text{Mean number of USVs engaged in Type I inspection that are reassigned to unID'd suspicious SBs and suspicious SBs being followed by UAVs}}}$$

$$- \underbrace{\lambda_W V_{II}(t)}_{\substack{\text{Mean number of suspicious SBs that leave region}}} - \underbrace{\mu_{VII} V_{II}(t)}_{\substack{\text{Mean number of USVs that complete Type II inspection}}}$$

$$\frac{dV_{II,R}(t)}{dt} = \underbrace{\mu_{VI} V_{I,R}(t) c_{Vrr}}_{\substack{\text{Mean number of USVs that are inspecting (Type II) hidden Red ID'd as suspicious by USVs}}}$$

$$+ \underbrace{\left\{\gamma_V \left[M_V - B_V(t)\right]^+\right\}\left[1 - e^{-\kappa_V\left(\frac{W_S(t)}{W_U(t)+R(t)}\right)^{\tau_V}}\right]\left[\frac{A_{F,R}(t)}{A_F(t)+A_{F,R}(t)}\right]A_{F,R}(t)}_{\text{Mean number of USVs that arrive at hidden Red that being followed by UAVs}}$$

$$+ \underbrace{\left\{\gamma_V \left[V_I(t)+V_{I,R}(t)\right]\right\}\left[e^{-\kappa_{VS}\left(\frac{\left[M_V - B_V(t)\right]^+}{V_I(t)+V_{I,R}(t)}\right)^{\tau_{VS}}}\right]A_{F,R}(t)}_{\substack{\text{Mean number of USVs engaged in Type I inspection that are reassigned to hidden Red being followed by UAVs}}} \qquad (2.28)$$

$$- \underbrace{\mu_{VII} V_{II,R}(t)}_{\substack{\text{Mean number of USVs that complete Type II inspection of hidden Red}}}$$

The following equation represents the rate of change of the probability ***R*** is not inspected over time.

$$\frac{dR(t)}{dt} = -\underbrace{\mu_{VI,R} V_{I,R}(t) c_{Vrr}}_{\substack{\text{Mean number of hidden Red that is ID'd as suspicious by USV after Type I inspection}}}$$

$$\underbrace{-\left\{\gamma_V\left[M_V - B_V(t)\right]^+\right\}\left[1 - e^{-\kappa_V\left(\frac{W_S(t)}{W_U(t)+R(t)}\right)^{\tau_V}}\right]\left[\frac{A_{F,R}(t)}{A_F(t)+A_{F,R}(t)}\right]A_{F,R}(t)}_{\text{Mean number of USVs that arrive at hidden Red being followed by UAVs}} \quad (2.29)$$

$$\underbrace{-\left\{\gamma_V\left[V_I(t)+V_{I,R}(t)\right]\right\}\left[e^{-\kappa_{VS}\left(\frac{\left[M_V - B_V(t)\right]^+}{V_I(t)+V_{I,R}(t)}\right)^{\tau_{VS}}}\right]A_{F,R}(t)}_{\substack{\text{Mean number of USVs engaged in Type I inspection that are reassigned to hidden Red being followed by UAVs}}}$$

The initial conditions for the state variables $W_U(t)$, $W_S(t)$, $W_I(t)$, $A_I(t)$, $A_F(t)$, $V_I(t)$ and $V_{II}(t)$ are the corresponding steady state values from equations (2.6) to (2.12). State variables $A_{I,R}(t)$, $A_{F,R}(t)$, $V_{I,R}(t)$ and $V_{II,R}(t)$ have initial condition equal to zero. $R(t)$ has value one as its initial condition.

Equations (2.18) to (2.29) are solved numerically using the author's implementation of the Euler method in MATLAB to determine the limits of the state variables.

The ***R*** is assumed to stay hidden for a deterministic time of T_R. The probability ***R*** is detected during its hidden time T_R is $\left[1-R(T_R)\right]$. Let K_B be the event in which ***R*** is detected in scenario B. An approximation of the probability of event K_B, given T_R, is displayed in equation (2.30).

$$P(K_B)=\left[1-R(T_R)\right]+\left[R(T_R)\right]P(K_A) \qquad (2.30)$$

9. Measure of Effectiveness

The MOE for the SB model is the probability of detecting a single Red boat in both threat scenarios given there are a certain number of UAVs and USVs in the strait.

THIS PAGE IS INTENTIONALLY LEFT BLANK

III. MODEL EXPLORATION AND SENSITIVITY ANALYSIS

A. LS THREAT MODEL

1. Significant Factors

The large ship (LS) threat model of chapter 2 is exercised for values of model parameters that form a nearly orthogonal Latin hypercube design (Sanchez 2006). The model is exercised at these parameter values to determine those parameters (factors) that have the most affect on the model output (the probability of neutralizing a hijacked LS). It is also used to determine the effects that varying the number of sub-regions, n, and the number of service periods, m, have on the model output. The factors are varied over ranges that are assessed to be likely practical variations in the D-vessel traffic and the PC's operational capability. A summary of the results follows. Details of the experimental design and detailed results are presented in Appendix B.

The number of sub-regions, n, into which the strait is divided affects the outcome of the model. As n increases, the probability of detection decreases for fixed values of the other parameters. The PCs are distributed uniformly over the sub-regions. When a D-vessel travels through a sub-region uninspected, only the PCs in the subsequent sub-regions have a chance to inspect it, independent of the previous sub-regions. Thus for large n, the time until the D-vessel is inspected has approximately an exponential distribution. Since the number of PCs per sub-region

becomes smaller as the number of sub-regions increases, the probability that the D-vessel is inspected becomes smaller. Hence, larger n has the effect of reducing the chance of inspecting a D-vessel. The effect of n on the model's outcome is also more significant for lower values of the number of PCs, M. On the other hand, the number of service periods in the PCs' boarding and inspection process, m, has a small effect on the probability of detecting the hijacked ship, except when $M \leq 3$. When $M \leq 3$, higher m results in a lower probability of detection. When M is small, the PCs will be busy most of the time and the representation of the service time distribution has more effect. For large values of m the service time distribution is approximately that of a constant. The values for n and m used in the remainder of this thesis are $n = 10$ for all values of M; $m = 8$ for $M \leq 3$; and $m = 2$ for $M > 3$. These values were chosen because they result in pessimistic values for the probability of detection (see Appendix B for details). These results also suggest that in a higher resolution model it is important to represent the distribution of time that a LS is available for inspection; it is less important to represent the distribution of the service time if the number of PCs considered is small.

The results displayed in Appendix B suggest that the most significant factor in determining the probability that Red vessel is detected ($P(K)$) is the number of active PCs (M) in the strait. The next most significant factors are the arrival rate of D-vessels (α) followed by the rate at which the PCs are able to inspect D-vessels once onboard (μ).

Table 1. Parameter values for Base Case LS model.

Parameter	**Symbol**	**Value**
Mean time from D-vessel entry to region and can be inspected until it reaches port (hours)	$\frac{n}{\lambda}$	2
Mean time for PC to inspect a D-vessel (hours)	$\frac{m}{\mu}$	4
Mean time for PC to travel to D-vessel (hours)	$\frac{1}{\gamma}$	1
Arrival rate of D-vessels to strait (per hour)	α	$20/24 \simeq 0.83$
Number of sub-regions in the strait	n	10
Number of service time periods in a boarding and inspection process	m	8 for $M \leq 3$ 2 for $M > 3$

2. Complementary Effect of M and α

This analysis examines the effects on the outcome of the model when M, number of PCs, and α, arrival rate of D-vessels, are varied. In a base case with α of 20 D-vessels per day, approximately 0.83 per hour, six PCs are required in the strait to achieve a $P(K) \simeq 0.90$ of detecting the hijacked D-vessel. This analysis determines how the $P(K)$ changes when the average number of arrivals ranges from 10 to 40 D-vessels per day, M is varied from 1 to 10, and all other factors are have values equal to those in the base case presented in Table 1.

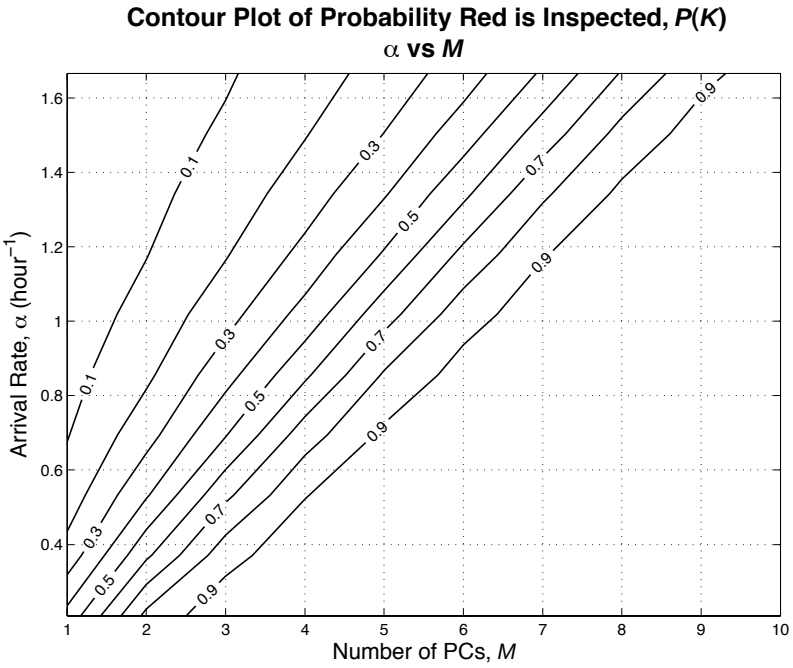

Figure 6. Contour plot of the probability that the Red vessel is detected versus the number of PCs active in the strait and the D-vessels' arrival rate

The contour plot of $P(K)$, displayed in Figure 6, indicates that there is a nearly linear relationship between α and M in maintaining a given level of $P(K)$. For every increment of 0.2 in arrival rate (or increment of 4.8 D-vessels per day), an additional PC is required to maintain $P(K)$ approximately 0.90 or higher. With six PCs active in the strait, the arrival rate of LSs may be as large as 25 D-vessels per day and still have a $P(K)$ of approximately 0.90.

3. Complementary Effect of M and μ

This analysis examines the effects on the outcome of the model when M, the number of PCs, and μ, where $\frac{1}{\mu}$ is the mean time boarding party from PC is on a D-vessel, are varied at the same time. M is varied from 1 to 7 while all other factors except μ are kept at their base case values as in Table 1.

From the contour plot displayed in Figure 7, it can be determined how much μ has to increase in order to allow reduction in M. In the base case with μ=0.25, six PCs are required to achieve $P(K)$>0.90 of detecting the hijacked D-vessel. If only five PCs are available, then μ must be at least 0.3 to achieve $P(K)$>0.90; that is a reduction of about ⅓ hour in the mean time taken by the personnel onboard a PC to board and inspect D-vessels $P(K)$. To maintain the same level of $P(K)$, every unit decrement in M

requires an exponential increment in μ. It is difficult in practice to decrease the mean inspection time. Thus, this model suggests decreasing the mean PC inspection time has a limited practical effect in reducing M. In summary, if a high level of search rate, μ, is achievable when boarding, it can compensate for a small number of boarding from PCs.

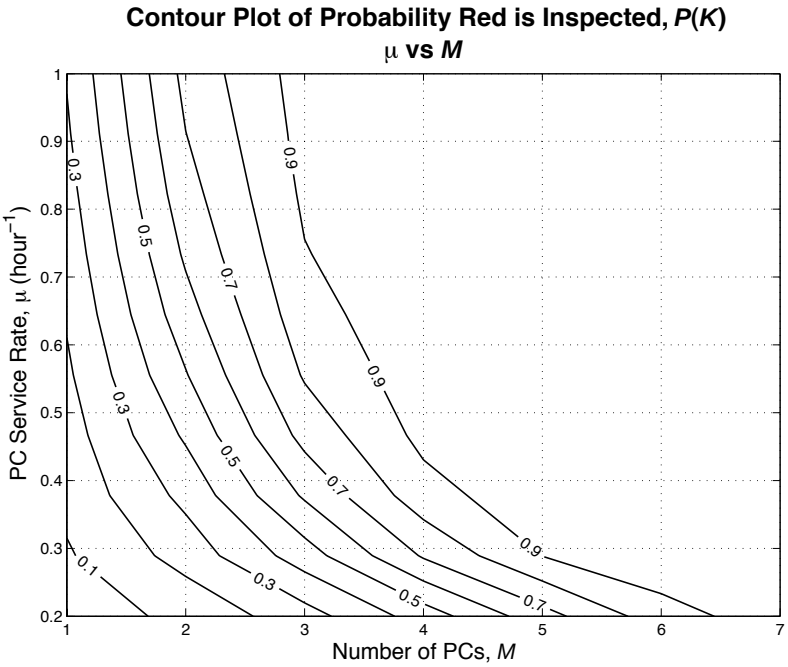

Figure 7. Contour plot of the probability that the Red vessel is detected versus the number of PCs active in the strait and the PC service rate; α=0.83.

4. Comparison of the Deterministic Fluid Model and A Birth-Death Model

This analysis is a comparison between the results from the deterministic fluid (DF) model described in Chapter 2 and two versions of a stochastic birth-death (BD) model. The BD models represent the effect of CONOPS of inspection

of LSs as a birth and death process of a system with processes that have times between events that are exponentially distributed. The second version of the BD models is a generalization of the first with the strait divided into a number of sub-regions. Descriptions of the two versions of the BD models are in Appendix C. The values used for the parameters in this analysis are the same as those displayed in Table 1, except for the number of sub-regions and service periods.

a. Case 1: DF Model versus BD Model 1 (BD-1)

Figure 8 displays the plot of the probability that the Red vessel is inspected versus the number of active PCs in the strait for both models. For consistency, the DF model has the number of sub-regions, n=1, and the number of service periods, m=1. From Figure 8, it is observed that the BD-1 model results are more pessimistic than those of the DF model for all M. The curve for BD model does not rise as rapidly as the DF one when M increases. The largest difference, in percentage, between the results of the two models is at M=3 where the BD-1 model's result is almost 40% lower. This suggests that the DF model may be optimistic. To achieve a probability of detection of more than 0.9, the DF model indicates that at least five PCs are required and the BD-1 model indicates at least eight PCs.

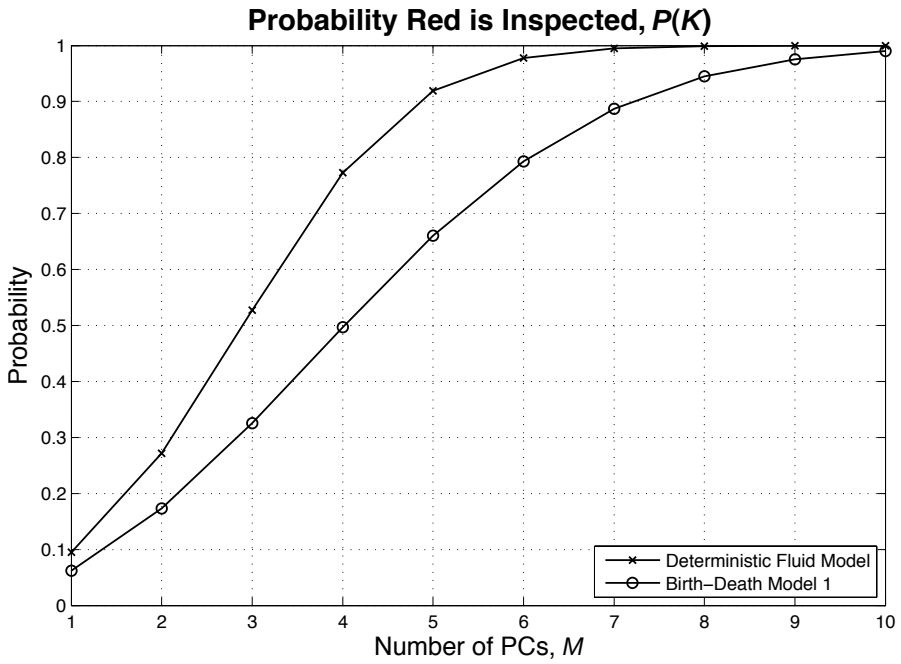

Figure 8. Plot of probability that the Red vessel is detected versus the number PCs active in the strait for the deterministic fluid model and birth-death model 1, with n=1 and m=1.

b. Case 2: DF Model versus BD Model 2 (BD-2)

Figure 9 plots the probability that the Red vessel is inspected versus the number of active PCs in the strait for both models. The DF model and the BD-2 model both have the number of sub-regions equal to the number of PCs, $n = M$, and the number of service periods, m=1. There is one PC per sub-region. From Figure 9 it is observed that both models produce very similar results. The BD-2 model, which is a generalized version of BD-1, gives slightly more optimistic results than the BD-1 model. The result of this comparison gives more confidence in the DF model.

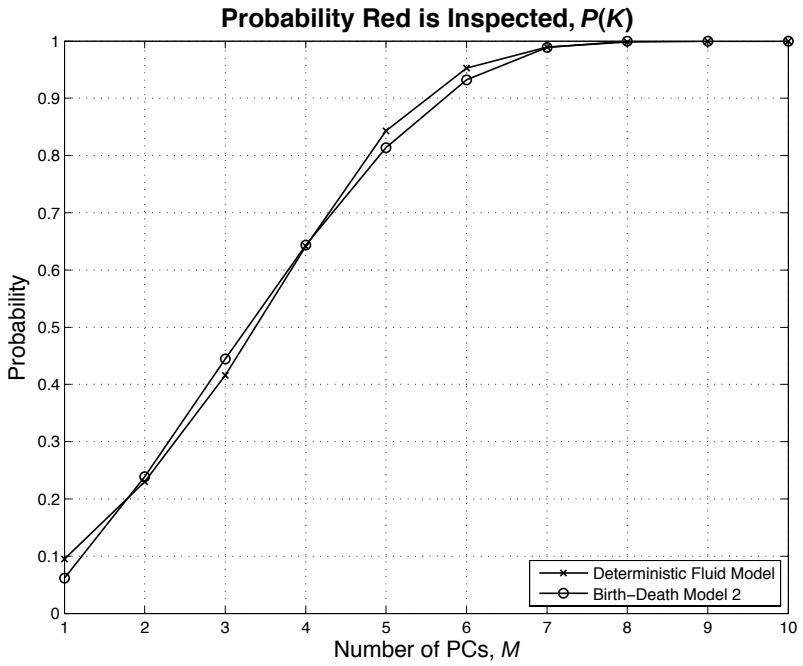

Figure 9. Plot of the probability that the Red vessel is inspected versus the number of PCs active in the strait for the deterministic fluid model and birth-death model 2, with $n = M$ and m=1.

5. Optimal PC Deployment Using BD-2 Model

In this analysis, the generalized birth-death model (BD-2) is used to study the optimal way of deploying a given number of PCs. Here the strait is divided into two sub-regions, n=2, and there are a total of five PCs deployed in both regions, M=5. The number of service periods is one: m=1. The values used for the other parameters in this analysis are the same as those displayed in Table 1.

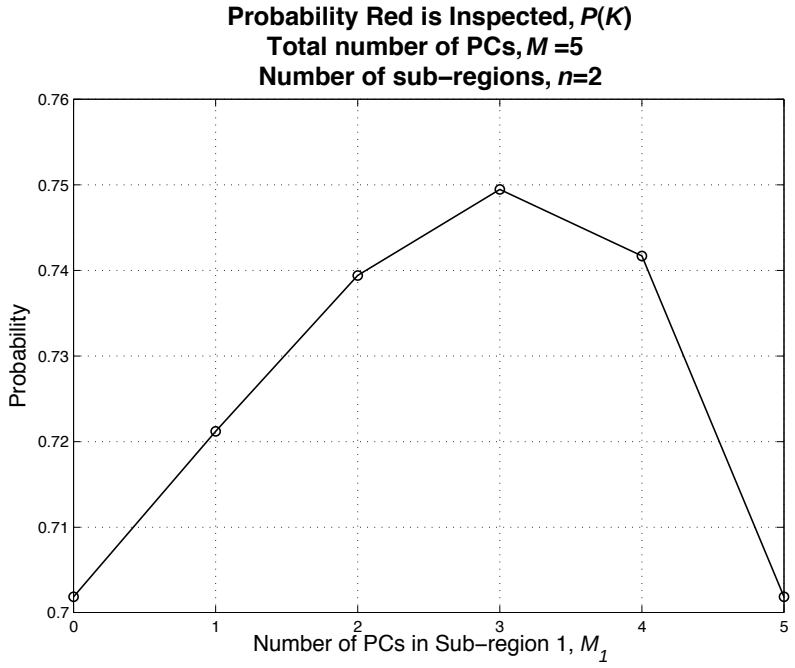

Figure 10. Plot of the probability that the Red vessel is inspected versus the number of PCs active in sub-region 1, with $n=2$, $m=1$, and $M=5$.

Figure 10 plots the probability that the Red vessel is inspected versus the number of PCs active in sub-region 1. Figure 10 shows that the probability is the highest when three PCs are deployed in sub-region 1. Detection is at the lowest when all PCs are deployed in either one of the sub-regions. The model suggests that the optimal deployment plan for a force of five PCs is to assign three and two PCs in sub-region one and two, respectively. Similar analysis should be carried out for other force sizes and numbers of sub-regions.

B. SB THREAT MODEL

Table 2 displays the parameters values for the surveillance platforms under good and poor visibility conditions that are used in the analysis in this chapter.

Table 2. Parameter values for SB model – surveillance platforms.

Parameter	Symbol	Good Visibility			Poor Visibility		
		UAV	USV	PC	UAV	USV	PC
Speed (nm per hour)	v_A, v_V	100	30	30	100	20	20
Sensor footprint (nm x nm)	f_A, f_V	1x1	0.5x 0.5	0.75x 0.75	0.8x 0.8	0.4x 0.4	0.6x 0.6
Mean time a UAV and USV (PC) takes to classify a SB as harmless or suspicious (Type I inspection) (minutes)	$\frac{1}{\mu_A}, \frac{1}{\mu_{V,I}}$	5	10	8	7	13	11
Mean time a USV (PC) requires to classify a suspicious SB a threat (Type II inspection) (minutes)	$\frac{1}{\mu_{V,II}}$	-	20	18	-	27	24
Probability a White SB is misclassified as suspicious by the UAV and USV (PC) during Type I investigation and must undergo Type II inspection	c_{Awr}, c_{Vwr}	0.1	0.1	0.01	0.15	0.15	0.05
Probability that the Red is classified correctly by a UAV and USV (PC)	c_{Arr}, c_{Vrr}	.95	.95	.99	.95	.95	.99

1. Suspicious SB Priority Parameters

The decision parameters, κ_A and κ_V, are used to represent the *modus operandi* for the UAV and USV

respectively. They are measures of how the platforms prioritize their inspections between suspicious and unsuspicious SBs. Larger parameter values mean that the platform gives higher priority to inspecting a suspicious SB; conversely, a value of zero means that unsuspicious SBs always have priority over suspicious SBs. It makes operational sense to always give priority to inspecting a suspicious SB. However, this analysis will study how different priority settings for the UAV and USV affect the MOE.

First, suitable values are determined for κ_A and κ_V that represent higher priority being given to suspicious SBs. The term

$$\left[1-\exp\left\{-\kappa_V\left(\frac{W_S(t)}{W_U(t)}\right)^{\tau_V}\right\}\right] \qquad (3.1)$$

is used in the differential equations to multiply the proportion of suspicious SBs that will be inspected by USVs; a similar term exists for UAVs. When κ_V is large, expression (3.1) approaches unity, and a free USV will almost always choose to inspect a suspicious SB rather than an unsuspicious SB. Conversely, when κ_V approaches zero, expression (3.1) tends to zero, and a free USV is more likely to choose an unsuspicious SB to inspect. The tuning factors τ_A and τ_V are (arbitrarily) set equal to two for all computations in this thesis. Figure 11 displays the plot of the probability that the Red boat is inspected versus the suspicious SB priority parameter κ, where $\kappa=\kappa_A=\kappa_V$. In Figure 11, the results are for nine USVs with

respective number of UAVs, M_A=0, 1 and 2, and the parameter values as displayed in Table 2. From Figure 11, it is observed that the probabilities become nearly constant for $\kappa > 200$, so those values are omitted. For the purpose of this thesis, a value of $\kappa_A = \kappa_V$=300 will be used to represent the effect of higher priority being given to suspicious SBs by both UAVs and USVs.

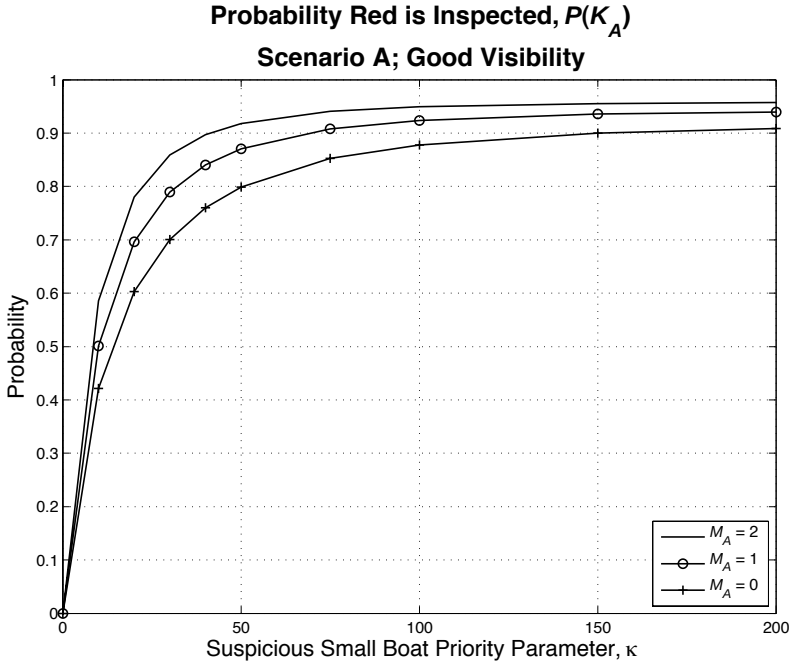

Figure 11. Plot of the probability that the Red is inspected in scenario A versus the suspicious SB priority parameter, for nine USVs under good visibility conditions.

An ORBAT mix of one UAV and nine USVs, in good visibility conditions, (parameters displayed in Table 2), are used as the basis for the next analysis. Figure 12 displays the contour plot of scenario A's $P(K_A)$ versus the USVs' priority parameter κ_V on the x-axis and the UAV's

priority parameter κ_A on the y-axis. Both parameters take values between 0 to 300 and are displayed on a log-scale in the figure. Figure 13 displays a similar plot for scenario B's $P(K_B)$.

Figure 12 shows that $P(K_A)$ is highly dependent on κ_V. For a given κ_V, larger values of κ_A result in a slightly lower $P(K_A)$. When the USVs' priority parameter increases, $P(K_A)$ increases rapidly because only a USV is able to detect a Red boat, which is a suspicious boat in scenario A. On the other hand, the model represents little to no benefit to having the UAV assigned to a suspicious SB detected by the shore-based radar. Only a USV can service such a suspicious SB. A UAV giving priority to a suspicious SB only keeps the UAV busy, and prevents it from identifying other unsuspicious SBs. Similar, but more pronounced, results are obtained for scenario B's $P(K_B)$.

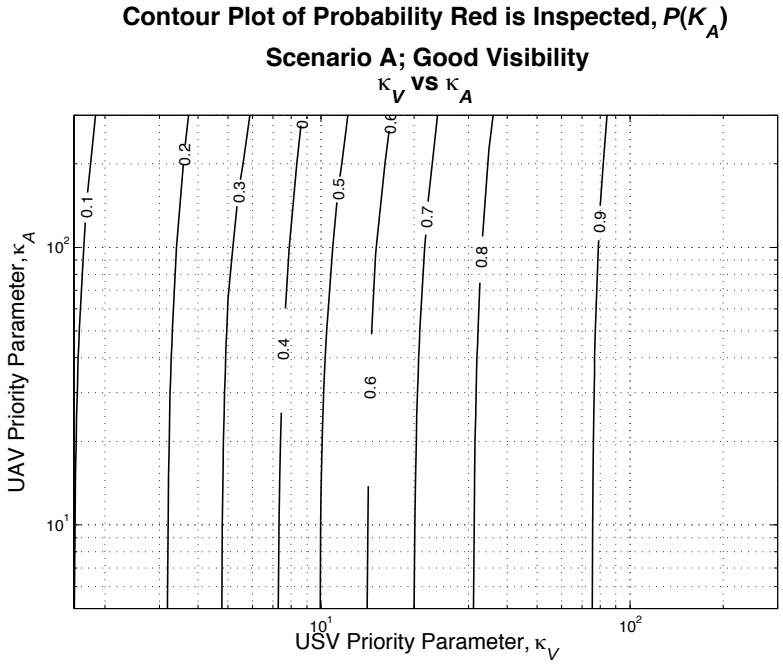

Figure 12. Contour plot of the probability that Red is inspected in scenario A versus the suspicious SB priority parameters for UAV and USV.

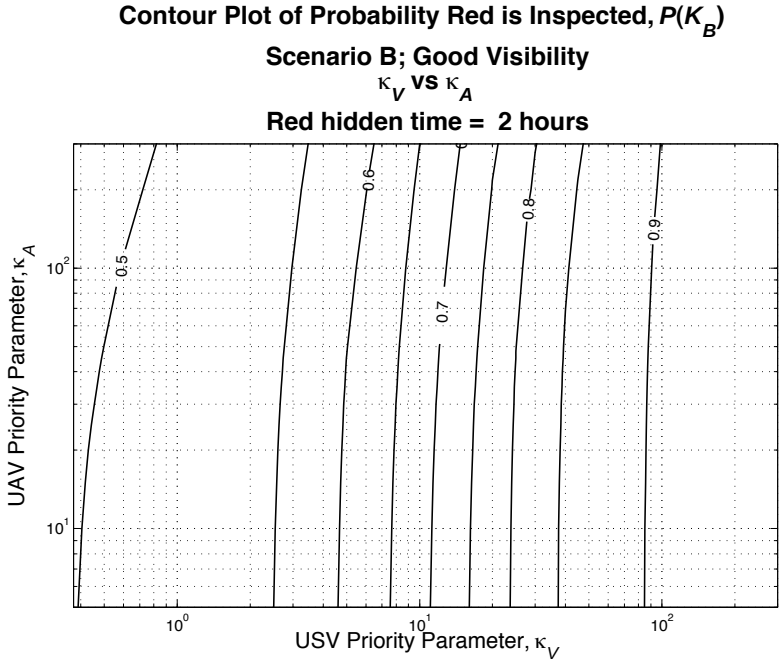

Figure 13. Contour plot of the probability that Red is inspected in scenario B versus the suspicious SB priority parameters for UAV and USV.

Figure 14 displays the plot of the probability Red is inspected and identified as Red versus the number of active USVs in the region with $\kappa_A=\kappa_V=300$. It is observed that for a small number of USVs (less than three), the addition of a UAV actually causes $P(K_A)$ to drop. The likely cause is that a small number of USVs (or PCs) can be overwhelmed by the additional workload created by the UAVs; when a UAV misclassifies a neutral SB (White) as suspicious, a USV or PC must travel to the SB and perform a Type II inspection. Consequently, there are fewer idle USVs (or PCs) to detect Red, which results in lower $P(K_A)$. This phenomenon is likely to be more apparent when the surface platforms are less effective, such as under poor visibility conditions. Figure 15 displays the corresponding plot of mean number of USVs not engaged in any inspection versus the number of those active in the region under the same conditions as in Figure 14. For three or fewer active USVs, it is observed that the addition of one UAV causes a significant drop in number of available USVs. A USV is said to be available if it is not engaging in an inspection or it has been reassigned from a Type I inspection to a Type 2 inspection. When the second UAV is added, the number of available USVs drops further, though not as much as for the first. When there is a sufficient number of USVs to deal with the workload generated by the UAVs, each USV addition increase the availability of USVs, as observed in Figure 15 for a number of USVs greater than three. It is further observed in Figure 15 that when there is no UAV, there is only a marginal increase in the mean number of available USVs when the number of active USVs increases. This marginal increase

is because the USVs' high priority to inspect suspicious SBs decreases the number of USVs available to inspect unsuspicious SBs, even though the mean number of unsuspicious SBs is much larger than the mean number of suspicious SBs. As a result, the mean number of available USVs is quite high compared to the number of active USVs; the number of active USVs equals the number deployed in the strait. This effect is most significant when there is only one active USV; for the parameter values used in Figure 15, the mean number of available USVs is 0.5, while the mean numbers of unidentified unsuspicious SBs and suspicious SBs are 41 and 3.5, respectively. When the USVs have no priority to inspect suspicious SBs and there is one active USV, the mean number of available USVs is only 0.06, and the mean number of USVs engaged in Type II inspections is zero. Table 3 displays the mean numbers of USVs engaged in Type I and II inspections, and those that are not busy with an inspection in scenario A under good visibility conditions, for the two cases when a USV has high versus no priority to inspect suspicious SBs. The number of reassigned USVs is not shown in Table 3 because in both cases, no USV is reassigned since there is a positive number of USVs not engaged in some form of inspection. When κ_V=300, the mean number of available USVs increases from 0.50 to 0.91 as the number of active USVs increases from one to four. Conversely, when a USV has a low priority to inspect suspicious SBs, the mean number of available USVs increases from 0.06 to 0.80 as the number of active USVs increases from one to four. If there is only one USV active in the region, it makes operational sense not to task it to inspect unsuspicious SBs, but to put it on standby to

inspect the less frequent suspicious SBs (as Red is a suspicious SB in scenario A).

Table 3. Table of number of USVs engaged in inspection and available to inspect Red in scenario A, under good visibility when (1) $\kappa_A=\kappa_V=300$ and (2) $\kappa_A=300$ and $\kappa_V=0$.

Active	(1) $\kappa_A=\kappa_V=300$			(2) $\kappa_A=300$, $\kappa_V=0$		
	Type I	Type II	Available	Type I	Type II	Available
0	0	0	0	0	0	0
1	0.35	0.15	0.50	0.94	0.00	0.06
2	1.10	0.32	0.58	1.83	0.00	0.17
3	1.84	0.47	0.69	2.60	0.00	0.40
4	2.51	0.58	0.91	3.20	0.00	0.80
5	3.06	0.67	1.26	3.61	0.00	1.39

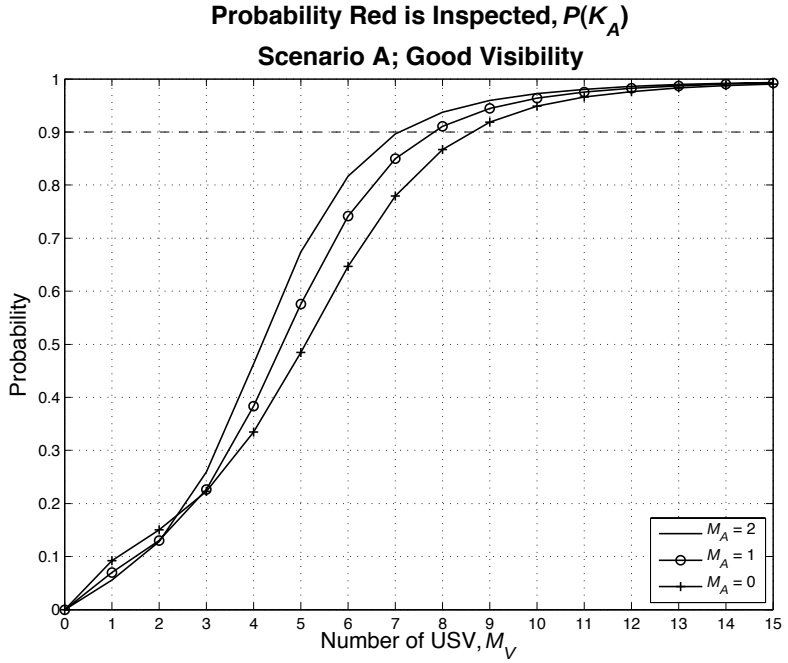

Figure 14. Plot of the probability that Red is inspected in scenario A versus the number of active USVs; under good visibility conditions, with $\kappa_A=\kappa_V=300$.

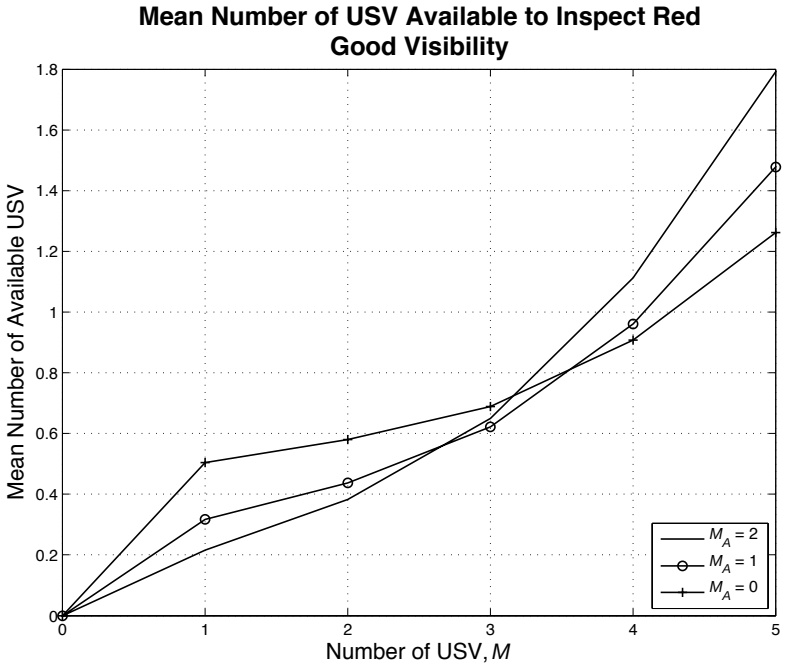

Figure 15. Plot of mean number of USVs available (not engaged in any type of inspection) to inspect Red in scenario A; under good visibility conditions, with $\kappa_A = \kappa_V = 300$.

Therefore, in this case, operating the UAV with no priority for following a suspicious SB detected by land-based radar and having the USV give a high priority to inspecting suspicious SBs will result in a better chance of detecting the Red boat, subject to there being enough USVs to manage the workload from the UAVs. An extension of the current model may have a term that represents the effect of UAVs being tasked to follow suspicious SBs detected by the land-based radar. One such effect may be that the SB ceases its suspicious behavior when the UAV is sighted. In the current model, the UAV should concentrate its efforts on reducing the number of unidentified, but not suspicious, SBs. The USV should give priority to inspecting suspicious SBs.

2. USV Reassignment Parameter

The decision parameter κ_{VS} is a measure of how likely a USV that is engaged in a Type I inspection will be reassigned to inspect another suspicious SB. The reassignment term

$$\left[\exp\left\{-\kappa_{VS}\left(\frac{\left[M_V - V_I(t) - V_{II}(t)\right]^+}{V_I(t)}\right)^{\tau_{VS}}\right\}\right] \qquad (3.2)$$

multiplies the number of USVs engaged in Type I inspection in equations (2.6) to (2.12).

Table 4 displays the values of expression (3.2) for all combinations of the integral mean number of USVs engaged in Type I and Type II inspections. This is for the case of a total of nine USVs active in the region with κ_{VS}=10 and τ_{VS}=0.25, 0.5 and 2. The other parameters have values representing good visibility conditions as displayed in Table 2. For τ_{VS}=0.25, it is observed that the probability of reassignment is zero or very low when total mean number of USVs engaged in Type I and II inspections is not nine, i.e. there are idle USVs. When the total mean number of USVs engaged in Type I and Type II inspections is equal to nine, the probability of reassignment is one, hence capturing the desired effect. For τ_{VS}=0.5 and 2, the situation when not all USVs are busy has higher probability of reassignment than when τ_{VS}=0.25. Hence, larger values for τ_{VS} do not represent the desired effect as well. Therefore, to ensure that reassignment only occurs when all USVs are

engaged in some form of inspection, the tuning factor τ_{VS} is set to a value 0.25 for the rest of the analyses in this thesis.

Figure 16 displays the plot of the probability the Red boat is inspected in scenario A versus the USV reassignment parameter for the case of nine USVs. The other parameters have values representing good visibility conditions as displayed in Table 2. From Figure 16 it is observed that when the USVs are always reassigned under all conditions, κ_{VS}=0, the probability of detecting the Red is the highest. That is, all USVs not engaged in Type II inspections are candidates to investigate a suspicious SB. As κ_{VS} increases, the probability of detecting the Red decreases slightly and becomes constant for κ_{VS}>8. As κ_{VS} increases, it is less likely that USVs are reassigned when there are idle (not engaged in any form of inspection) USVs. The tuning factor, τ_{VS}, ensures that, (for the parameters used in this analysis), reassignment is less likely to happen when there are idle USVs. For the purpose of this thesis, a value of κ_{VS}=10 will be used to model the reassignment of USVs. With this choice, it is unlikely that there will be a reassignment of busy USVs when there are idle USVs.

Table 4. Table of equation (3.2) as a function of the mean numbers of USVs engaged in Type I and Type II inspections; for nine USVs active in the region; κ_{VS}=10 and τ_{VS}=0.25, 0.5 and 2.

Mean number of USVs engaged in Type II inspections $V_{II}(t)$	Mean number of USVs engaged in Type I inspections $V_I(t)$	Probability of reassignment, equation (3.2) for		
		τ_{VS}=0.25	τ_{VS}=0.5	τ_{VS}=2
1	1	0	0	0
1	2	0	0	0
1	3	0	0	0
1	4	0	0	0
1	5	0.0002	0.0004	0.0273
1	6	0.0005	0.0031	0.3292
1	7	0.0021	0.0228	0.8154
1	8	1	1	1
2	1	0	0	0
2	2	0	0	0
2	3	0	0	0
2	4	0.0001	0.0002	0.0036
2	5	0.0004	0.0018	0.2019
2	6	0.0017	0.0169	0.7575
2	7	1	1	1
3	1	0	0	0
3	2	0	0	0
3	3	0	0	0
3	4	0.0002	0.0008	0.0821
3	5	0.0012	0.0114	0.6703
3	6	1	1	1
4	1	0	0	0
4	2	0	0	0
4	3	0.0001	0.0003	0.0117
4	4	0.0008	0.0067	0.5353
4	5	1	1	1
5	1	0	0	0
5	2	0	0	0
5	3	0.0005	0.0031	0.3292
5	4	1	1	1
6	1	0	0	0
6	2	0.0002	0.0008	0.0821
6	3	1	1	1
7	1	0	0	0
7	2	1	1	1
8	1	1	1	1

*When the first two columns sum to nine (shaded rows), i.e. all active USVs are engaged in inspections, then the probability of reassignment is one.

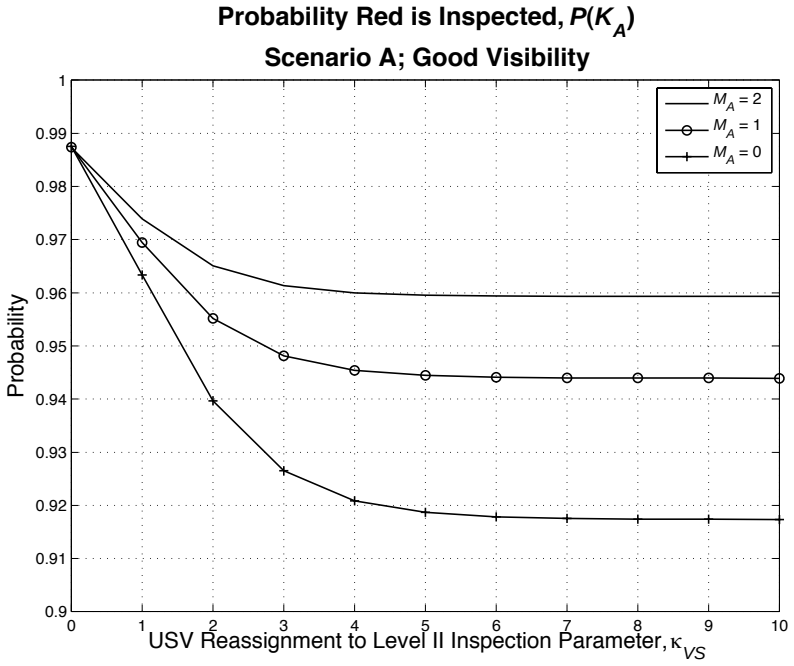

Figure 16. Plot of probability that Red is inspected in scenario A versus the USV reassignment parameter for nine USVs under good visibility conditions; κ_A=0 and κ_V=300.

3. White SB Classification Probabilities

The platforms' accuracies in classifying unsuspicious White boats are modeled as the probability of correctly classifying unsuspicious SBs. The classification parameters for the UAV and USV are c_{Aww} and c_{Vww}, respectively. This analysis compares how the accuracy of the classification of White boats by the UAV and USV affects the probability of inspecting the Red boat. The parameters will take values from 0.5 to 1.0, which is deemed an operationally reasonable range. As before, the basis of this analysis will be an ORBAT mix of one UAV and nine USVs and good visibility conditions for all other parameters. The parameter values are displayed in Table 2.

Figure 17 displays the contour plot of scenario A's $P(K_A)$ versus the platforms' accuracies in classifying White boats. Figure 18 displays a similar plot for scenario B's $P(K_B)$. In general, the larger probabilities of correct classification result in fewer false suspicious SBs being generated for Type II inspections by the USVs. Consequently, the probability of detecting Red is higher due to greater availability of the USVs. The UAV makes the greatest contribution to a high probability of detecting the Red when it is highly accurate (c_{Vww}>0.95) in classifying White SBs. In Figure 17, it is observed that when the UAV's c_{Aww}>0.95, the USVs need only to be fairly accurate, i.e. with c_{Vww}>0.65, in order to achieve $P(K_A)$=0.9. On the other hand, if the USV is highly accurate, the accuracy of the UAV is not really important. Similar observations are also made for scenario B's $P(K_B)$. The same results hold for a smaller number of USVs; see Figure 19 for the same case but with one UAV and three USVs.

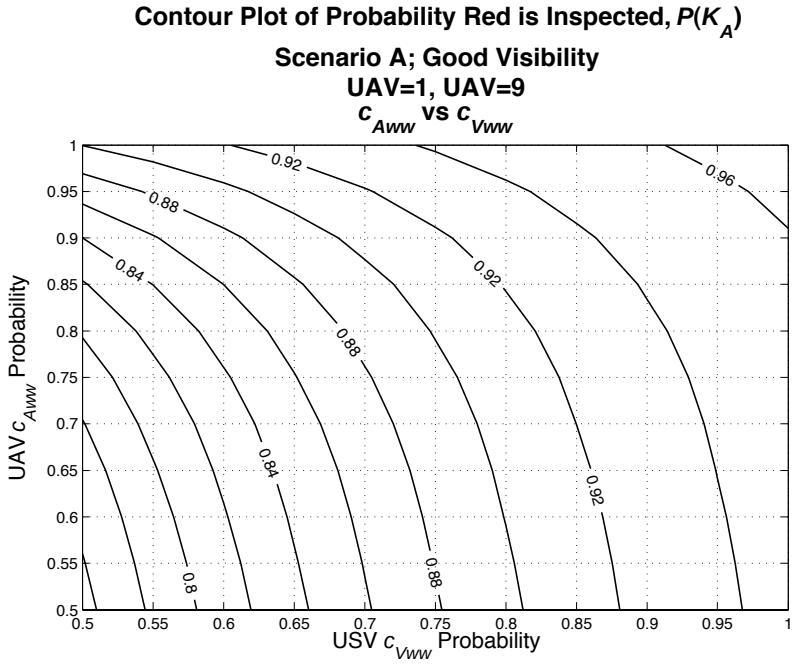

Figure 17. Contour plot of the probability that Red is inspected in scenario A versus the probability of correctly classifying White for UAV and USV; UAV=1 and USV=9; κ_A=0 and κ_V=300.

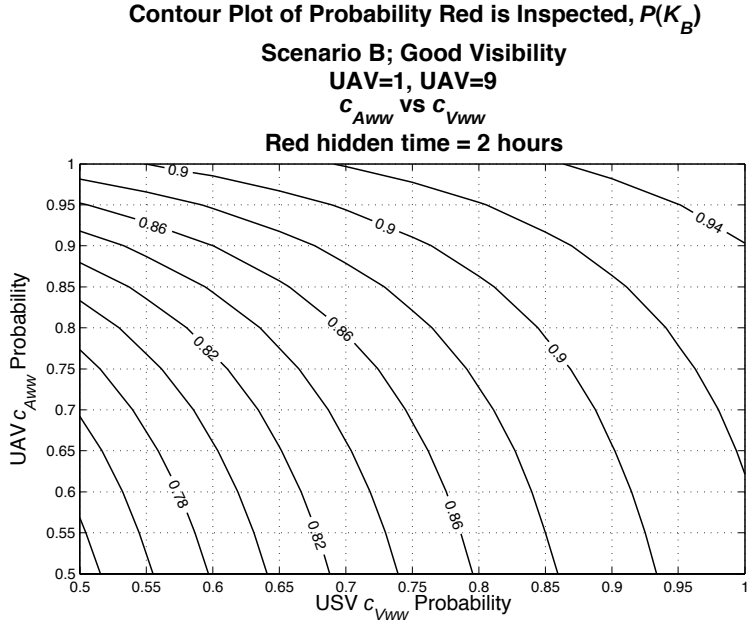

Figure 18. Contour plot of the probability that Red is inspected in scenario B versus the probability of correctly classifying White for UAV and USV; UAV=1 and USV=9; κ_A=0 and κ_V=300.

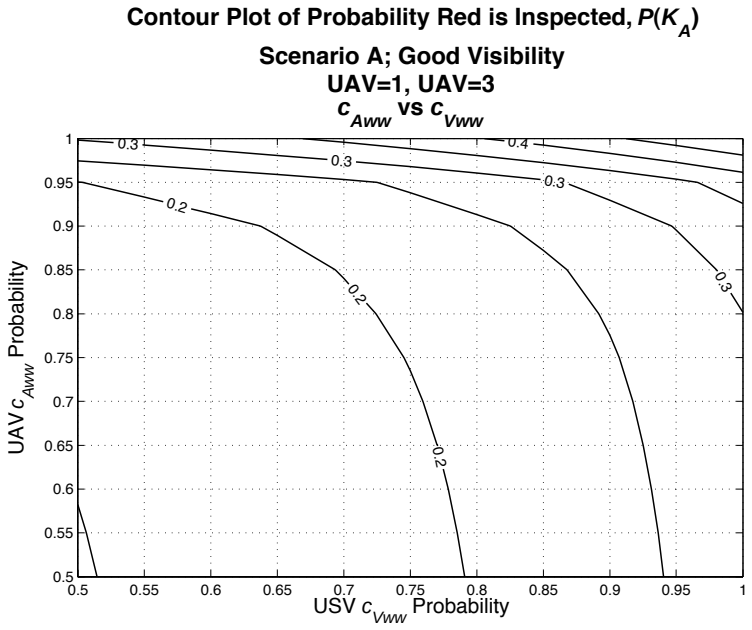

Figure 19. Contour plot of the probability that Red is inspected in scenario A versus the probability of correctly classifying White for UAV and USV; UAV=1 and USV=3; κ_A=0 and κ_V=300.

To summarize, if UAVs are to be deployed with USVs, the UAV should have a high c_{Aww} in order to make a significant positive contribution to the outcome of detecting Red. The generation of false positives by the UAV ($c_{Awr} = 1 - c_{Aww}$) is actually not high but there are many opportunities for misclassifying a White as suspicious SB. There are two consequences of misclassification; the UAV must follow the apparently suspicious SB and so is unable to identify other SBs; in addition a USV must conduct a Type II inspection and so is unavailable to conduct other inspections.

4. Red's Hidden Time in Scenario B

This analysis considers how the mean time the Red boat attempts to hide, T_R, affects scenario B's $P(K_B)$. Four values are considered for T_R: 0.5, 1, 2, and 5 hours, and a mixed ORBAT of one UAV and some USVs.

Figure 20 displays the plots of the probability Red is inspected/neutralized as a function of the number of USVs under good and poor visibility conditions. The four curves in each plot correspond to different values for T_R. In general, it is observed that, as expected, $P(K_B)$ is higher when T_R is longer. Given one UAV and nine USVs under good visibility conditions, if T_R is shortened from two hours to half an hour, $P(K_B)$ drops from 0.92 to 0.86, about 7%. See Figure 21 for the plot $P(K_B)$ versus T_R for the ORBAT mix of one UAV and nine USVs.

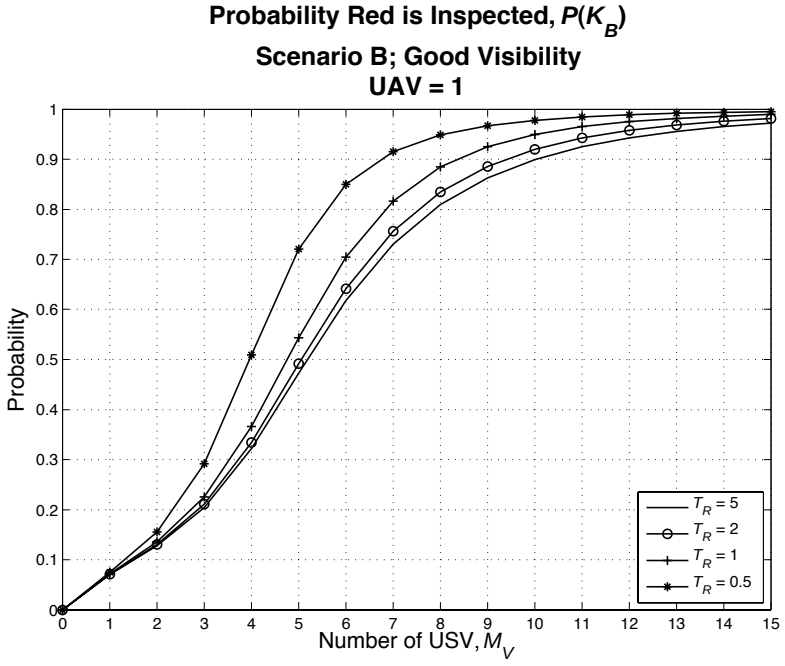

(a)

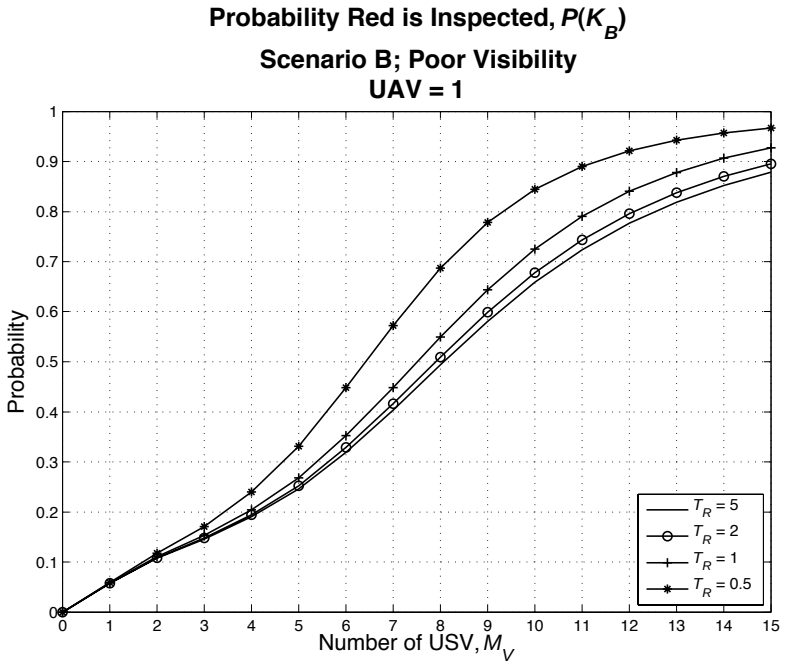

(b)

Figure 20. Plot of the probability that Red is inspected in scenario B versus the number of active USVs for different Red hidden times under (a) good visibility and (b) poor visibility; κ_A=0 and κ_V=300.

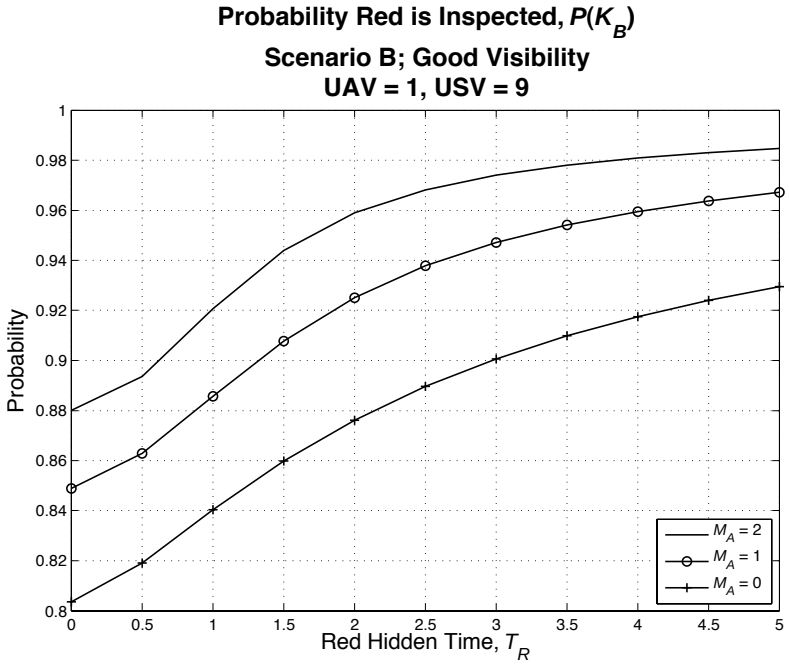

Figure 21. Plot of probability that Red is inspected versus Red hidden time in scenario B under good visibility, for ORBAT mix of one UAV and nine USVs, κ_A=0 and κ_V=300.

5. UAV's Mean Inspection Time

This analysis considers how the UAV's mean time to conduct a Type I inspection, $\frac{1}{\mu_A}$, affects the probability of inspecting the Red boat. The basis for this analysis is an ORBAT mix of one UAV and various numbers of USVs under good visibility conditions for all other parameters, as displayed in Table 2. The values for the UAV's mean inspection time vary from one minute to 10 minutes.

Figure 22 displays the contour plot of scenario A's $P(K_A)$ versus $\frac{1}{\mu_A}$ and the number of active USVs. It can be

observed that the UAV's mean inspection time has very little impact on $P(K_A)$ for the case examined. For a given number of active USVs, a shorter UAV mean inspection time only results in a slight increase in $P(K_A)$. When there are eight USVs, if the UAV mean inspection time is reduced from five minutes to one minute, $P(K_A)$ only increases from 0.91 to 0.92. Similar observations are made for $P(K_A)$ under poor visibility conditions (see Figure 23). Therefore, for this case with the given USV parameters for good visibility conditions, efforts to reduce UAV mean inspection time will not help much in improving $P(K_A)$. It should be noted that longer UAV inspection times could potentially result in an increased probability of correct classification. This effect is not represented in the current model and could be investigated in future work. It should also be noted that variability in the inspections times is also not represented in this model.

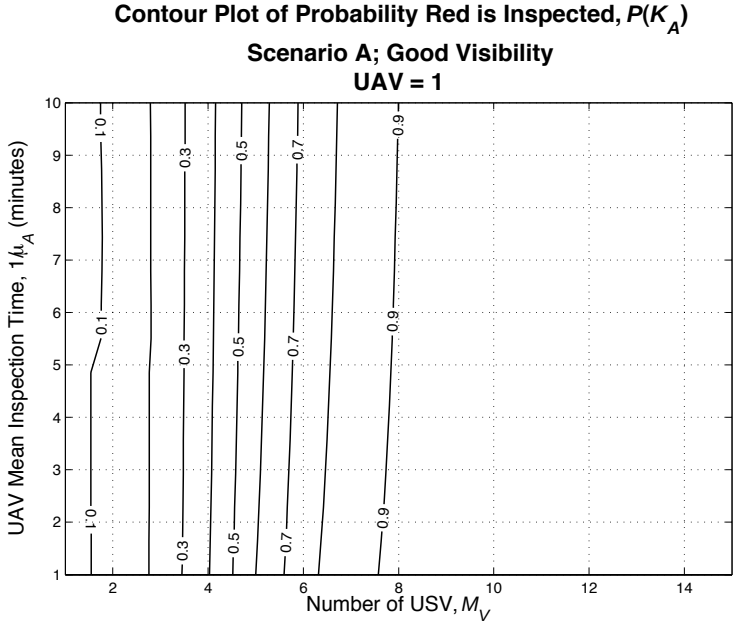

Figure 22. Contour plot of the probability that Red is inspected in scenario A versus the UAV's mean inspection time and the number of active USVs, under good visibility conditions, κ_A=0 and κ_V=300.

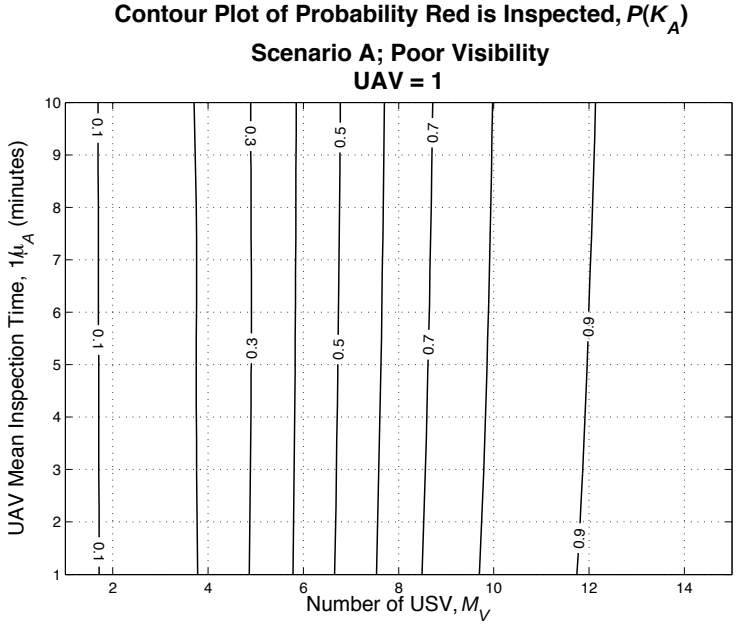

Figure 23. Contour plot of the probability that Red is inspected in scenario A versus the UAV's mean inspection time and the number of active USVs, under poor visibility conditions, κ_A=0 and κ_V=300.

6. USV Mean Inspection Time for Type I and Type II Inspections

This analysis considers how the USV's mean inspection times, $\frac{1}{\mu_{V,I}}$ and $\frac{1}{\mu_{V,II}}$, affect the probability of inspecting the Red boat. The basis for this analysis is an ORBAT mix of one UAV and nine USVs under good visibility conditions for all other parameters, as displayed in Table 2. The values for $\frac{1}{\mu_{V,I}}$ and $\frac{1}{\mu_{V,II}}$ are varied from five to 10 minutes and 10 to 30 minutes respectively.

Figure 24 displays the contour plot of scenario A's $P(K_A)$ versus $\frac{1}{\mu_{V,I}}$ and $\frac{1}{\mu_{V,II}}$. It can be observed that the partial derivative of $P(K_A)$ with respect to $\frac{1}{\mu_{V,I}}$ is higher than that with respect to $\frac{1}{\mu_{V,II}}$. Assume that the original mean values for $\frac{1}{\mu_{V,I}}$ and $\frac{1}{\mu_{V,II}}$ are 10 and 20 minutes, respectively, with $P(K_A)$=0.94, and there are technology or procedures to make it possible to reduce either mean time by 20%. Reducing $\frac{1}{\mu_{V,I}}$ to eight minutes increases $P(K_A)$ to about 0.96, while reducing $\frac{1}{\mu_{V,II}}$ to 16 minutes increases $P(K_A)$ to about 0.95. Therefore, for the given parameters,

efforts on reducing the USV's mean time taken for a Type I inspection will result in a slightly greater impact on increasing $P(K_A)$ as long as there is no decrease in the probability of correct classification. Once again, the effects of variability in the inspection times are not represented in the model.

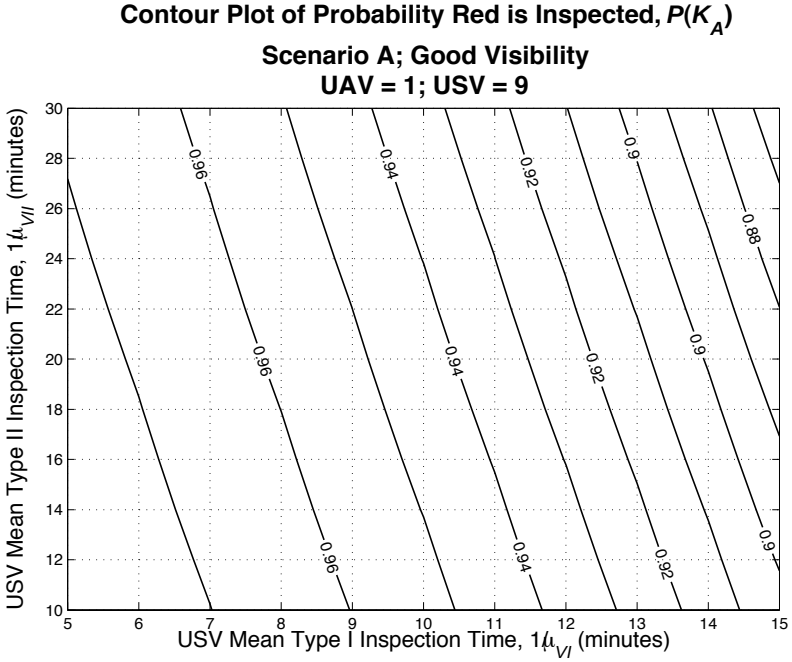

Figure 24. Contour plot of the probability that Red is inspected in scenario A versus USV mean inspection times for Type I and Type II inspections, under good visibility conditions with 1 UAV and 9 USVs; κ_A=0 and κ_V=300.

THIS PAGE IS INTENTIONALLY LEFT BLANK

IV. RESULTS AND ANALYSIS

In this chapter, the models described in Chapter 2 are used to estimate the number of surveillance platforms required to detect the two types of maritime threats, large ship (LS) and small boat (SB). The analyses in Chapter 3 provide insights on the mechanics of the model under different decision parameters settings and form the basis for specifying their values in this chapter.

The required detection criterion for each type of threat is a probability of Red detection of at least 0.9. As a PC is the only platform deemed suitable for the LS threat, the required number to attain the criterion will be proposed. For the SB threat, it is possible to use USVs, PCs, or both, with or without UAVs. Some combinations of USVs, PCs, and UAVs that can achieve the criterion for the SB threat will be proposed and their estimated costs discussed. For the background setting of the two models, the notional strait is represented by a 36 nm[7] by 5 nm rectangle region. The port is situated 18 nm from either end of the strait. The parameter values concerning the LS and SB traffic in the strait are described in the respective sections for each model. The settings for the parameters concerning surveillance platform characteristics and performance are based on the author's assessment of reasonable values.

[7] Nautical miles.

A. LS THREAT

1. Measure of Effectiveness (MOE)

The CONOPS developed for the LS threat requires only one type of sensor platform, which is the PC. The MOE used in this analysis is the probability of detecting a single hijacked D-vessel given M number of PCs active in the strait dedicated to inspecting D-vessels.

2. Parameters

D-vessels arrive at the strait at a rate of about 20 vessels per day. It takes an average of two hours for the D-vessels to transit to the port. The mean time PCs take to transit and prepare to board a D-vessel is one hour and another four hours to conduct the inspection. Table 5 displays the parameter used in the LS model. The number of PCs active in the region, M, is a variable that ranges from 1 to 10.

Table 5. Parameter values for LS model

Parameter	Symbol	Value
Mean time from when D-vessel enters region until it reaches port if it is not inspected by PC (hours)	$\frac{n}{\lambda}$	2
Mean time for PC to inspect a D-vessel (hours)	$\frac{m}{\mu}$	4
Mean time for PC to travel to D-vessel (hours)	$\frac{1}{\gamma}$	1
Arrival rate of D-vessels to strait (per hour)	α	20/24
Number of sub-regions in the strait	n	10
Number of service time periods in a boarding and inspection process	m	8 for $M \leq 3$ 2 for $M > 3$

3. Results and Analysis

Figure 25 displays the plot of the probability of detecting a hijacked D-vessel as a function of the number of PCs active in the strait. The marginal increase in the probability of detection falls when the number of active PCs is more than four. In order to achieve a detection probability that is greater than 0.9, at least six PCs are required to be deployed in the strait. This minimum number of PCs ensures that there are sufficient idle PCs (a mean of at least 2.7) available to inspect the hijacked D-vessel when the latter enters the strait.

From Figure 26, it is observed that the mean number of uninspected PCs is small when there are more than six PCs active in the strait. The mean number of busy PCs when six PCs are active is about 3.3 (see Figure 27).

Therefore, six PCs should be deployed in the strait achieving a 0.95 probability of detecting a hijacked D-vessel.

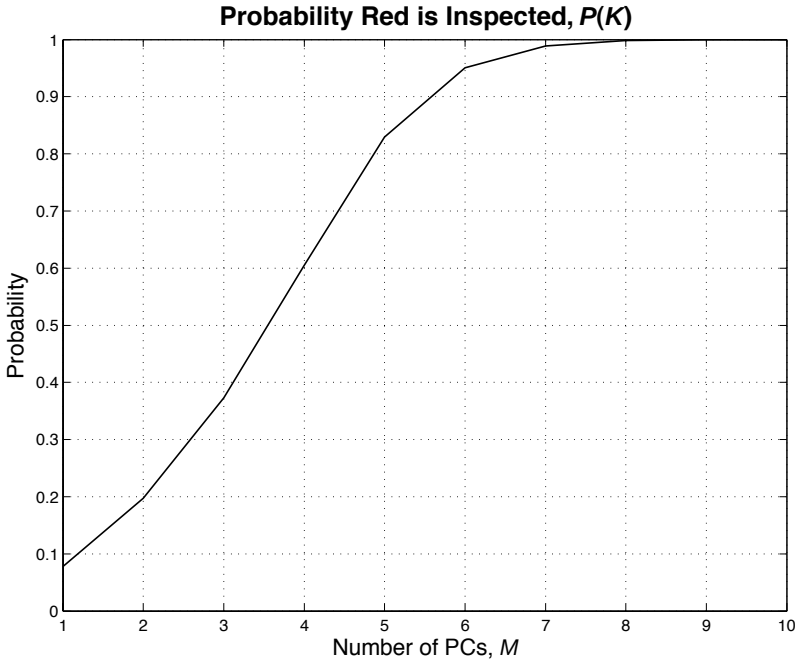

Figure 25. Plot of probability of detection of Red vessel against the number of PCs active in the strait.

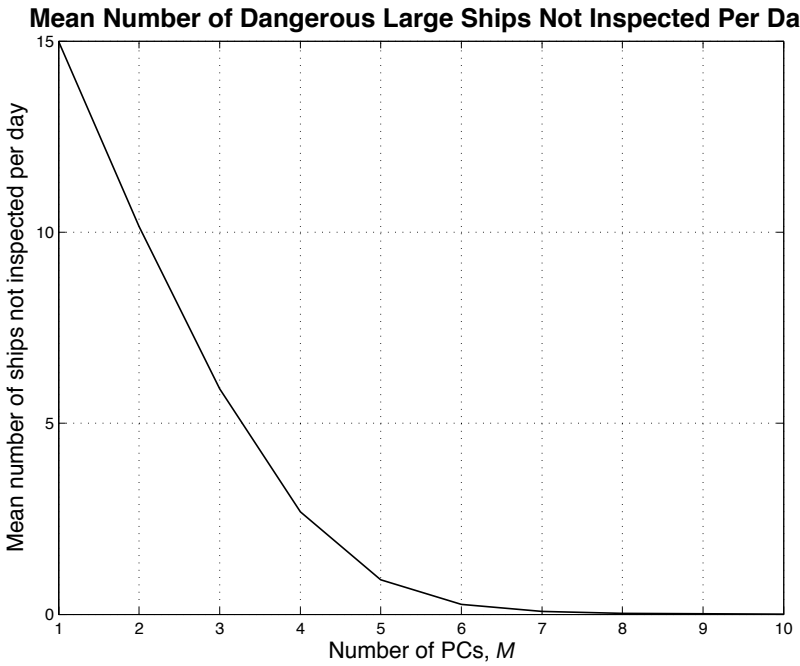

Figure 26. Plot of mean number of D-vessels not inspected per day against the number of active PCs active in the strait.

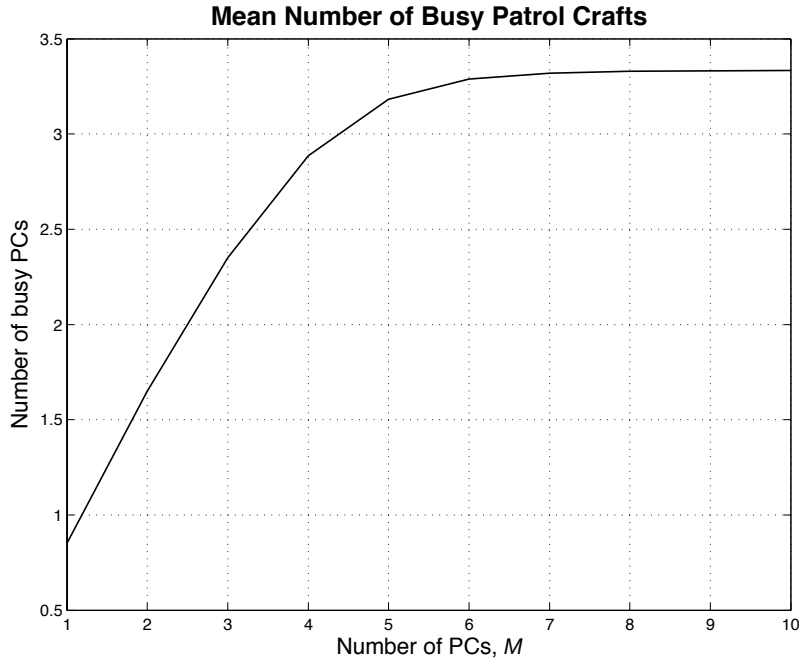

Figure 27. Plot of mean number of busy PCs against the number of active PCs in the strait.

B. SB THREAT

1. Measure of Effectiveness (MOE)

The MOE used in this analysis is the probability of detecting a single Red given M_A number of UAVs and M_V number of USVs active in the strait. Recall that due to airspace restriction, a maximum of two UAVs can be deployed above the strait. Both $P(K_A)$ and $P(K_B)$ of the two threat scenarios A and B, respectively, will be considered. First a comparison of the cost effectiveness of the USV versus PC will be done because they essentially perform the same function in this scenario. Then, the number of USVs or PCs, with and without UAVs, required to achieve a given probability of detection will be determined. Cost comparison of the assets will be based on the cost estimates of the respective surveillance platforms as given in Table 6 (see Appendix D for details). The unit costs are based on 10 years of operating life, and include annual operating and support costs.

Table 6. Estimated unit acquisition and operating cost of surveillance platforms based on 10 years operating life (in millions US$ FY2007).

	UAV	USV	PC
Cost per unit per year	1.88	0.49	0.92

2. Parameters

Two types of environmental conditions for the model are considered; good and poor visibility in the strait. The SB arrival rate, the mean length of time SBs spend in the strait, and the proportion of SBs that act suspicious are the same under both conditions. However, under poor visibility conditions, SBs will remain tracked for a shorter period of time. The SBs of concern here are those that do not have AIS. There are an average total of 48 such SBs in the strait at all times. Table 7 displays the values of parameters concerning the SB traffic in the strait for both visibility conditions.

Table 7. Parameter values for SB model – SB traffic.

Parameter	Symbol	Good Visibility	Poor Visibility
Arrival rate of SBs into the strait (per hour)	α_W	12	
Mean time each SB remains in the strait (hours)	$\frac{1}{\lambda_W}$	4	
Probability that a SB acts suspicious before leaving the strait	p_{SS}	0.1	
Mean time identified SBs remain tracked (hours)	$\frac{1}{\beta}$	2	1.3

It is assumed that Red for scenario A takes a mean time of 15 minutes to cross the strait to its target, i.e., the mean of $\boldsymbol{T}_{R,A}$ is 15 minutes. It is also assumed that in scenario B Red will attempt to hide among other SBs in the strait for a period of two hours. Thereafter, Red will take a mean time of $\boldsymbol{T}_{R,A}/2$ to reach its target, i.e., 7.5 minutes.

These parameters concerning Red are the same for both good and poor visibility conditions.

Table 2 displays the values of the parameters concerning the surveillance platforms. The parameters for USVs and PCs share the same symbols. The PCs are modeled to have shorter mean inspection times and to be much more accurate in classifying SBs than the USVs. Hence, the key differences between them are that a PC has a larger sensor footprint, slightly higher inspection rates, and much lower probabilities of misclassifying a Red and suspicious SBs. Both platforms are less effective under poor visibility conditions, i.e., longer inspection times, slower platform speeds, shorter sensor ranges, and higher misclassification rate for white SBs. In general, a platform's performance in the respective parameters is degraded by about 30%. However, it is assumed that the platform's effectiveness in classifying a Red remains unchanged under both visibility conditions.

The decision parameters (κ_A, κ_V, and κ_{VS}) concern how the surveillance platforms set their priorities in selecting targets for inspection. The CONOPS assumes the USVs (or PCs) are more likely to inspect a suspicious SB than unsuspicious ones; i.e., κ_V= 300. A UAV has no priority in inspecting suspicious SBs; instead it will focus on inspecting unsuspicious SBs, i.e., κ_A=0. The tuning factors for both priority parameters are set at $\tau_A = \tau_V$=2. A USV (or PC) already engaged in a Type I inspection is only reassigned to conduct a Type II inspection on an unidentified suspicious SB when all USVs

(PCs) are engaged in some activities; this is represented by setting κ_{VS}=10 and τ_{VS}=0.25.

Table 8. Parameter values for SB model – surveillance platforms.

Parameter	Symbol	Good Visibility			Poor Visibility		
		UAV	USV	PC	UAV	USV	PC
Speed (nm per hour)	v_A, v_V	100	30	30	100	20	20
Sensor footprint (nm x nm)	$f_A,\ f_V$	1x1	0.5x 0.5	0.75x 0.75	0.8x 0.8	0.4x 0.4	0.6x 0.6
Mean time a UAV and USV (PC) take to classify a SB as harmless or suspicious (Type I inspection) (minutes)	$\frac{1}{\mu_A}, \frac{1}{\mu_{V,I}}$	5	10	8	7	13	11
Mean time a USV (PC) takes to classify whether a suspicious SB is a threat (Type II inspection) (minutes)	$\frac{1}{\mu_{V,II}}$	-	20	18	-	27	24
Probability a White SB is misclassified as suspicious by the UAV and USV (PC) during a Type I inspection and must undergo a Type II inspection	c_{Awr}, c_{Vwr}	0.1	0.1	0.01	0.15	0.15	0.05
Probability that the Red is classified correctly by a UAV and USV (PC)	c_{Arr}, c_{Vrr}	.95	.95	.99	.95	.95	.99

3. Results and Analysis

Figure 28 displays the plots of scenario A's $P(K_A)$ against the number of USVs active in the strait in good and poor visibility conditions. The three curves on each plot are for the cases with no UAV, one UAV, and two UAVs deployed. Similar plots for PCs are displayed in Figure 29.

In order to achieve $P(K_A)$>0.9 under good visibility conditions and with no UAV contribution, at least nine USVs or eight PCs are required to be deployed in the strait. Under poor visibility conditions, $P(K_A)$ for nine USVs or eight PCs (without a UAV) drops by almost 30% to 0.68 for USVs and 0.70 for PCs. The contribution of UAVs in improving $P(K_A)$ is not very significant; each additional UAV is equivalent to about one USV or PC for cases of $P(K_A)$>0.9 for both good and poor visibility. Furthermore, UAVs are more costly to acquire and operate than USVs or PCs; see Table 6.

Figure 30 displays the plots of scenario B's $P(K_B)$ versus the number of USVs active in the strait under good and poor visibility conditions. The three curves on each plot are for the cases with no UAV, one UAV, and two UAVs deployed. Figure 31 displays similar plots for PCs. In general, it is observed that the UAVs are making a higher contribution in scenario B compared to scenario A. For example, for eight USVs, two UAVs increase $P(K_B)$ by 0.11 (about a 14% increment) compared to an increment of 0.07 or about 8% in $P(K_A)$. The UAVs' higher rate of inspection for Whites is assisting in detecting the Red while it is hidden among the other Whites. However, even with the larger contribution, each additional UAV remains equivalent to about one USV or PC. In order to achieve $P(K_B)$>0.9 under good visibility conditions and no UAV contribution, at least 10 USVs or eight PCs are required. When compared with scenario A, one additional USV is required; for PCs, the number required remains the same. In scenario B, Red is

hidden among other White SBs for a period of two hours, and when it becomes suspicious the idle USVs have only half the time they have in scenario A to detect Red. From Figure 32, it is observed that, with 10 USVs and no UAV, the probability of detecting Red within its hidden time is 0.42. The additional USV for scenario B as compared to scenario A, is needed to ensure at least a 0.83 probability of detecting Red within the shorter time after it becomes suspicious in Scenario B. This is so that the total probability of detecting Red is more than 0.90 Under poor visibility conditions, $P(K_B)$ for 10 USVs or eight PCs (without a UAV) drops by about 30% to 0.67 for USVs and 0.72 for PCs.

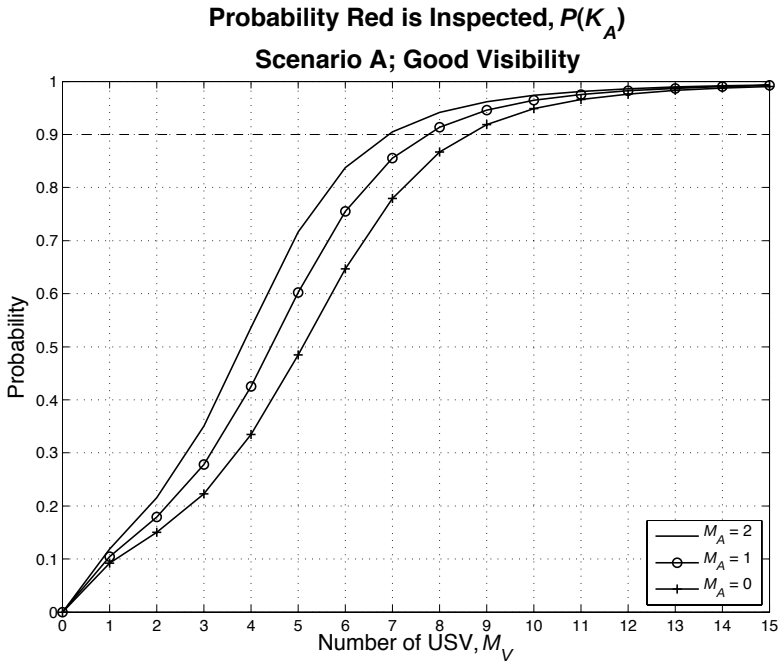

(a)

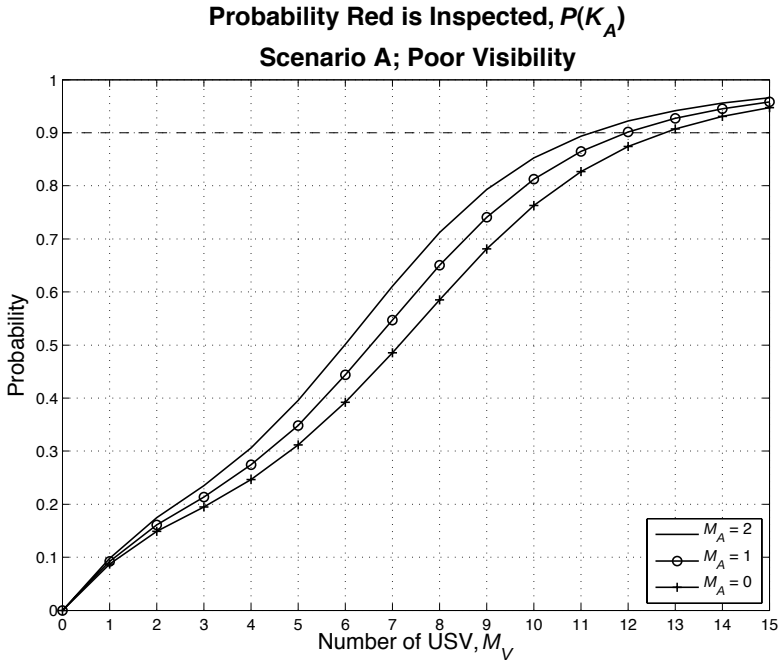

(b)

Figure 28. Plot of probability that SB threat is detected in scenario A against the number of active USVs in the strait under (a) good and (b) poor visibility conditions.

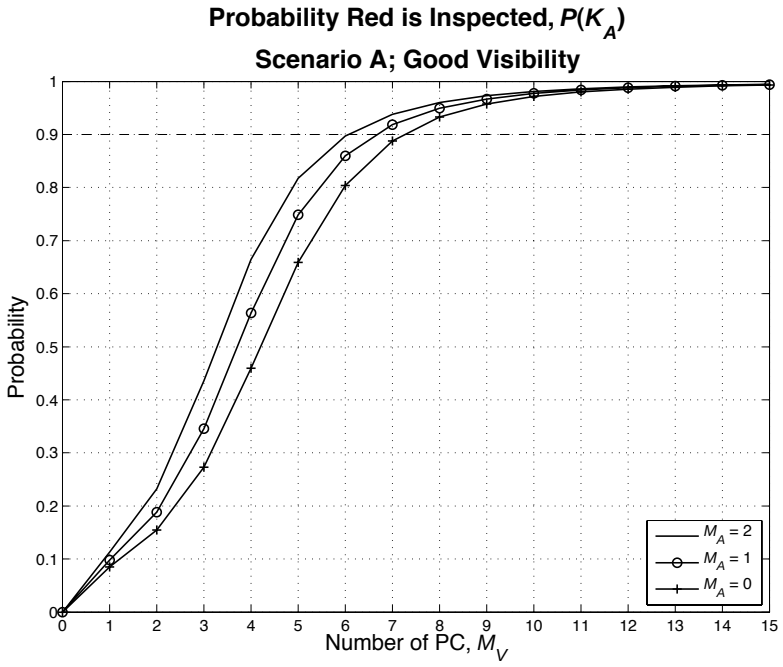

(a)

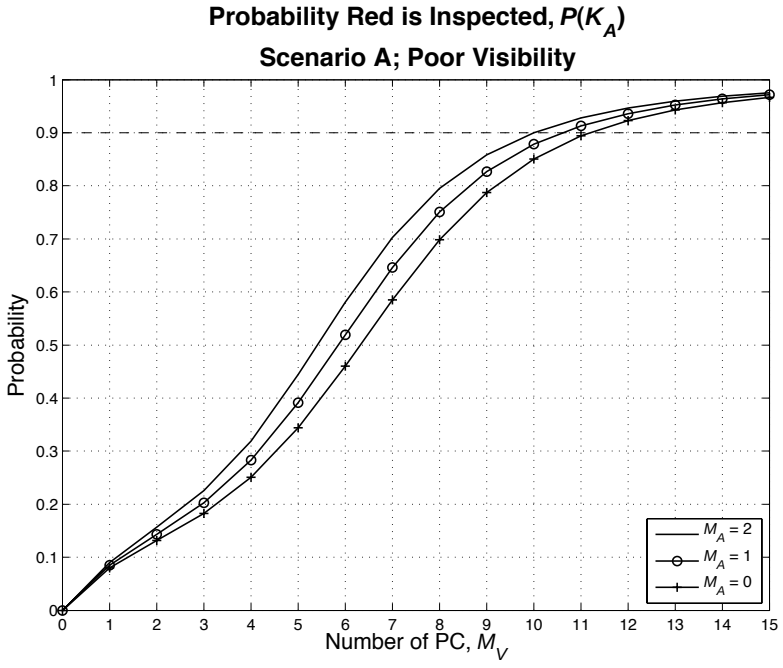

(b)

Figure 29. Plot of probability that SB threat is detected in scenario A against the number of active PCs in the strait under (a) good and (b) poor visibility conditions.

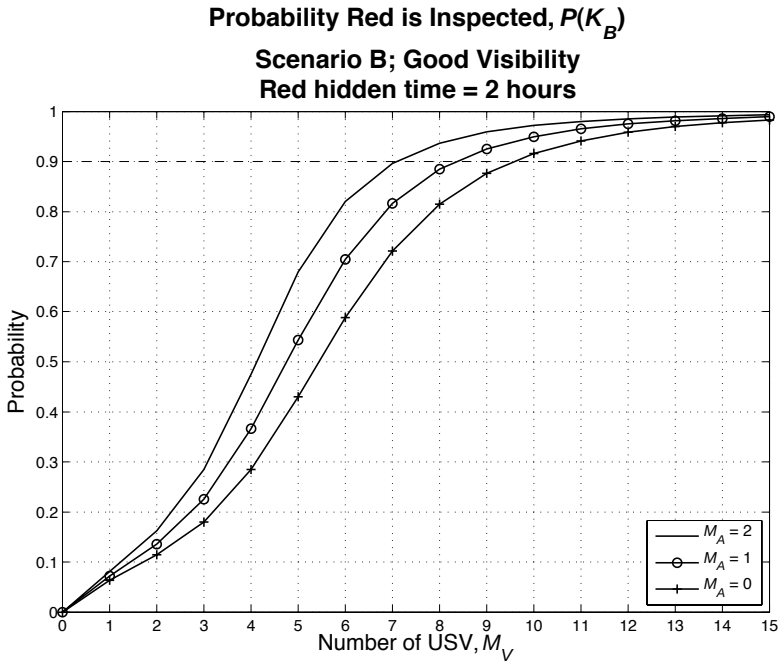

(a)

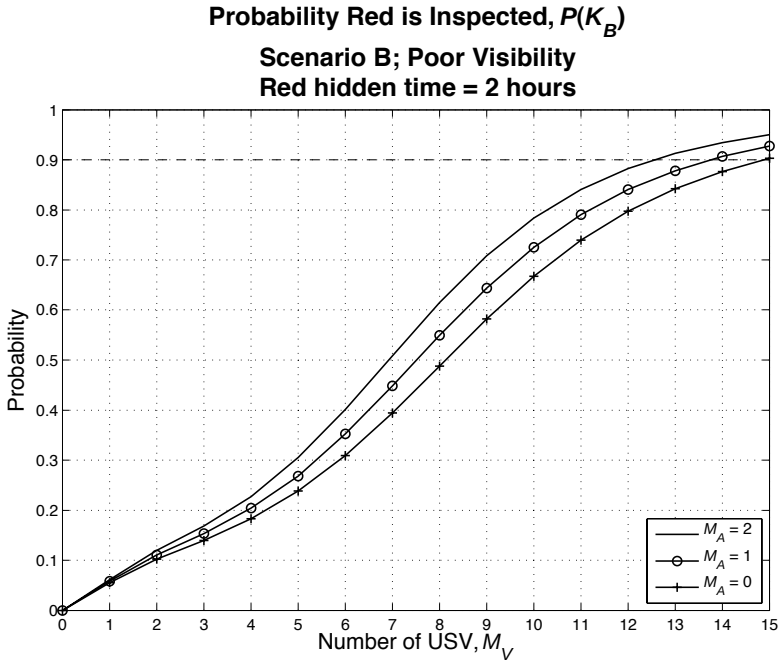

(b)

Figure 30. Plot of probability that SB threat is detected in scenario B against the number of active USVs in the strait under (a) good and (b) poor visibility conditions.

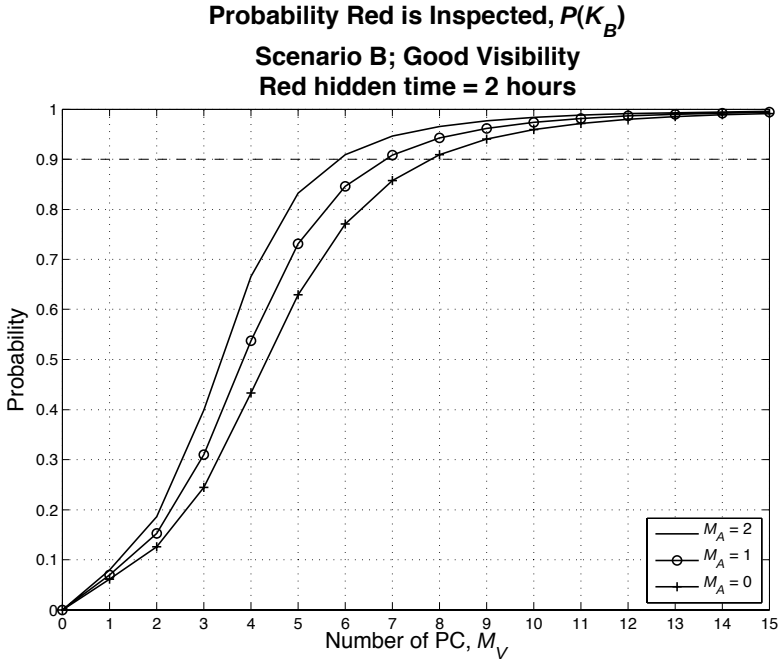

(a)

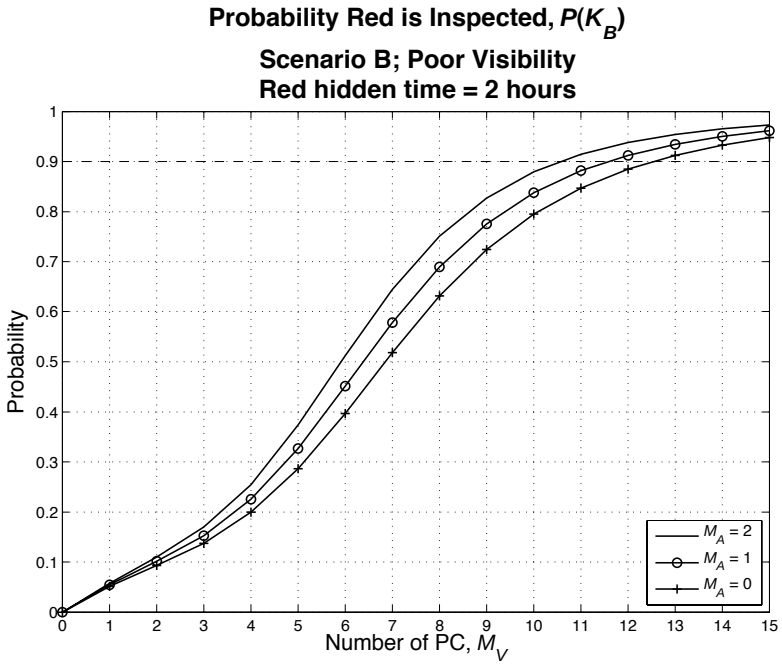

(b)

Figure 31. Plot of probability that SB threat is detected in scenario B against the number of active PCs in the strait under (a) good and (b) poor visibility conditions.

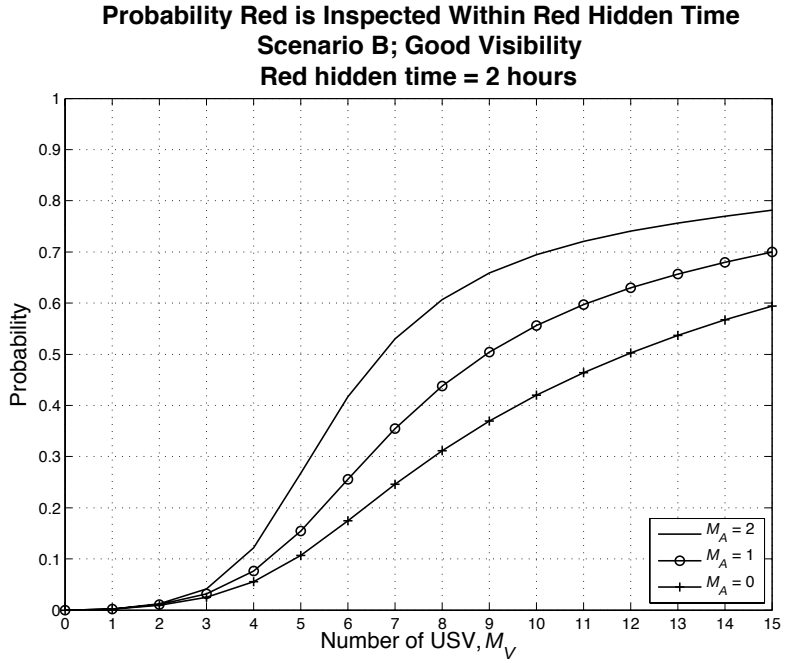

Figure 32. Plot of probability Red is inspected in scenario B within its hidden time of 2 hours, under good visibility.

4. Cost Effectiveness Analysis and Recommendations

The effectiveness of the PCs in the SB model is only marginally better than the USVs while costing two times more than the USVs. For the conditions examined, to achieve a probability of detection of greater than 0.9, the number of PCs required is only one to two less than the number of USVs. From a purely cost-effectiveness standpoint, having an order of battle (ORBAT) of all USVs seems to be the better choice. However, from an operational perspective a mixed ORBAT of USVs and PCs is more robust. A mixed USV and PC ORBAT allows operator flexibility in the deployment of assets; it allows for manned platforms to take over in the

event that a USV is unable to complete a surveillance task. The manned PCs will also likely have a higher deterrence effect and exercise better ground judgments than a USV. Note also that use of PCs puts human operators at risk. Since a pure USV ORBAT will require about 10 USVs and a pure PC ORBAT will require about eight PCs, a mixed ORBAT is estimated to require a total of about eight to 10 surface platforms. A possible ratio for the mix is one PC to two USVs, i.e., a total of three PCs and six USVs.

The model results show that a UAV does not greatly improve the probability of detection. One UAV is equivalent to about one surface platform in terms of achieving a probability of detection of more than 0.9. However, the model does not take into account some capabilities of the UAV as part of the whole surveillance system. First, the UAV has a deterrence effect; it is a conspicuous airborne sensor. Second, the UAV's airborne sensor provides a plane view perspective of targets. This additional perspective adds another dimension to the situational picture, which will improve situational awareness. Representing the consequences of these capabilities in the model requires research in future studies.

Therefore, to achieve a probability of detection of at least 0.9, it is recommended to have an ORBAT of a total of nine surface platforms comprising three PCs and six USVs. The estimated cost of this ORBAT mix is US$5.7 million per year for a period of 10 years. If one UAV is added to the ORBAT mix, one less surface platform is required. For an ORBAT mix comprising one UAV, two PCs, and six USVs, the estimated cost is US$6.7 million per year for a period of

10 years. For an ORBAT mix comprising one UAV, three PCs, and five USVs, the estimated cost is US$7.1 million per year for a period of 10 years.

V. CONCLUSION AND RECOMMENDATIONS

A. CONCLUSION

Two CONOPS were developed to address the surveillance requirements to counter two types of maritime terrorism threats in the congested strait of a littoral state. The first maritime threat concerns the use of large ships (LSs) carrying highly dangerous cargo (D-vessels) to inflict extensive damage to port facilities or other ships. The CONOPS against this threat in this thesis is to use coastal radars and boarding teams from PCs to conduct boarding and inspection of D-vessels in order to detect a LS that has been hijacked by, or is in the hands of terrorists (Red). If such a LS is not detected and disabled it can instill severe damage to a port. The second maritime threat concerns the use of small boats (SBs) to inflict damage on infrastructure, e.g. the port, or other vessels. These terrorist SBs are called *Red boats*. The CONOPS against this second threat, here consisting of one Red boat, is to use cooperative coastal radar, UAVs, USVs, and PCs. The UAV is used to rapidly identify unsuspicious SBs; USVs and PCs are used to inspect suspicious SBs detected by the coastal radar and the UAVs, and to detect the Red boat. Two possible scenarios are considered for the SB threat, one is a direct attack by the single Red boat, and the other is a sneak attack where the one Red boat attempts to hide among other neutral (White) SBs for some time before attacking. Two environmental conditions, good and poor visibility, are considered in the analysis. For both CONOPS, the analyses considered only attacks from a single Red; consideration of

attacks by a team of Red boats, involving both lethal Reds and use of Red decoys are not taken in this thesis.

B. RECOMMENDATIONS FOR SURVEILLANCE PLATFORM MIX AND MODUS OPERANDI AGAINST LS AND SB THREAT

The LS model is applied to a situation with an arrival rate of 20 D-vessels per day. In order to have a probability of detecting the Red vessel greater than 0.9, an order of battle (ORBAT) of at least six PCs is required to be deployed. An additional PC is required for every increment of four to five more D-vessels to arrive per day.

The SB model is applied to a situation with an arrival rate of 12 SBs per hour and an average of 48 unidentified SBs in the strait at any time. These SBs are the portion of the total in the strait that require inspection to ascertain identity. The criterion for the ORBAT mix is to achieve a probability of detection of the Red boat of at least 0.9. In good visibility conditions, the recommended ORBAT mix of six USVs and three PCs without any UAVs results in an estimated cost of US$5.7 million per year for a period of 10 years. A mixed USV and PC ORBAT is recommended because the presence of PCs makes a more robust surveillance force in terms of deterrence and exercising ground judgment. USVs are useful in situations when it is not necessary to risk human lives. If a UAV is included, the recommended mix is one UAV, two PCs, and six USVs at an estimated cost of US$6.7 million per year for a period of 10 years.

The analysis of the SB model results also provides some insight on the possible modus operandi for the surveillance platforms. The UAV's contribution is only significant when it is highly reliable in correctly classifying White small boats. The UAV must be able to quickly identify SBs and classify them as suspicious or not suspicious. If the UAV mistakenly classifies a non-suspicious SB as suspicious, a USV or PC must do a Type II inspection on the SB. Thus, UAVs increase the workload for the USVs and PCs. If deployed, a UAV should have low priority in following suspicious SBs detected by land-based sensors; in this model there is no advantage to having the UAV follow such a suspicious SB. Conversely, the USV should give highest priority to inspecting suspicious SBs to achieve higher probabilities of detecting the Red. In addition, the UAV mean inspection time appears not to have much impact on the probability of detection; this result assumes the probability of correct classification is not affected by the classification time. Reducing USV mean inspection time for Type I inspections, instead of Type II inspections, has a larger impact in increasing probability of detection. Once again, the probability of correct classification as suspicious or not suspicious that results from a Type I inspection is assumed not to depend on the length of time spent conducting the inspection.

C. RECOMMENDATION FOR FUTURE WORK

This thesis identifies several possible refinements to the SB model. The first refinement is to include possible suspicious SBs' behavioral change when they are being

followed by UAVs. This would allow for the suspicious SBs to change to unsuspicious SBs when they detect they are being followed by a UAV; this reduces the probability of having USVs do a Type II inspection. A second refinement is to have the probability of correct classification of White SBs by both UAVs and USVs be functions of the Type I inspection times. This would allow for possible determination of the optimal length of inspection times. Incorporation of the deterrence effect of having assets visibly patrol the straits may influence the number of assets required.

A comparison between the probabilities of detecting the Red showed that they are similar for the deterministic fluid model and a generalized birth-death stochastic model for the LSs. Further formulation and study of stochastic models for the two scenarios can further inform decision makers concerning the number of UAV, USV, and PC assets needed to respond to the threats. They can also be used to study the allocation of surveillance assets to different sub-regions.

Another extension to the model that can be explored is to consider teamed-attack by Red boats, instead of the current Red tactics of a single attacker. One possible teamed-attack tactic by the Red is the use of a decoy and an attacker SB.

APPENDIX A: ESTIMATION OF PARAMETERS

A. INTRODUCTION

This appendix discusses the methods used in estimating the following parameters:

$\frac{1}{\delta_A}, \left(\text{respectively, } \frac{1}{\delta_V} \right)$ = Mean time taken by an idle UAV and (respectively, USV) to proceed to an unidentified small boat;

$\frac{1}{\gamma_V}$ = Mean time taken by an idle USV to proceed to a UAV shadowing a suspicious small boat.

B. METHOD FOR $\frac{1}{\delta_A}$ AND $\frac{1}{\delta_V}$

The region is rectangular with sides M_x and M_y. If the number of UAVs, M_A>1 (respectively USVs, M_V>1), each platform is assigned a fraction $\frac{1}{M_A}$ (respectively $\frac{1}{M_V}$) of the region. We assume that a UAV (respectively USV) has a square footprint with side f_A (respectively f_V); the area that can be seen by the sensor on the platform is f_A^2 (respectively f_V^2). The sub-region assigned to a UAV (respectively USV) is tiled with the square footprints with

a total of $\frac{M_x M_y}{M_A f_A^2}$ (respectively $\frac{M_x M_y}{M_V f_V^2}$) tiles (see Figure 33).

Let v_A (respectively v_V) be the speed of a UAV (respectively USV). The time for a UAV (respectively USV) to cross one footprint along the x-direction (or y-direction) is f_A / v_A (respectively f_V / v_V). The mean time for a UAV (respectively USV) to travel over the entire sub-region assigned to it (using a raster scan pattern) is $\frac{T_A}{M_A} = \frac{M_x M_y}{M_A f_A^2} \frac{f_A}{v_A} = \frac{M_x M_y}{M_A f_A v_A}$ (respectively $\frac{T_V}{M_V} = \frac{M_x M_y}{M_V f_V v_V}$).

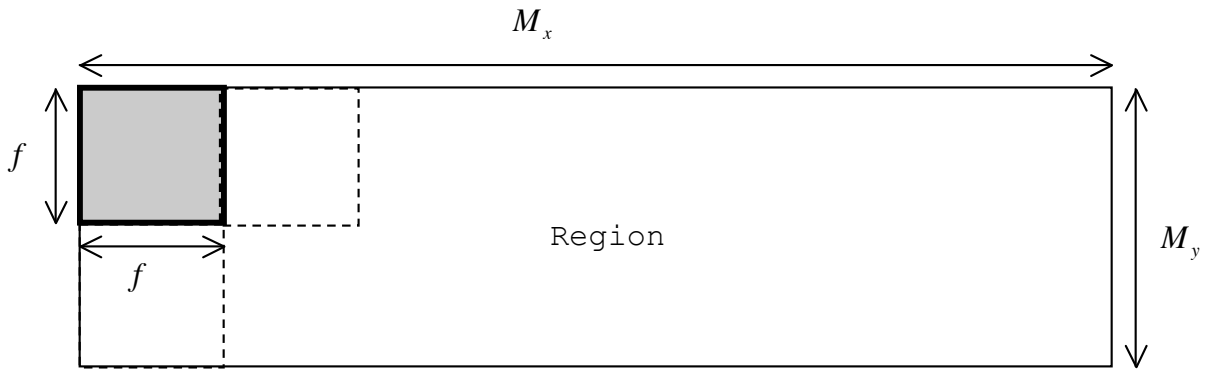

Figure 33. Schematic diagram of the tiling of the region by a platform sensor footprint.

We assume that there are $\frac{W_U}{M_A}$ (respectively $\frac{W_U}{M_V}$) unidentified small boats in each sub-region for a UAV (respectively USV), where W_U is the mean number of unsuspicious SBs. Therefore, the mean time taken by a UAV

(respectively USV) to travel between the unidentified small boats is $\frac{1}{\delta_A} = \frac{T_A}{M_A}\frac{M_A}{W_U} = \frac{T_A}{W_U}$ (respectively $\frac{1}{\delta_V} = \frac{T_V}{W_U}$).

C. METHOD FOR $\frac{1}{\gamma_V}$

The time taken for each USV to travel around its sub-region is $\frac{T_V}{M_V}$. An estimate of the mean travel time of a USV to respond to a report of a suspicious small boat is $\frac{1}{\gamma_V} = \frac{T_V}{2M_V}$.

THIS PAGE INTENTIONALLY LEFT BLANK

APPENDIX B: DESIGN OF EXPERIMENT FOR THE EXPLORATION OF THE LARGE SHIP THREAT MODEL

A. OBJECTIVE

The objective of this design of experiment (DOE) is twofold. First is to determine the effects of varying the number of sub-regions, n, and the number of service periods, m, on the outcomes of the large ship (LS) model. The values of n and m should be at least 1. Second is to determine the most significant factors in the model.

B. DOE

The design points for all parameters of the model, except n and m, are generated by the Nearly Orthogonal Latin Hypercube (NOLH) design method (Sanchez 2005) used in designing simulation experiments. Table 9 displays the ranges of the parameter values considered and the 17 design points generated. For each design point, the probability that Red is detected ($P(K)$) is determined as the number of sub-regions, n, varied from 1-25 and the number of service periods, m, is set at five levels (1, 2, 4, 8, 16). Recall that a service time for a PC is the sum of m service periods of equal length.

Table 9. DOE design points

	Parameters (Ranges)				
Design Point	**λ** $(1/3 - 1)$	**μ** $(1/5 - 1/2)$	**γ** $(2/3 - 4/3)$	**α** $(5/12 - 5/4)$	***M*** $(1 - 10)$
1	0.79	0.5	1.21	0.73	3
2	0.96	0.28	1.25	0.89	1
3	0.92	0.33	0.71	0.63	7
4	0.88	0.39	0.88	1.25	6
5	0.5	0.48	0.96	0.52	4
6	0.33	0.29	0.92	1.09	2
7	0.58	0.26	1.33	0.68	9
8	0.63	0.46	1.17	1.2	8
9	0.67	0.35	1	0.83	6
10	0.54	0.2	0.79	0.94	8
11	0.38	0.43	0.75	0.78	10
12	0.42	0.37	1.29	1.04	4
13	0.46	0.31	1.13	0.42	5
14	0.83	0.22	1.04	1.15	7
15	1	0.41	1.08	0.57	9
16	0.75	0.44	0.67	0.99	2
17	0.71	0.24	0.83	0.47	3

C. RESULTS

1. The Effects of Varying *n* and *m*

Figure 34 displays the 17 sub-plots of the results from the LS model for the 17 design points. Each sub-plot is the plot of $P(K)$ against n and each curve on the sub-plot is for m set at different levels. From Figure 34, it appears that m has no significant effect on the $P(K)$ in the LS model except for those runs when the number of active PCs (M) is three or fewer [see Figure 34 (b), (f), (p), and

(q)]. When $M \leq 3$, higher m results in lower $P(K)$. In run 2 where M=1, the difference in $P(K)$ between m=1 and m=8 is 30% (at n=10). This suggests that when $M \leq 3$, m should take a larger value such as m=8. When $M > 3$, m could take a smaller value such as m=2. $P(K)$ tends to decrease as n increases. In all 17 design points, the largest drop in $P(K)$ occurs from n=1 to 10. At n=10 and m=8, the percentage drop in $P(K)$ ranges from near zero to about 30% across the 17 design points. The sub-plots also appear to indicate that the effect of n is more significant when there is a smaller number of active PCs. This suggests that the parameter n should be set to a value around n=10 for this size region.

The recommendations of this analysis are that for the size of the region considered and the service time considered, n should be set to a value of n=10; for $M > 3$, m should be equal to two; and for $M \leq 3$, m should be equal to eight.

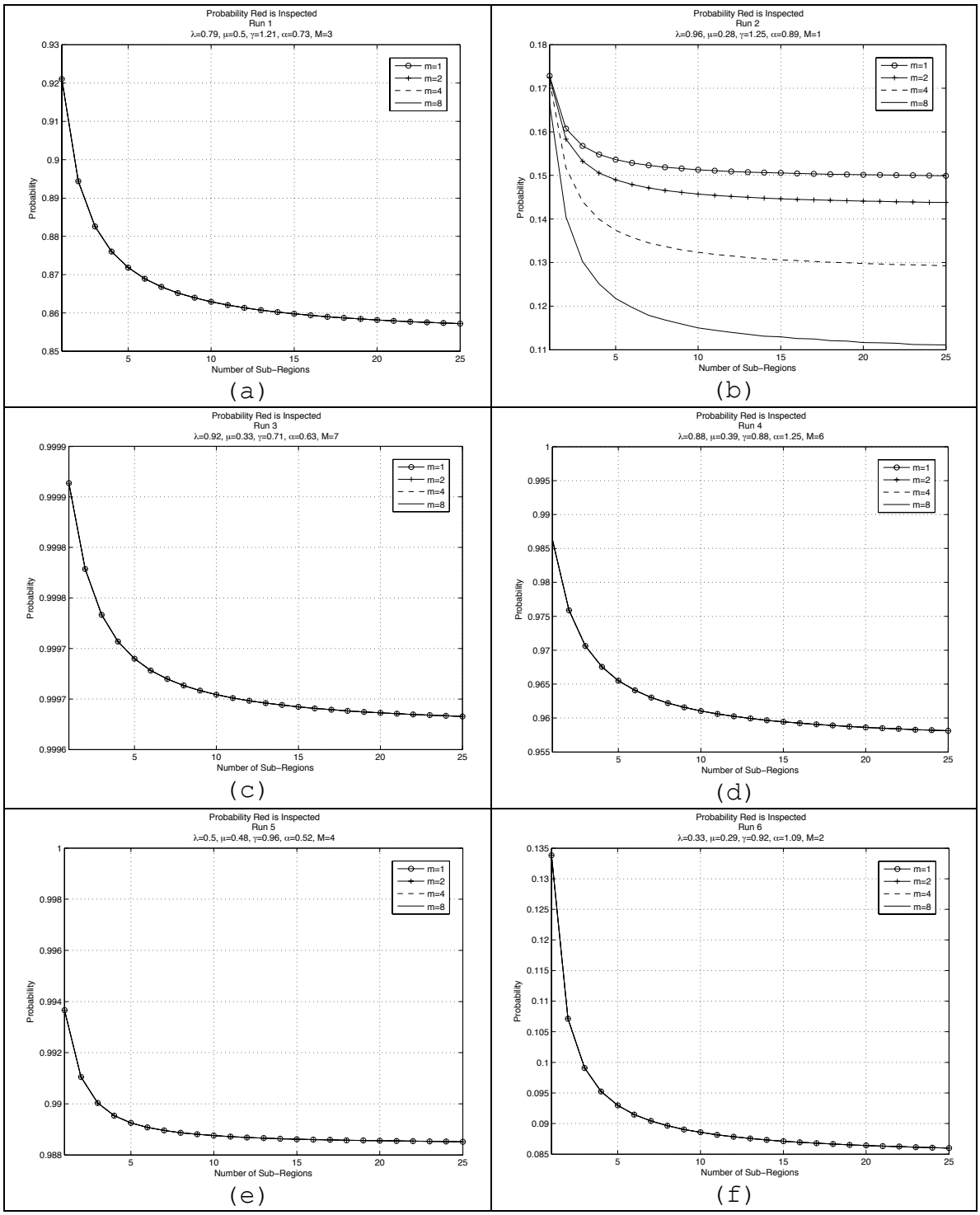

Figure 34. (a)-(f). Plot 1 to 6 of probability of detection versus the number of sub-regions, n, for various numbers of service time periods, m.

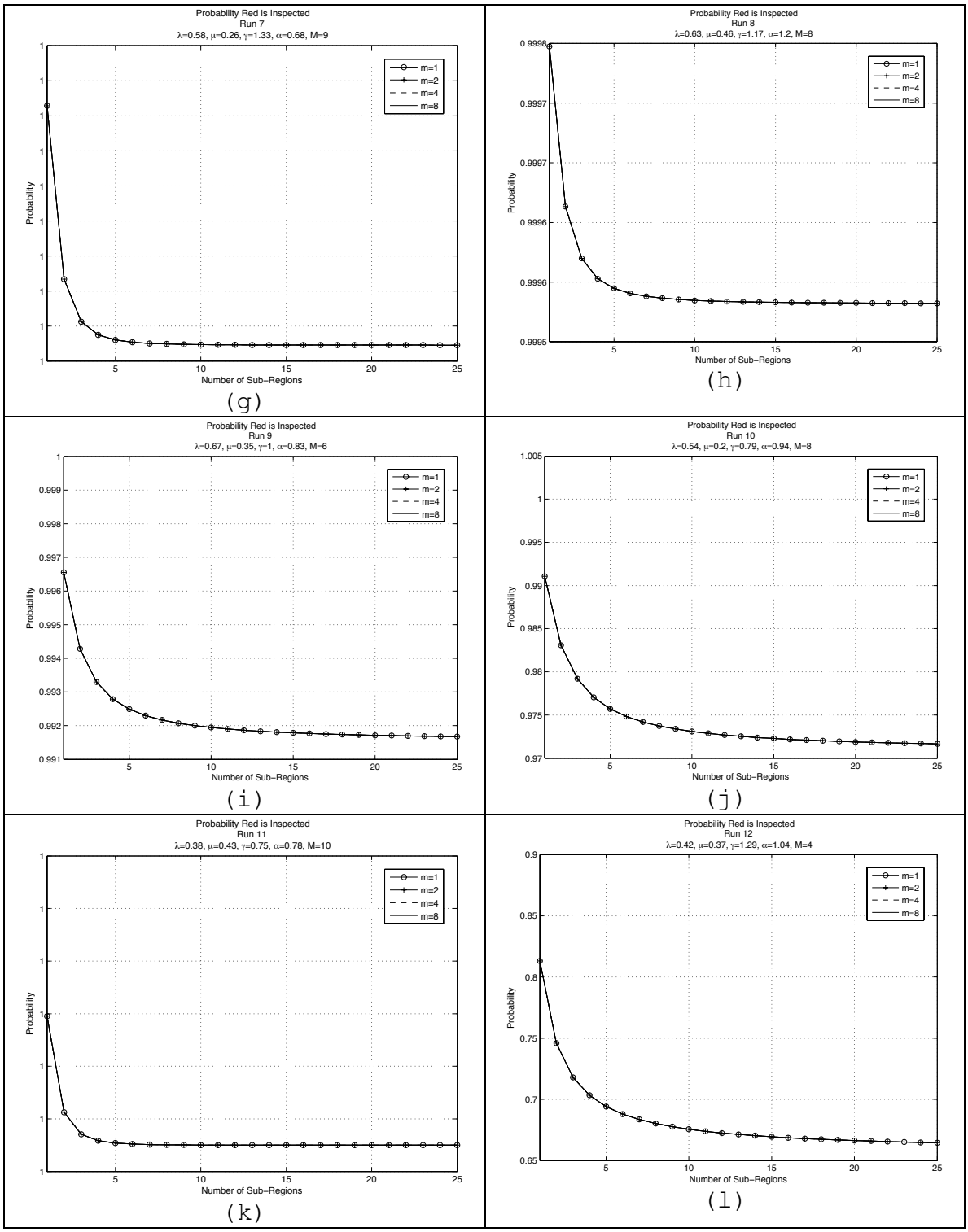

Figure 34. (g)-(l). Plot 7 to 12 of probability of detection versus the number of sub-regions, n, for various numbers of service time periods, m.

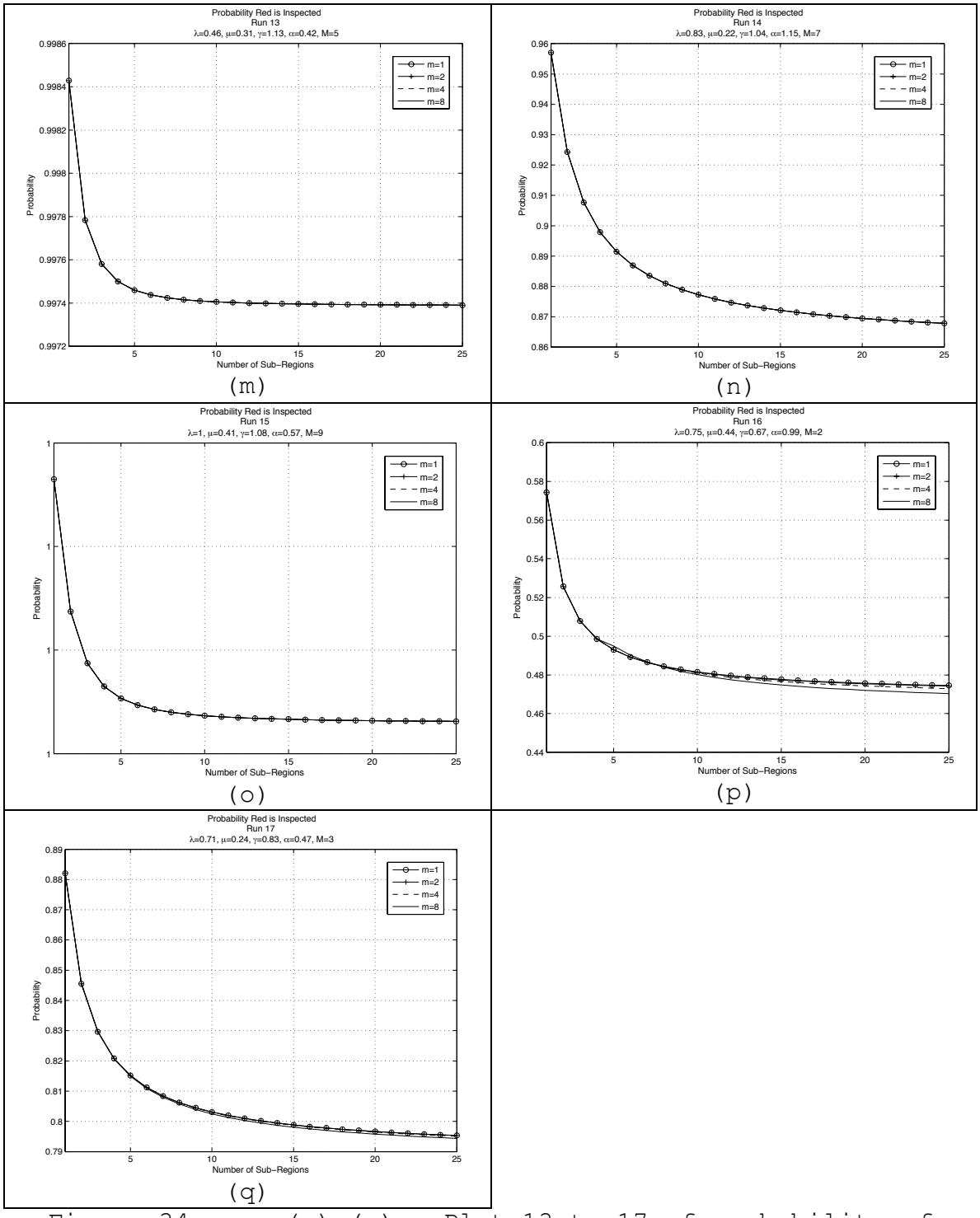

Figure 34. (m)-(q). Plot 13 to 17 of probability of detection versus the number of sub-regions, n, for various numbers of service time periods, m.

2. Significant Factors in the LS Model

Values of the model parameters considered appear in Table 9. The values of these parameters form a nearly orthogonal Latin hypercube design (Sanchez 2006). The model results are summarized by a linear regression with explanatory variables the model parameters M, α, μ, λ, and γ; the resulting R-square value is 0.96. The estimates of the coefficients and their significance in the model are displayed in Figure 35. The polynomial and interaction terms are centered at the means of the corresponding individual factors.

The factor M, the number of PCs, is the most significant in this model, followed by the arrival rate of D-vessels (α) and the service rate of the PC (μ), i.e., the rate at which the PCs board and inspect the D-vessels. The rate at which D-vessels transit the strait (λ) and the rate at which PCs get to the next un-inspected D-vessel (γ) are the least significant factors in the model.

Sorted Parameter Estimates

Term	Estimate	Std Error	t Ratio	Prob>|t|
M	0.0789696	0.006669	11.84	<.0001*
(M-5.52941)*(M-5.52941)	-0.016784	0.003218	-5.22	0.0006*
alpha	-0.330338	0.070518	-4.68	0.0011*
mu	0.6676073	0.197	3.39	0.0080*
(alpha-0.83412)*(M-5.52941)	0.1244455	0.038197	3.26	0.0099*
lambda	0.086608	0.088008	0.98	0.3508
gamma	-0.027024	0.088397	-0.31	0.7668

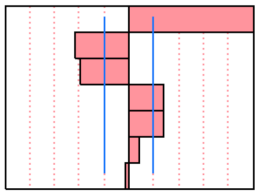

Figure 35. Sorted estimates of the parameter of the fitted model.

THIS PAGE IS INTENTIONALLY LEFT BLANK

APPENDIX C: COMPARISON OF THE DETERMINISTIC FLUID MODEL AND A BIRTH-DEATH MODEL OF THE LARGE SHIP PROBLEM

The models presented in this appendix are reproduced from a working paper by Gaver and Jacobs (2007).

A. MODEL C-1: A TIME-HOMOGENEOUS MARKOV/BIRTH-DEATH VERSION OF LARGE SHIP MODEL

Suppose there are $\boldsymbol{L}(t)$ un-inspected large ships (LSs) in the strait at time t; $\boldsymbol{L}(t)=\{0,1,2,\ldots,L\}$. For simplicity $L=\infty$ can be tolerated.

Let the probability that there are l LSs at time t, given there are l_0 LSs as the initial condition when t=0 be

$$P\left\{\boldsymbol{L}(t)=l\middle|\boldsymbol{L}(0)=l_0\right\} \qquad \text{(C.1)}.$$

1. Transition Probabilities

The transition probabilities between states for $\boldsymbol{L}(t)$ are displayed in the equations (C.2) and (C.3).

$$P\left\{\boldsymbol{L}(t+dt)=l+1\middle|\boldsymbol{L}(t)=l\right\}=\alpha_l dt+o(dt) \qquad \text{(C.2)}$$

Note this generalizes Poisson arrivals since if $\boldsymbol{L}(t)=\bar{L}>0$ more arrivals cannot occur. α_l is the rate of arrival of LSs, given l uninspected LSs are in strait at time t.

$$P\left\{\boldsymbol{L}(t+dt)=l-1\middle|\boldsymbol{L}(t)=l\right\}$$
$$=\begin{cases}\mu l dt+o(dt) & \text{for } 0\le l\le M \\ \mu M dt+\lambda\left[l-M\right]^{+}+o(dt) & \text{for } l>M\end{cases} \qquad \text{(C.3)}$$

Note this combines the act of joining a PC with a LS and the act of PC boarding with $\frac{1}{\mu}=\frac{1}{\mu_J}+\frac{1}{\mu_B}$ where $\frac{1}{\mu_B}$ is the mean time to board and inspect the LS and $\frac{1}{\mu_J}$ is the mean time for the PC to travel to and prepare to board (join with) the LS. M is the number of active PCs in the strait and $\frac{1}{\lambda}$ is the mean time a LS remains in the strait. The first line expresses the rate of service when there are more than enough PCs; the second represents the situation in which all M PCs are occupied and so the remainder of the LSs, $\boldsymbol{L}(t)-M$, escape the region (e.g. reach the port) at individual rate λ.

2. Long-run / Steady-State Solution

Let

$$\alpha_l dt+o(dt)=P\left\{\boldsymbol{L}(t+dt)=l+1\middle|\boldsymbol{L}(t)=l\right\} \qquad \text{(C.4)}$$

and

$$\mu_l dt+o(dt)=P\left\{\boldsymbol{L}(t+dt)=l-1\middle|\boldsymbol{L}(t)=l\right\} \qquad \text{for } l\ge 1$$
$$=\begin{cases}\mu l dt+o(dt) & \text{for } 0\le l\le M \\ \mu M dt+\lambda\left[l-M\right]^{+}+o(dt) & \text{for } l>M\end{cases} \qquad \text{(C.5)}.$$

The limiting probabilities:

$$\pi_l = P\left\{\boldsymbol{L}(\infty) = l\right\} \qquad \text{(C.6)}$$

always exist if $\boldsymbol{L}$ is finite, or $\lambda > 0$.

The solution of the Balance Equations, see Ross (2007, p. 387), is

$$\pi_l = \pi_0 \frac{\alpha_0 \alpha_1 \cdots \alpha_{l-1}}{\mu_1 \mu_2 \cdots \mu_l} \qquad \text{(C.7)}$$

where π_0 is found by normalization. For the special case of stationary Poisson arrivals, $\alpha_i \equiv \alpha$, and $i \in (0, 1, 2, \ldots)$,

$$\pi_0 = \frac{1}{1 + \sum_{n=1}^{\infty} \frac{\alpha^n}{\mu_1 \mu_2 \cdots \mu_n}} \qquad \text{(C.8)}.$$

3. Probability of Detecting Red Vessel

A Red vessel (hijacked LS) enters the strait. Let K be the event that the Red vessel is detected. For the parameters (rates) used here, the Red vessel is detected when the number of un-inspected LSs is less than the number of active PCs in the strait when Red enters the strait. Hence, the probability of detecting Red vessel for M active PCs is

$$P(K \mid M) = \sum_{l=0}^{M-1} \pi_l \qquad \text{(C.9)}.$$

An important generalization, not covered here, deals with streams or surges of Red entrants bound for the port.

B. MODEL C-2: A GENERALIZED TIME-HOMOGENEOUS PSEUDO-MARKOV/BIRTH-DEATH VERSION OF LARGE SHIP MODEL WITH SEQUENTIAL SUB-REGIONS

The strait is next subdivided into n contiguous sub-regions traversed sequentially. Let $\boldsymbol{L}_j(t)$ be the number of un-inspected LSs in sub-region j, $j \in (0, 1, 2, \ldots, J)$. LSs enter the strait in sub-region 1. Let M_j be the number of PCs assigned to sub-region j; these PCs only inspect LSs in sub-region j.

1. Transition Probabilities

The transition probabilities between states for $\boldsymbol{L}(t)$ are displayed in the expressions (C.10) and (C.11).

$$P\left\{\boldsymbol{L}_j(t+dt) = l_j + 1 \,\middle|\, \boldsymbol{L}_j(t) = l_j,\ \boldsymbol{L}_{j-1}(t) = l_{j-1}\right\}$$
$$= \begin{cases} \alpha_{l_j}\, dt + o(dt) & \text{for } j = 1 \\ n\lambda\left[l_{j-1} - M_{j-1}\right]^+ dt + o(dt) & \text{for } j > 1 \end{cases} \qquad \text{(C.10)}$$

Note that this generalizes Poisson arrivals since if $\boldsymbol{L}_j(t) = \bar{L}_j > 0$ more arrivals can be prevented. Such cases are not addressed in this thesis; here $\alpha_j \equiv \alpha$ constant.

First,

$$
\begin{aligned}
& P\left\{\boldsymbol{L}_j\left(t+dt\right)=l_j-1\middle|\boldsymbol{L}_j\left(t\right)=l_j\right\} \\
&= \begin{cases} \mu l_j dt + o\left(dt\right) & \text{for } 0 \le l_j \le M_j \\ \mu M_j dt + n\lambda\left[l_j - M_j\right]^{+} + o\left(dt\right) & \text{for } l_j > M_j \end{cases} \\
&\equiv \mu_{l_j}\left(j\right)dt + o\left(dt\right)
\end{aligned}
\qquad \text{(C.11)}.
$$

Approximation of the limiting distribution (*assuming independence between strait segments*):

$$
\lim_{t\to\infty} P\left\{\boldsymbol{L}_1\left(t\right)=l_1,\ldots,\boldsymbol{L}_n\left(t\right)=l_n\right\} \approx \prod_{i=1}^{n}\pi_{l_i}\left(i\right) \qquad \text{(C.12)}
$$

where

$$
\pi_{l_j}\left(j\right) = \begin{cases} K_1 \dfrac{\alpha^{l_j}}{\mu_1\left(1\right)\cdot\mu_2\left(1\right)\cdot\ldots\cdot\mu_{l_j}\left(1\right)} & \text{for } j=1 \\ K_j \dfrac{n\lambda A_{j-1}^{l_j}}{\mu_1\left(j\right)\cdot\mu_2\left(j\right)\cdot\ldots\cdot\mu_{l_j}\left(j\right)} & \text{for } j>1 \end{cases} \qquad \text{(C.13)}
$$

and K_j is a normalizing constant as in the Model C-1 in this appendix (same limiting distribution but with $n\lambda$ instead of λ and M_j instead of M. Additionally,

$$
K_j = \begin{cases} \dfrac{1}{1+\sum_{k=1}^{\infty}\dfrac{\alpha^k}{\mu_1\left(1\right)\cdot\mu_2\left(1\right)\cdot\ldots\cdot\mu_k\left(1\right)}} & \text{for } j=1 \\ \dfrac{1}{1+\sum_{k=1}^{\infty}\dfrac{\left(n\lambda A_{j-1}\right)^k}{\mu_1\left(j\right)\cdot\mu_2\left(j\right)\cdot\ldots\cdot\mu_k\left(j\right)}} & \text{for } j>1 \end{cases} \qquad \text{(C.14)}
$$

$$A_j = \sum_{k=M_j}^{\infty} \left(k - M_j\right)\pi_k\left(j\right) \qquad \text{for } j > 0 \qquad \text{(C.15)}.$$

The probability an entering Red is detected is (approximately Markov, hence "sub M"):

$$P_M\left(K\right) = \left\{1 - \prod_{j=1}^{n}\left[1 - \sum_{l=0}^{M_j - 1} \pi_l\left(j\right)\right]\right\}. \qquad \text{(C.16)}.$$

APPENDIX D: COST ESTIMATES

A. PLATFORM ACQUISITION COST

The acquisition cost estimates for each of the platforms are based on awarded contracts of similar platforms in recent years or program reports.

According to a report from the Fire Scout UAV program, each UAV unit is estimated to cost FY2007 US$9.4 million (*Defense Industry Daily*, 2007).

The unit cost of the Rafael Protector USV is unavailable in open sources and has to be estimated from the cost of other USVs. In 2006, a US$12.7 million contract was awarded to provide four USVs for the Littoral Combat Ship's (LCS) Anti-Submarine Warfare (ASW) Mission Module. It is assumed here that the LCS's USV with the ASW payload is similar in cost to the Protector USV with EO/IR, and radar sensors, and a small caliber weapon system. Hence the estimated cost of one Protector USV unit is FY2006 US$3.2 million.

The estimated cost of the PCs is based on the Israeli Navy's US$40 million program to acquire eight fast patrol crafts (FPCs) in 2002. Hence the estimated acquisition cost for one unit PC is US$5 million (FY2002).

Table 10 displays the FY2007 normalized acquisition cost for the platforms.

Table 10. Table of platform acquisition cost normalized to FY2007.

	UAV	**USV**	**PC**
Unit acquisition cost (US$ million)	9.4 (FY 2007)	3.2 (FY 2006)	5.5 (FY 2002)
Inflation rate (%)	1.00	1.02	1.11
Unit acquisition cost (US$ million FY2007)	9.40	3.26	6.11

B. EXPECTED LIFE SPAN OF THE PLATFORMS

It is assumed the platform will be deployed for a period of ten years.

C. OPERATION AND SUPPORT (O&S) COST

As no open-sourced data is available on the O&S of these platforms, they are estimated as a proportion of their respective unit acquisition cost. It is assumed that the unit annual O&S costs for each of the platforms is 10%, 5% and 5% for UAVs, USVs, and PCs respectively.

D. ESTIMATED COST PER UNIT PER YEAR

Table 11 displays the estimated total cost per unit year.

Table 11. Estimated total cost per unit per year for each platform.

	UAV	**USV**	**PC**
Unit acquisition cost (US$ million FY2007)	9.40	3.26	6.11
Expected life span	10	10	10
Unit acquisition cost per year of life span (US$ million FY2007)	0.94	0.33	0.61
O&S cost per year (US$ million FY2007)	0.94	0.16	0.31
Total cost per unit per year (US$ million FY2007)	1.88	0.49	0.92

THIS PAGE INTENTIONALLY LEFT BLANK

LIST OF REFERENCES

Bateman, S. (2006). Assessing the Threat of Maritime Terrorism: Issues for the Asia-Pacific Region, *Security Challenges, Octr 2006, Vol. 2, No. 3,* 84-85.

Defense Industry Daily (Sep 18, 2007). *The Fire Scout VTUAV Program: By Land and By Sea (updated)*. Retrieved Sep 28, 2007, from http://www.defenseindustrydaily.com/the-fire-scout-vtuav-program-by-land-and-by-sea-updated-01316/#more.

Defense Industry Daily (Oct 23, 2006). *US Navy Spends Another $12.7M for ASW Module USVs*. Retrieved Sep 28, 2007, from http://www.defenseindustrydaily.com/us-navy-spends-another-127m-for-asw-module-usvs-02735/#more.

Defense Update (n.d.). *Israel Navy Acquire new Fast Patrol Boats*. Retrieved Sep 28, 2007, from http://www.defense-update.com/news/FPBs-IN.htm.

Department of Defense Dictionary of Military and Associated Terms Joint Publication 1-02. (2001, amended 2007) Retrieved Nov 9, 2007, from http://www.dtic.mil/doctrine/jel/doddict.

Efe, Murat, Yilmaz, A. E., & Dura Donmez, Ozlem (2005). Data fusion for a surveillance system: addressing some practical problems. *Systems Engineering, 2005. ICSEng 2005. 18th International Conference on 16-18 Aug*. 342-347.

Gaver, D.P., Jacobs, P.A., Chng, K.C., & Alderson, D. (2007). Slides on Domain Protection Methodologies presented at the INFORMS Annual Meeting 2007.

Gaver, D.P., Jacobs, P.A. (2007). *A Birth-Death Model for for the Large Ship Problem in Maritime Domain Protection Methodology*. Draft paper. Operations Research Department, Naval Postgraduate School, Monterey, CA.

International Maritime Organization. AIS transponders. Retrieved Nov 9, 2007, from http://www.imo.org.

Ross, S.M. (2007). *Introduction to probability models* (9th ed.). London: Academic Press.

Sanchez, S. M. (2005). Spreadsheet for generating orthogonal and nearly-orthogonal LH designs in natural levels. Retrieved on Aug 1, 2007, from http://diana.cs.nps.navy.mil/SeedLab.

Sanchez, S. M. (2006). Work smarter, not harder: guidelines for designing simulation experiments. *Proceedings of the 2006 Winter Simulation Conference*, eds. L.F. Perrone, F.P. Wieland, J. Liu, B. G. Lawson, D. M. Nicol, and R.M. Fujimoto, 52-53.

U.S. Coast Guard Navigation Center. Automatic ID Systems. Retrieved on Nov 5, 2007, from http://www.navcen.uscg.gov/enav/ais

INITIAL DISTRIBUTION LIST

1. Defense Technical Information Center
   Ft. Belvoir, Virginia

2. Dudley Knox Library
   Naval Postgraduate School
   Monterey, California

3. Professor Patricia A. Jacobs
   Department of Operations Research
   Naval Postgraduate School
   Monterey, California

4. Distinguished Professor Donald P. Gaver
   Department of Operations Research
   Naval Postgraduate School
   Monterey, California

5. CAPT USN (Ret) Wayne P. Hughes, Jr.
   Senior Lecturer
   Department of Operations Research
   Naval Postgraduate School
   Monterey, California

6. CAPT USN (Ret) Jeffrey E. Kline
   Senior Lecturer
   Department of Operations Research
   Naval Postgraduate School
   Monterey, California

7. Assistant Professor David Alderson
   Department of Operations Research
   Naval Postgraduate School
   Monterey, California

8. LTC Malcolm Shee
   Head Operations Research Branch (Navy)
   SAF Operations Research Office
   Joint Plans and Transformation Department
   Ministry of Defence, Singapore
   Singapore